

Authors' response to Referee 1

Journal: Ocean Sciences

Title of paper: Impact of intraseasonal wind bursts on SST variability in the far eastern Tropical Atlantic Ocean during boreal spring 2005 and 2006. Focus on the mid-may 2005 event.

Authors: Herbert Gaëlle, Bourlès Bernard.

We thank Reviewer 1 for his comments and suggestions that allowed improvements of our paper. We have made all needed information to make the figures easily understandable and conforming with general publications criteria (figures size, labels, etc). We also worked to make the manuscript easier to read and understand, by adding some information and removing others.

RC: Referee's comment; **AC:** Authors' comment; **MC:** Manuscript changes

Response to major comments

1. RC: The study focusses on the years 2005 and 2006. Most of the features discussed in section 4.2, however, appear to occur in both of these year. Maybe it would be more instructive to contrast 2005 to an interannual warm event year?

AC: To contrast interannual events in 2005 and in a warm year (like 1998) would be indeed also interesting. However, the comparison with the year 2006, considered as a “normal year”, shows that the interannual events are a common feature impacting the SST variability in the studied area and highlights what makes the year 2005 as a “cold” year. To illustrate, the figure X1 (not added in the revised manuscript) below shows the longitude-time diagram of the SST in CLR (Figure X1 a & f) as well as the intraseasonal variations of the wind stress speed (Figure X1 c & h), the 20°C-isotherm depth (Figure X1 d & i), and the sea surface heat flux (Figure X1 e & j) for 1998 (warm year) and 2005 (cold year). We see indeed that the SSTs in boreal spring are higher in spring 1998 than spring 2005. The wind bursts during spring 1998 are not as stronger than during spring 2005. Moreover, the 20°C-isotherm is deeper in spring 1998 than during 2005, making the SST less reactive to wind intensification.

What makes the particularity of the year 2005 is not the occurrence of intraseasonal events but their time of occurrence, their strength, and the favorable combination of local and remote forcing with the arrival of Kelvin wave at the time of strong local winds which induces shallower thermocline.

Thus, we have not described the conditions for 1998 because we have preferred to focus on the year 2005 and understand what makes it an anomalous year compared to a “normal” year. However, it would be interesting to add in the Discussion section some lines about the conditions of a warm year such as 1998.

MC: These lines have been added in the conclusion:

“It should be noted that the occurrence of intraseasonal wind intensification in CLR is not specific to the spring/summer 2005 and 2006 and is observed every year over the 1998-2008 period of study (not shown). However, their impact on SST variability in the region is modulated depending on the strength of wind intensification and of the subsurface preconditioning. For example, the year 1998, known as a ”warm year”, is characterized by anomalous warm SST in boreal spring/summer in the CLR., associated with anomalous weak winds and anomalous deep thermocline.”

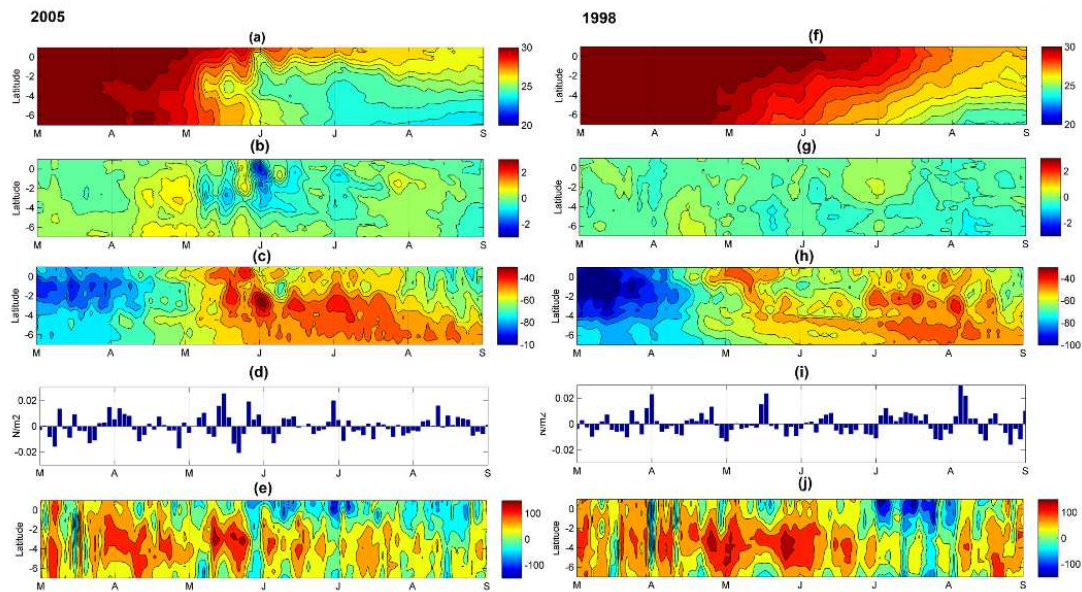


Figure X1: (a & f) Latitude-time diagram of 2-daily SST (°C) ; (b & g) intraseasonal variations of SST (°C); (c & h) intraseasonal variations of wind stress; (d & i) 20°C-isotherm depth ; (e & j) surface heat flux; from 1st March to 31 August 2005 (left panels) and 1998 (right panels) and averaged from 5°E to 12°E. The intraseasonal variations are computed by remove the 30 days low-pass filtered field to the total field.

2. RC: Also, it is not clear whether the processes discussed in section 4 and 5 are specific to 2005 or whether some of them play a role in every spring cooling and/or other interannual cold events as well. In other words: Do intraseasonal wind bursts impact SST in the Cape Lopez region in every summer or during every interannual cold event or just in very specific years as 2005?

AC: The comparison with 2006, considered as a “normal” year, precisely shows that the intraseasonal wind bursts also occur in spring/summer during normal conditions and that is not a particularity of the year 2005. However, in 2005, there are successive strong wind bursts in April-May combined with favorable subsurface conditions (shallow thermocline) due to the arrival of Kelvin wave, that make the cooling more efficient than in 2006 and which occurs earlier than usual. In order to clarify this point in the text, some lines have been added in the conclusion as mentioned in response to the previous question.

3. RC: Related to point 1 and 2, the time scales discussed tend to get mixed up a bit. The relationship between the intraseasonal wind bursts, the seasonal cycle of SST, and interannual variations should be sorted out more clearly.

AC & MC: In order to sort out the different times scales more clearly, we decide to show the interannual component of SST/winds/vertical current shear/Ekman pumping variability on figure 4, by removing the 30-days low-pass filtering to the annual time series. An effort has been made in the text in order to describe more clearly the time scales studied. In addition, some lines have added in section 4.3 (“Westward extension of the CLR cooling”) about the climatological behavior of the connection between CLR and equatorial region and the particularity of the year 2005.

Response to Specific comments:

1. RC: I am missing a motivation on why the Cape Lopez region is of interest.

AC: The initial reason that motivates the study of the SST variability in the Cape-Lopez region is the observation in satellite SST data of cold coastal waters independent from those observed off shore in the cold tongue region around 10°W (see the map of satellite SST data for the 8 June 2005 shown on the Figure X2) which raises the question of the link of such cooling with the cold tongue development.

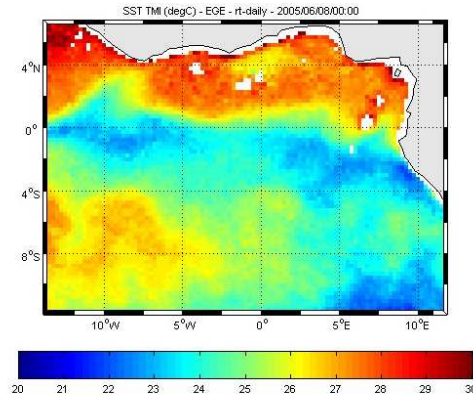


Figure X2: SST (°C) from TMI satellite data on 8 June 2005.

The equatorial region and the processes implied in the cold tongue development are largely studied contrary to the Cape-Lopez region. Other several studies focus on SST variability in more southern region such as Angola-Benguela front, but very few in the Cape-Lopez region. However, we thought that better describe the SST variability in the Cape-Lopez region is needed and interesting especially because of the numerous processes in play notably due to the presence of the coast and the proximity of the equator. In addition, some studies (such as DeCoëtlogon et al., 2010) suggest that at short time scale (a few days), more than half of the cold SST anomaly around the equatorial cooling could be explained by horizontal oceanic advection controlled by the winds. Therefore, a better understanding of the SST variability in the CLR may also help to better understand the SST variability in the equatorial region.

MC: Some lines have been added in the Introduction:

“The question of the processes implied in the SST variability in the Cape-Lopez region was raised based on an observation in satellite SST data of cold coastal waters during spring independent from those observed off shore in the cold tongue region around 10°W which also raised the question of the link of such cooling with the cold tongue development.” [...] “In addition, some studies (such as DeCoëtlogon et al., 2010) suggest that at short time scale (a few days), more than half of the cold SST anomaly around the equatorial cooling could be explained by horizontal oceanic advection of upwelled cold coastal waters controlled by the winds. Therefore, a better understanding of the SST variability in the CLR may also help to better understand the SST variability in the equatorial region.”

2. RC: Related to comment (3) above, the time scales of interest should be specified somewhere in the beginning, and it should be stated whether the data were filtered or averaged over time to focus on them individually.

AC: In order to isolate the interannual component, we removed the low-pass filtering (cutoff frequency of 30 days) of the annual time series to the total field.

MC: As suggested, we have added this information in the text, in Sect. 2:

“Note that throughout the whole text and figure captions, the term “intraseasonal variations” is used to designate the field obtained after the removing of the 30 days low-pass filtered field to the total field of the given year, while “intraseasonal anomaly” refers to the field obtained after the removing of the 30 days low-pass filtered field averaged over 1998-2008 to the total field of the given year.”

3. RC: line 184/185: The highest temperatures occur more towards boreal spring than winter.

AC & MC: Thank you for the remark. Indeed, the highest temperatures occur at the end of March, i.e. at the late of boreal winter and the beginning of boreal spring. The text has been modified accordingly.

4.RC: line 188/189: I think all of the references given here discuss biases in coupled climate models while in this study an ocean-only model is used.

AC: Thanks to point this.

MC: The phrase line 188/189 has been changed as following:

“Despite a warm bias ($\sim 1^{\circ}\text{C}$) compared to satellite observations, the model pretty well reproduces the satellite pattern. While this warm bias in the eastern tropical Atlantic is well known in coupled climate models (e.g. Zeng et al., 1996; Davey et al., 2002; Deser et al., 2006; Chang et al., 2007; Richter and Xie, 2008), results from Large and Danabasoglu (2006) show that a warm SST bias may also be present along the Atlantic coast of southern Africa in forced ocean-only simulation.”

5. RC: lines 200-202: A number of previous studies have shown this and could be cited (e.g. Schouten et al., 2005).

AC: Thank you for point this.

MC: Reference has been added as following (section 3):

“The region is also characterized by a shallow thermocline which depicts a strong semi-annual cycle (Fig. 1d). The evolution of z_{20} reveals a shoaling of the thermocline during May-July and a deepening up to October-November when it exhibits a maximum depth, in agreement with previous studies such as the one realized by Schouten et al. (2005) who find a similar seasonal cycle from SSH altimetric data.”

6. RC: It is hard to directly compare the conditions in 2005 and 2006 as they are presented in different figures (Fig. 3 and 4) on different pages of the manuscript. I would suggest to combine those figures. Also, the individual dates given in the text (e.g. lines 231 to 233, lines 257 to 259) are impossible to identify in these figures and should be illustrated in a different way.

AC: The choice to separate 2005 and 2006 has been made to highlight the correlation between the different fields.

MC: In order to have better clarity, we decided to show the total field of SST and 20°C-isotherm depth for 2005 and 2006 on Figure 3 and the intraseasonal variations (by removing the 30-days low-pass filtered data from the total field) of SST/wind/vertical current shear/Ekman pumping for 2005 and 2006 on the same Figure 4, in order to better highlight the intraseasonal events. In addition, we have made a zoom on March-August period for better visibility of the events.

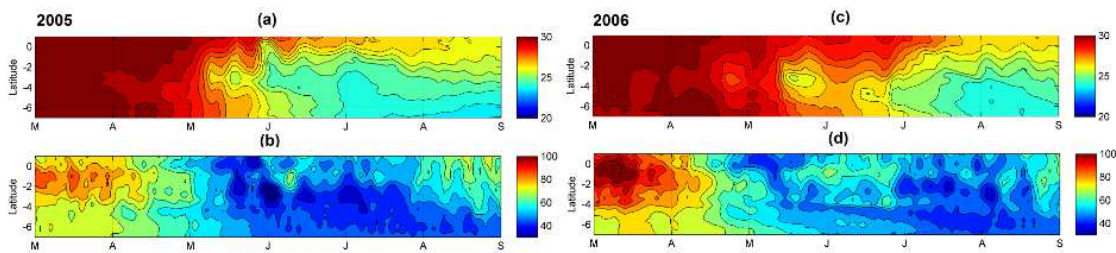


Figure 3: (a & c) Latitude-time diagram of the sea surface temperature ($^{\circ}\text{C}$); (b & d) Latitude-time diagram of the 20 $^{\circ}$ C-isotherm depth (m); from 1st March to 31 August 2005 (left panels) and 2006 (right panels) and averaged between 5 $^{\circ}$ E and 12 $^{\circ}$ E.

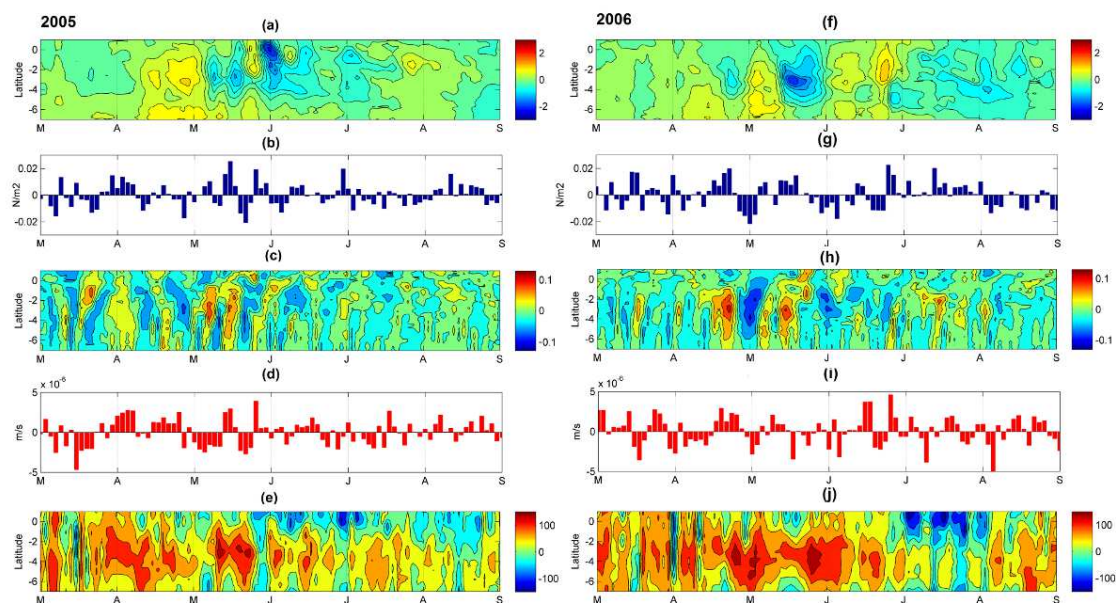


Figure 4: (a & f) Time-latitude diagram, from 7° S to 1° N, of the intraseasonal variations of sea surface temperature (in °C) averaged between 5° E and 12° E; (b & g) Time evolution of the intraseasonal variations of wind stress amplitude (N.m^{-2}) averaged between 5° E and 12° E and between 3° S and 0° S; (c & h) Latitude-time diagram of the intraseasonal variations of the maximum of the current vertical shear magnitude (m.s^{-1}) averaged between 5° E and 12°E; (d & i) Longitude-time diagram of the intraseasonal variations of Ekman Pumping (m.s^{-1}) averaged over the CLR. Ekman pumping values >0 indicate upwelling; (e & j) Latitude-time diagram of the net heat flux (W.m^{-2}) averaged between 5° E and 12° E; from 1st March to 31 August 2005 (left panels) and 2006 (right panels). For details about calculations of intraseasonal variations, see Sect. 2.

Modifications have also been made on the plot of 20°C-isotherm depths, Fig.3 : weaker values of 20°C-isotherm depths indicate shallower thermocline to be consistent with the modifications made on the Fig.1, Fig.5, Fig. 9, Fig. 7 and Fig. 13 (Fig 12 in revised version).

7.RC: lines 254/255: Are the data filtered to focus on the intraseasonal time scale? (see comment above)

AC: Yes, the wind stress magnitude field shown on Figure 4 has been obtained after remove the low-pass filtering (cutoff frequency of 30 days) to the total field (see the modified Figure 4 in the response of the previous question).

MC: Indications about how the calculations have been made for each figure have been added in the text, in Section 2 : *“Note that throughout the whole text and figure captions, the term “intraseasonal variations” is used to designate the field obtained after the removing of the 30 days low-pass filtered field to the total field of the given year, while “intraseasonal anomaly” refers to the field obtained after the removing of the 30 days low-pass filtered field averaged over 1998-2008 to the total field of the given year.”*

8. RC: line 336: How did the timing of the preconditioning impact the intensity of the cooling?

AC: In 2005, the arrival of the upwelling Kelvin wave in CLR brings the thermocline close to the surface that makes the wind burst, which occurs simultaneously, more efficient in cooling the SST. As explained in line 336, stronger wind intensification and simultaneously favorably preconditioned oceanic subsurface conditions, made the coupling between surface and subsurface ocean processes more efficient than in 2006, resulting in stronger cooling.

9. RC: Fig. 7 and Fig. 10 are very small and thus hard to read.

AC & MC: The Figure 7 has been modified and zoomed over January-June. The Figure 10 has been also modified and the wind and precipitation pattern have been separated for more visibility.

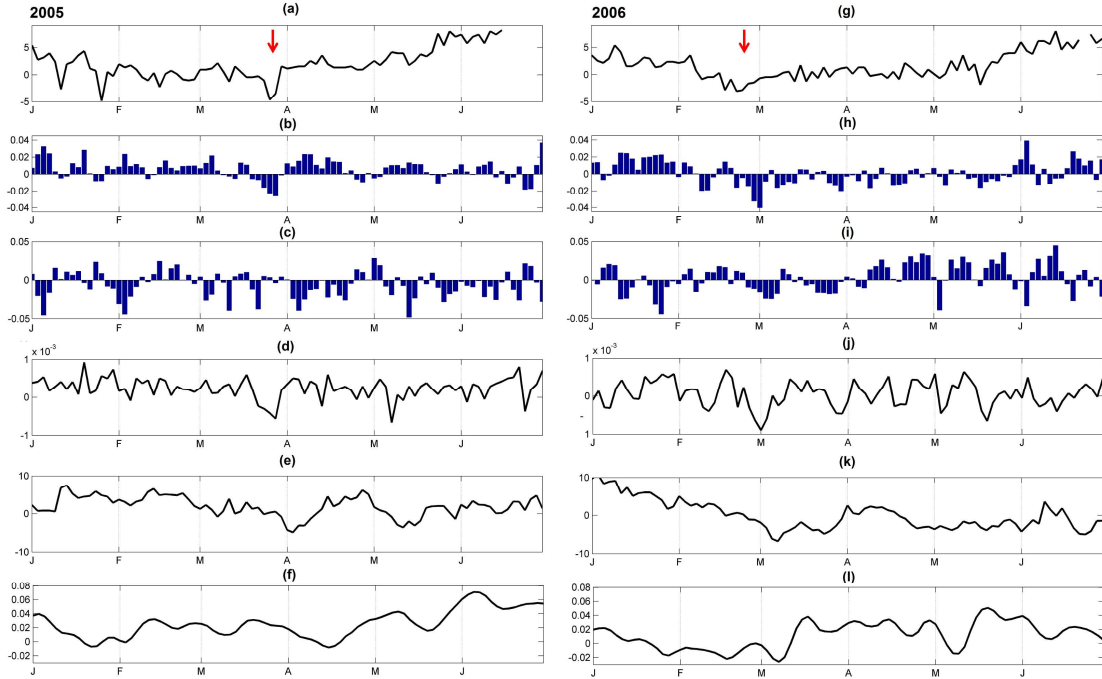


Figure 7: Time evolution, from 2-days averaged model outputs over Jan-June 2005 (left) and Jan-June 2006 (right); of (a & g) the position (in latitude, between 5° S and 10° N) where the meridional wind stress value equal zero (indicator of the position of the ITCZ); (b & h) the intraseasonal anomaly of the meridional wind stress (N.m^{-2}) averaged between 50° W and 35° W and between 1° S and 1° N; (c & i) same as (b & h) but for intraseasonal anomaly of zonal wind stress (N.m^{-2}); (d & j) the intraseasonal anomaly of the wind stress curl (N.m^{-2}); (e & k) the intraseasonal anomaly of the 20° C isotherm depth (m); (f & l) the intraseasonal anomaly of the sea level (m). The red arrow in (a & g) indicates the southward shift of the ITCZ before the excitation of the Kelvin wave (see text). For details about the calculations of anomalies, see Sect. 2

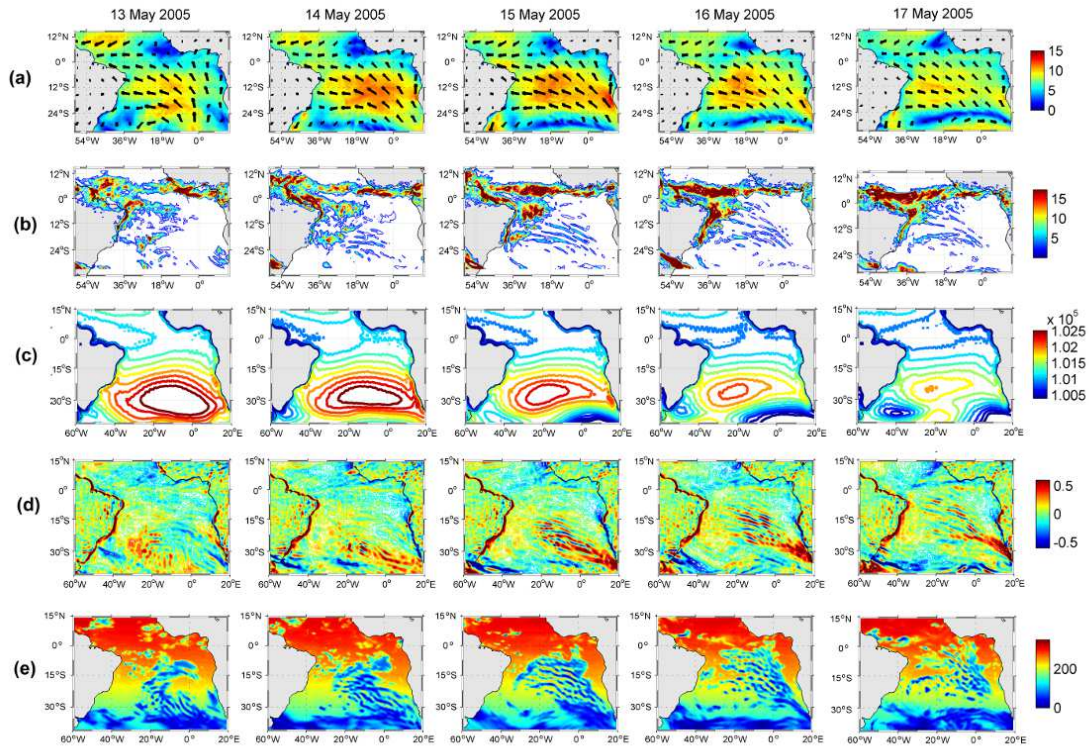


Figure 10: Daily-averaged, from 13 May to 17 May 2005 (left to right panels), of (a) the precipitation rate ($\text{kg}\cdot\text{m}^{-2}/\text{day}$); (b) the wind speed vectors superimposed with wind magnitude ($\text{m}\cdot\text{s}^{-1}$) from CFSR fields; (b) the surface pressure (hPa) from ERA-20C reanalysis; (c) the wind speed curl ($\text{m}\cdot\text{s}^{-1}$) computed from CFSR wind speed fields; and (d) the downward short-wave radiation ($\text{W}\cdot\text{m}^{-2}$) from CFSR fields.

10. RC: Section 5.2: You mention in the introduction that the monsoon onset happened early in 2005, but this information should be repeated in this section.

AC & MC: The following sentences have been added as an introduction of the section 5.2.:
“The mid-May 2005 wind event was found to be involved in the early onset of the ACT development (Marin et al. 2009, Caniaux et al., 2011). The influence of the cold tongue on the WAM onset has been suggested by several authors (Okumura and Xie, 2004; Caniaux et al., 2011; Nguyen et al., 2011; Thorncroft et al., 2011). At the seasonal time-scale, Caniaux et al. (2011) suggest that it comes from strong interactions between the SST cooling and wind pattern in the eastern equatorial Atlantic: the ACT serves to accelerate (decelerate) winds in the northern (southern) hemisphere contributing to the northward migration of humidify and convection, and pushes precipitation to the continent. Thus, due to its impact on ACT development, the mid-May wind event is also linked to the onset of the WAM in 2005 which has been the earliest over 1982-2007 period from Caniaux et al. (2011). In this section we aim to better understand how this single wind event may have such impact. For further

information on the WAM, the reader can refer to Leduc-Leballeur et al. (2013) and Caniaux et al. (2011).”

11. RC: Fig. 13 looks rather strange because of the discontinuities between May of one and April of the next year. Maybe you could separate the years more clearly with vertical black lines.

AC & MC: Vertical black thick lines have been added and the figure 13 has been modified for more clarity.

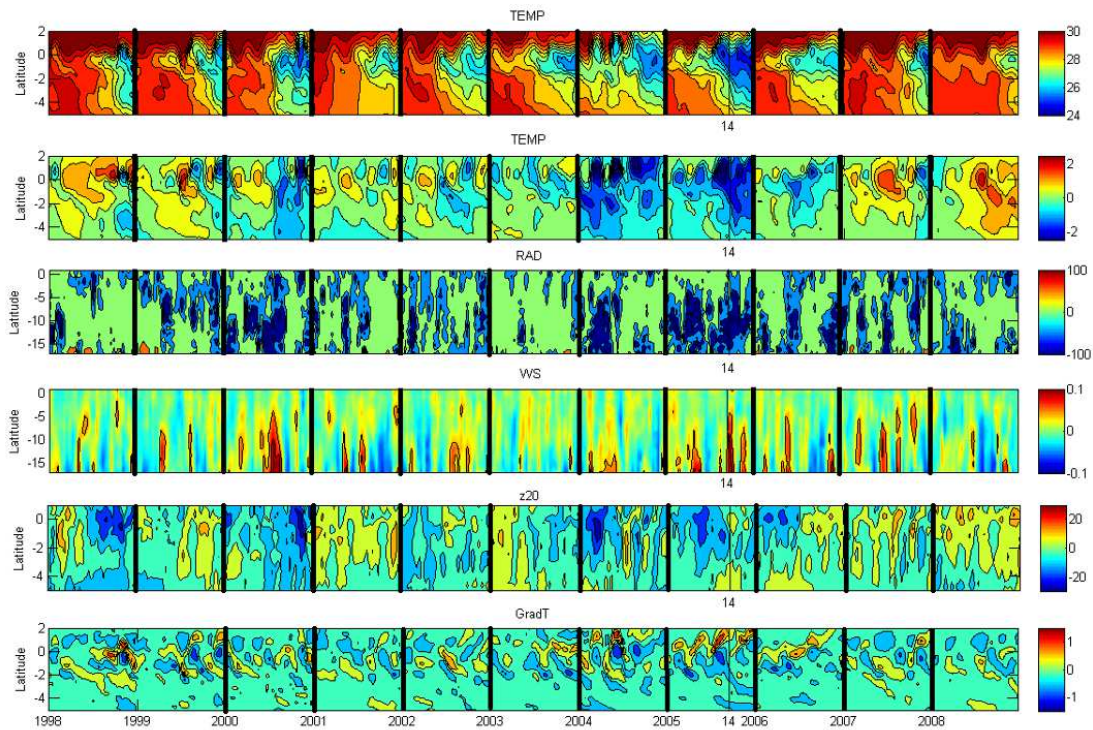


Figure 13 (“Figure 12” in the revised manuscript): Time-latitude diagrams for April-May along the 1998-2008 period, of 2-days average, from top to bottom i) SST (°C); ii) intraseasonal anomaly of SST (°C); , iii) intraseasonal anomaly of wind stress magnitude ($N.m^{-2}$) from CFSR fields; iv) intraseasonal anomaly of short-wave radiation surface flux ($W.m^{-2}$) from CFSR fields; v) intraseasonal anomaly of 20°C-isotherm depth (m) computed from the forced model SST; vi) intraseasonal anomaly of meridional SST gradient (every 0.5° of latitude), from the forced model; averaged over 10° W-6° W. The vertical black thin line indicates the date of 14 May, 2005. For details about the calculations of the anomalies, see Sect. 2.

Modifications have also been made on the plot of 20°C-isotherm depths : weaker values of 20°C-isotherm depths indicate shallower thermocline to be consistent with the modifications made on the Fig.1, Fig.3, Fig.5, Fig. 9 and Fig. 7.

12. RC: Instead of Fig. 14 a and b, I would suggest to show a map of the surface pressure for May 2005. The time series can then highlight that the pressure gradient was special.

AC: Thank you for the suggestion. In fact, maps of the surface pressure from May 13 to May 17 2005 are already shown on figure 10.

MC: We decided to remove the figure 14 and to modified the comments of the figure 10 about the surface pressure as following (section 5.1.1) :

“The strong winds during the event were associated with high pressure core of the Saint Helena Anticyclone, especially on 13-14 May, also associated with particularly low pressure under the ITCZ 4 days later (Fig. 10c). The pressure fall during the mid-May 2005 event appeared as the lowest in May over the whole decade (not shown). The meridional surface pressure gradient during the event is thus found to be the strongest over 1998-2008 period. That suggests strong Hadley circulation intensity during the mid-May event and therefore strong equatorward moisture flux, allowing the deep atmospheric convection in the Gulf of Guinea to be triggered at a self-sustaining level, as previously described in Sect. 5.2.”

13. RC: Please check that the figures are numbered in the order in which they are referenced in the text.

AC: Thanks, this was checked.

RC: Fig.1: I would suggest to plot the line for 2005 on top of the other lines as it is very hard to see. It would also be helpful to plot a larger area in the maps on the right hand side. What are the vectors shown in Fig.1b and Fig.1c ?

AC & MC: Thanks for suggestions. The modifications have been made (see Fig.1). The vectors shown in Fig.1b and Fig.1c are respectively the wind vectors and the surface current vectors. The indications have been added in the legend. In addition, modifications have been made on the plot of 20°C-isotherm depth: weaker values of 20°C-isotherm depth indicate shallower thermocline to be consistent with the modifications made on Fig.3, Fig.5, Fig.7, Fig. 9, and Fig. 13 (Fig. 12 in revised version).

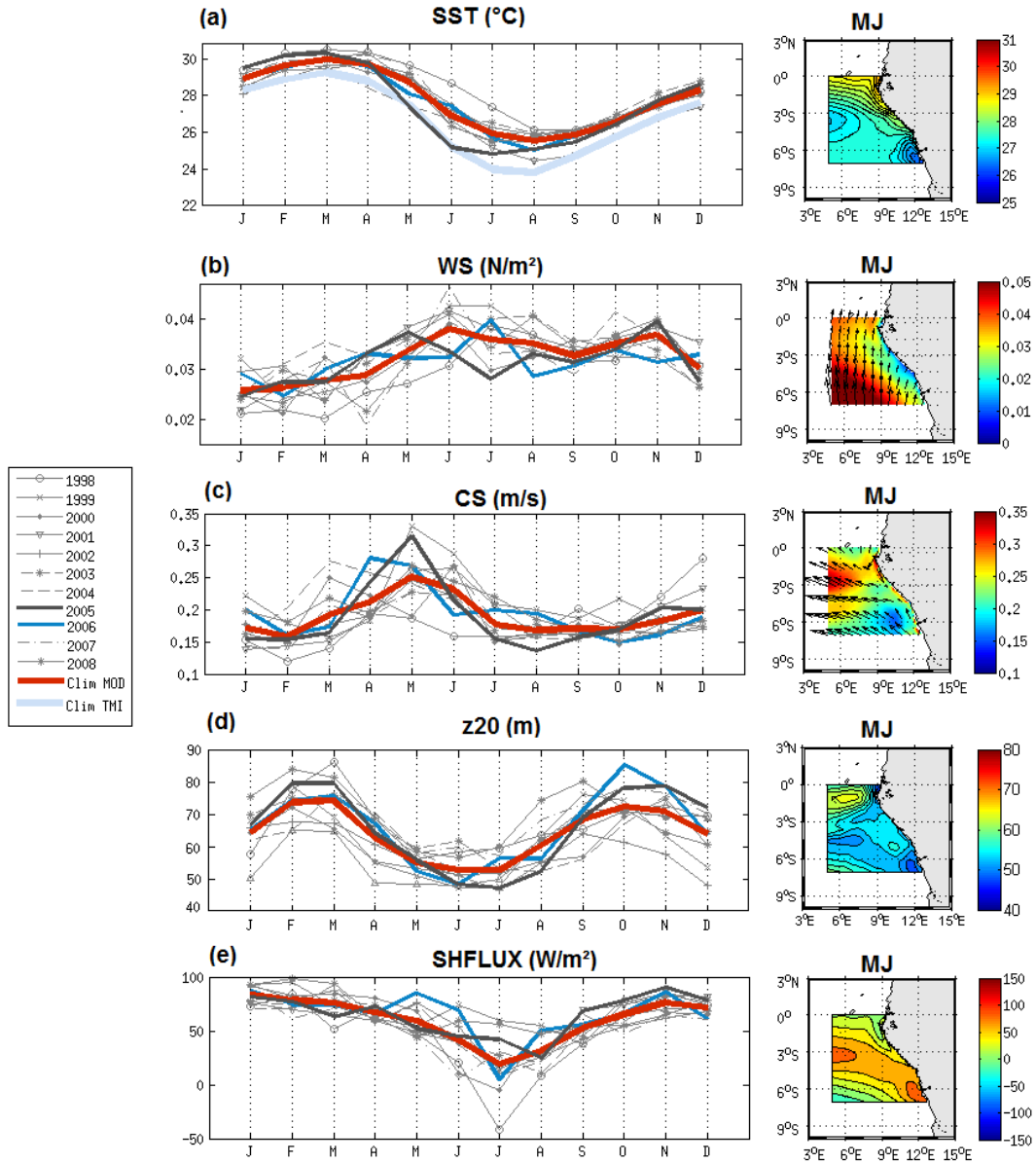


Figure 1: Monthly average of the (a) sea surface temperature ($^{\circ}\text{C}$); (b) wind stress direction (vectors) and magnitude (color field) ($\text{N}\cdot\text{m}^{-2}$); (c) horizontal surface current direction (vectors) and speed (color field) ($\text{m}\cdot\text{s}^{-1}$); (d) 20°C -isotherm depth (m); and (e) surface heat flux ($\text{W}\cdot\text{m}^{-2}$; positive values indicate downward flux) from January to December from 1998 to 2008 and for the climatology (averaged over 1998-2008) simulated by the model (red curve) and from the observations : monthly average TMI 3-daily SST data (light blue curve in (a)); averaged over 5°E - 14°E and 7°S - 0°S . Right panel: maps of each variable over May-June.

RC: Fig.5 : I would suggest to use red for deeper and blue for shallower thermocline to be consistent with SST.

AC& MC: Thanks for suggestion. The modifications have been made on Fig. 1, Fig.3, Fig. 5, Fig. 9, Fig. 7, and Fig. 13 (Fig 12 in revised version).

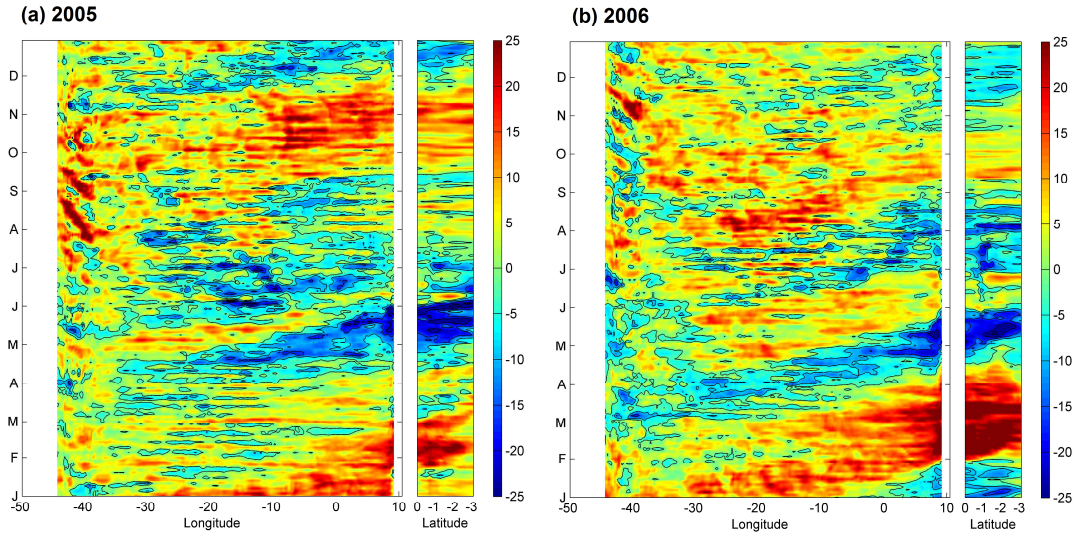


Figure 5: Time evolution of the intraseasonal anomaly of 20° C-isotherm depth (m) along the equator (between 54° W and 12° E) and along 9° E (between the equator and 3° S) for 2005 (left) and 2006 (right). Negative values indicate a 20°C isotherm depth closer to the surface. For details about calculations of the anomalies, see Sect. 2.

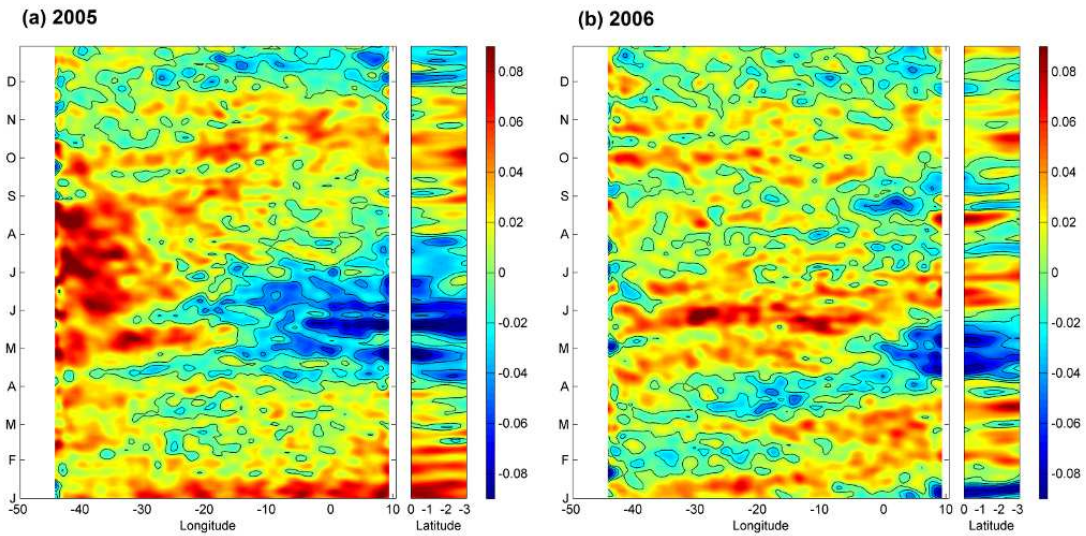


Figure 6: Time evolution of the sea level anomaly (m) along the equator (between 54° W and 12° E) and along 9° E (between the equator and 3° S) for 2005 (left), and 2006 (right) from AVISO data.

Additional authors' comments: Thanks a lot for the technical notes. The corrections have been made in the text.

Authors' response to Referee 2

Journal: Ocean Sciences

Title of paper: Impact of intraseasonal wind bursts on SST variability in the far eastern Tropical Atlantic Ocean during boreal spring 2005 and 2006. Focus on the mid-May 2005 event.

Authors: Herbert Gaëlle, Bourlès Bernard.

We thank Reviewer 2 for his comments and suggestions that allowed improvements of our paper. We have made all needed information to make the figures more understandable and conforming with general publications criteria (figures size, labels, etc). We also worked to make the manuscript easier to read and understand, by adding some information and removing others. The abstract has been also modified taking into account the reviewer's comments (the sentence about the NE Brazil has been removed and some words about the West African Monsoon have been added).

RC: Referee's comment; **AC:** Authors' comment; **MC:** Manuscript changes

Response to specific Comments

1. RC: I wonder for many of the plots, especially when discussing the May 2005 event, if it would be better to plot the difference from the climatological mean (an anomaly). It might make the 2005 event stand out. As the figures are, it is difficult to tell that this event is different from some of the other events in the 1998-2005 range.

AC: Thanks for the suggestion. Indeed, plot the anomalies allow to better identify the particularity of the mid-May 2005 event.

MC: We have modified the figure 13, enlarged it and the 30-days low-filtered data averaged over 1998-2008 period has been removed to each total field except for the first panel where the SST is shown. In addition, black thick lines have been added to separate each year.

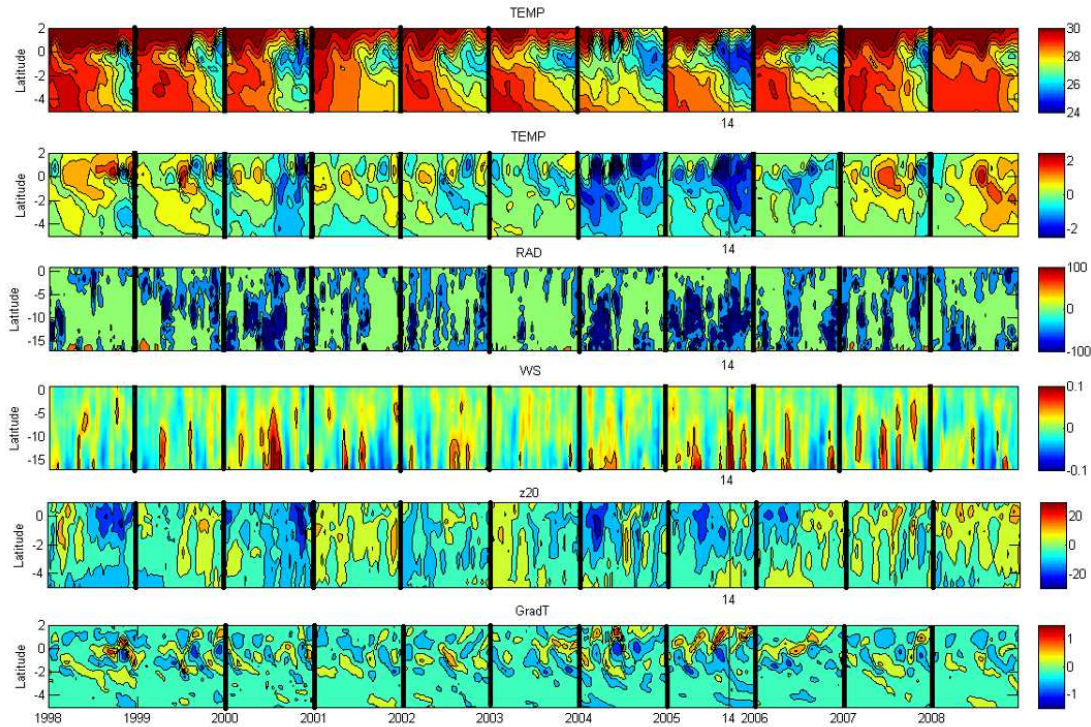


Figure 13 (“**Figure 12**” in the revised manuscript): Time-latitude diagrams for April-May along the 1998-2008 period, of 2-days average, from top to bottom i) SST (°C); ii) intraseasonal anomaly of SST (°C) ; iii) intraseasonal anomaly of wind stress magnitude (N.m^{-2}) from CFSR fields; iv) intraseasonal anomaly of short-wave radiation surface flux (W.m^{-2}) from CFSR fields; v) intraseasonal anomaly of 20°C -isotherm depth (m) computed from the forced model SST; vi) intraseasonal anomaly of meridional SST gradient (every 0.5° of latitude), from the forced model; averaged over 10°W - 6°W . The vertical black thin line indicates the date of 14 May, 2005. For details about the calculations of the anomalies, see Sect. 2.

Modifications have also been made on the plot of 20°C -isotherm depths : weaker values of 20°C -isotherm depths indicate shallower thermocline to be consistent with the modifications made on the Fig. 1, Fig.3, Fig.5, Fig7 and Fig. 9.

2. RC: For all figures, it would be helpful to increase the fontsize for the x and y-axis labels. The figures are very difficult to read.

AC: Thanks for this suggestion. Modifications have been made.

3. RC: It is unclear in the different sections whether the region being discussed is the Cape Lopez region, the equatorial Gulf of Guinea, or the western part of the basin. One confusing discussion revolves around the wind bursts. They are sometimes discussed in the Cape Lopez region associated with southerly winds and sometimes in the western

basin as westerly wind bursts associated with Kelvin and Rossby waves. The text mostly just says “wind burst” so it’s difficult to tell which is being referenced.

AC: Thanks for the remark. Indeed, in the first part of the paper we focused on the Cape-Lopez-region and then extend the analysis at more global scale when we focused on the mid-May wind event.

MC: For greater clarity, “wind bursts” has replaced by “southerly wind bursts” when they are discussed in the Cape-Lopez region and by “easterly wind bursts” when they are discussed in the western part of the basin.

4. RC: On line 13, you say “some particular events iii) a decrease of incoming surface shortwave radiation,” but in fact, you only described one event this applied to (May 2005). This can be fixed by changing the word “some” to “one.”

AC: Thanks for the remark. In fact, another event occurs in spring 2006 (on 2 April).

MC: Thus, we included the description of this event in the comments of Figure 4: *“A strong net cooling (-30 W.m^{-2}) occurred during the 26-28 May 2005 event. It was mainly due to a sudden decrease of incoming surface short wave radiation (drop of about 80 W.m^{-2} in the CLR between 22 and 28 May; not shown) suggesting increased cloud cover. Another strong net cooling occurred on 2 April 2006 with a mean value in the CLR reaching -95 W.m^{-2} . It is more sudden than the end-May 2005’s one, and was almost exclusively restricted to the CLR region with values reaching locally -185 W.m^{-2} (not shown). For both events, the net cooling did not concern the equatorial region west of 0°W .”* Thus, the sentence in the abstract has not been changed.

5. RC: Many times in the paper, a season (spring, etc.) is discussed. Please indicate boreal or austral.

AC & MC: “spring” has been replaced by “boreal spring”.

6. RC: The paper discusses connections between the South Atlantic and the Cape Lopez region, specifically in relation to the St. Helena Anticyclone. A paper by Bates (J. Clim., 2008) discusses an anomalous low pressure originating in the South Atlantic that migrates northeast-ward, influencing the Southern Trade Winds and thus affecting SST in the Cape Lopez region (though she refers to it as coastal Angola). I don’t know if the feature you discuss and the feature she discusses are the same thing. Papers by Bohua Huang and others at the Center for Ocean Land Atmosphere Studies from the

2000s time range also discuss variability in the South Atlantic. You may want to reference these papers if they would add something to your discussion. That is up to the authors to decide.

AC: Thanks for this suggestion. Indeed, Bates et al. (2008) show that the patterns of variability in the coastal Angola region is related to fluctuations in the southeast trade winds through two mechanisms: i) Bjerknes mechanism and ii) variability in subtropical high in South Atlantic. The phenomenon which is at work during May 2005 event related to anomalous strong St Helena Anticyclone, may correspond to the inverse feature that they describe (anomalous low pressure originating in the South Atlantic that migrates northeastward, affecting the SST in coastal Angola region with a peaking SST anomalies by approximately 4 months), but at smaller time scale.

7. RC: Because you discuss the NE coast of Brazil and the West African Monsoon, it would be nice to have them documented in the seasonal variability section to show how they fit into the normal seasonal cycle.

AC: Thanks for the suggestion. However, the NE coast of Brazil is only mentioned in Section 5.1.2 when we describe the anomalous precipitation pattern associated with the mid-May event (early SICZ development linked to the anomalous early development of the equatorial cold tongue). We have thus noted that “This convective zone, located between the ITCZ north of the equator and the South Atlantic Convergence Zone (SACZ) in southern tropics, is the Southern Intertropical Convergence Zone (SICZ) (Grotsky and Carton, 2003). This zone forms usually later, by June-August, when the southern branch of the convection separated from the ITCZ which moves north of the equator.”

Thus, it appears to us not necessary to add other information about seasonal variability in this area. More detailed information about ‘normal’ precipitation conditions in this area can be found in Grotsky and Carton (2003).

About the West African Monsoon, the important point for 2005 is the particularly early onset date, as reported by several authors (such as Caniaux et al. (2011)) associated with the particularly early development of the equatorial cold tongue. The role of the mid-May event in this phenomenon is explained in Section 5.2. We think that it is not necessary to describe more in details the seasonal variations of the West African Monsoon. If the reader needs to have more information about the coastal onset phase of the monsoon in the Gulf of Guinea, he can refer to Leduc-Leballeur et al. (2013), as cited in the text (section 5.2).

MC: However, we added these sentences as introduction of the section 5.2:

“The mid-May 2005 wind event was found to be involved in the early onset of the ACT development (Marin et al. 2009, Caniaux et al., 2011). The influence of the cold tongue on the WAM onset has been suggested by several authors (Okumura and Xie, 2004; Caniaux et al., 2011; Nguyen et al., 2011; Thorncroft et al., 2011). At the seasonal time-scale, Caniaux et al. (2011) suggest that it comes from strong interactions between the SST cooling and wind pattern in the eastern equatorial Atlantic: the ACT serves to accelerate (decelerate) winds in the northern (southern) hemisphere contributing to the northward migration of humidity and convection, and pushes precipitation to the continent. Thus, due to its impact on ACT development, the mid-May 2005 wind event is also linked to the onset of the WAM in 2005 which has been the earliest over 1982-2007 period from Caniaux et al. (2011). In this section we aim to better understand how this single wind event may have such impact. For further information on the WAM, the reader can refer to Leduc-Leballeur et al. (2013) and Caniaux et al. (2011).”

8. RC: When discussing the thermocline, do you mean shoaling instead of thinning and deepening instead of thickening? You also mention on line 202 that it is at a minimum, I believe you mean “minimum depth.”

AC: Thanks for pointing this. Indeed, when we say “thinning” we mean “shoaling” and when we say “thickening” we mean “deepening”. “minimum” is indeed used for “minimum depth”. However, following other comments, we modified the sign of z20, therefore, in the modified Fig. 1 the z20 values are positive.

MC: Thus, the related sentence has been modified as follows (section 3):

“The region is also characterized by a shallow thermocline which depicts a strong semi-annual cycle (Fig. 1d). The evolution of z20 reveals a shoaling of the thermocline during May-July and a deepening up to October-November when it exhibits a maximum depth, in agreement with previous studies such as the one realized by Schouten et al. (2005) who find a similar seasonal cycle from SSH altimetric data “

9. RC: Figure 1 has no scale for the wind speed.

AC: In fact, the colorbar at the right of the May-June averaged map indicates the scale for the wind stress magnitude.

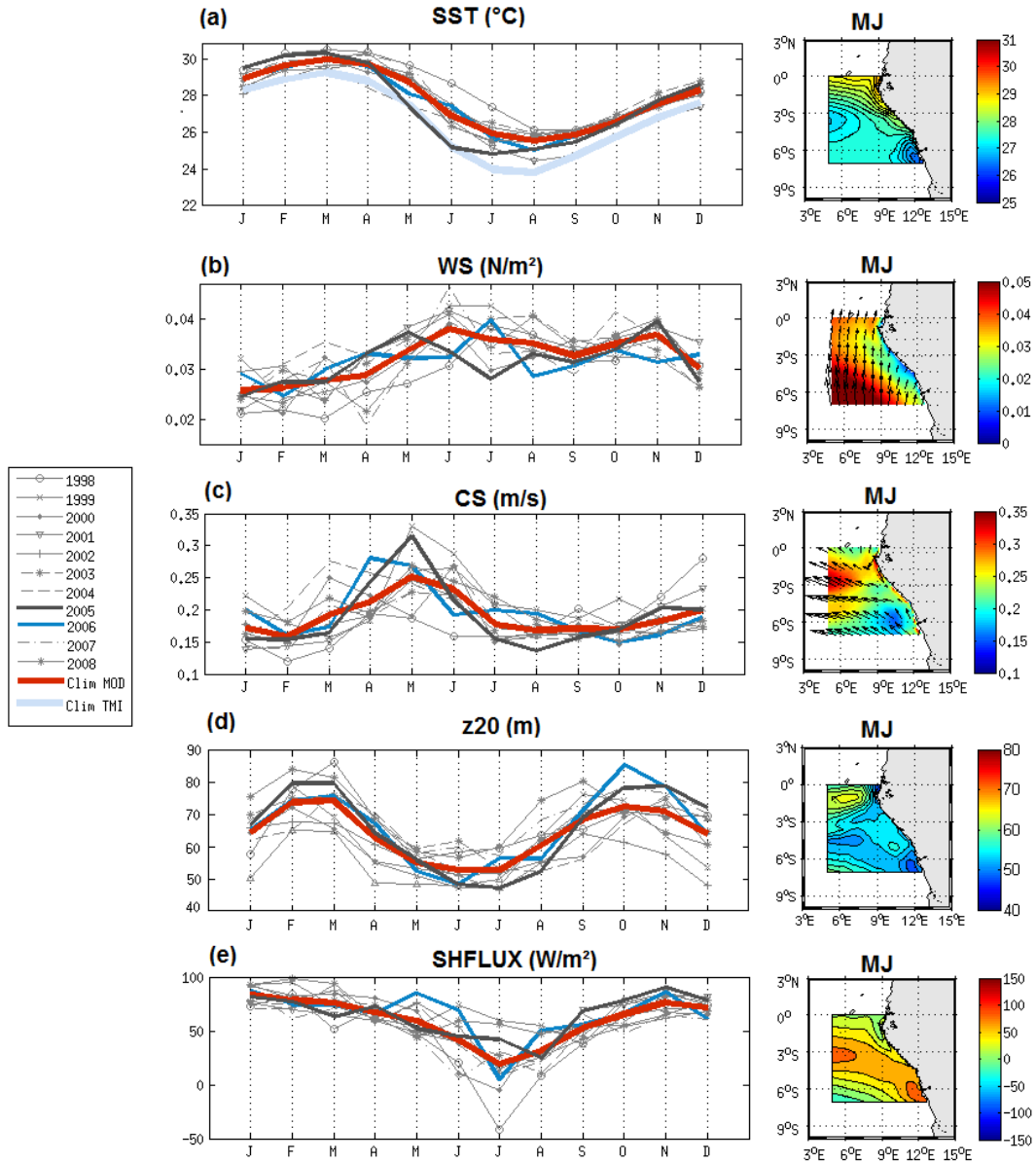


Figure 1: Monthly average of the (a) sea surface temperature ($^{\circ}\text{C}$); (b) wind stress direction (vectors) and magnitude (color field) ($\text{N}\cdot\text{m}^{-2}$); (c) horizontal surface current direction (vectors) and speed (color field) ($\text{m}\cdot\text{s}^{-1}$); (d) 20°C -isotherm depth (m); and (e) surface heat flux ($\text{W}\cdot\text{m}^{-2}$; positive values indicate downward flux) from January to December from 1998 to 2008 and for the climatology (averaged over 1998-2008) simulated by the model (red curve) and from the observations : monthly average TMI 3-daily SST data (light blue curve in (a)); averaged over 5°E - 14°E and 7°S - 0°S . Right panel: maps of each variable over May-June.

MC: In addition, modifications have been made on Fig. 1:

- weaker values of 20°C -isotherm depth indicate shallower thermocline to be consistent with the modifications made on Fig.3, Fig.5, Fig.7, Fig. 9, and Fig. 13 (Fig. 12 in revised version).

- May-June averaged maps have been enlarged to better locate the CLR.

10. RC: I don't think your discussion of Figure 1d on lines 203-205 reflect what is seen in the plot.

AC: Do you mean "Figure 1e" rather than Figure 1d ? Because the Figure 1d is discussed on lines 200-202 and not on lines 203-205. For the discussion of Figure 1e, the text has been modified as indicated in our response to the question 8.

11. RC: When you discuss the surface heat flux, please designate whether it is positive downward (into the ocean) or upward (out of the ocean).

AC & MC: The sentence "positive values indicate downward flux" has been added in the legend of Fig.1.

12. RC: The individual events mentioned on line 232 are difficult to see. Maybe only plot April-July or change the y-axis.

AC: Thanks for the suggestion.

MC: The figures 3 and 4 have been modified in this sense (plot over March-August only). In addition, the intraseasonal variations (removing of the 30 days low-pass filtered field to the total field) of SST/wind stress magnitude/vertical current shear/Ekman pumping are shown on Figure 4 in order to better highlight the intraseasonal events. Modifications have also been made on the plot of 20°C-isotherm depth: weaker values indicate shallower thermocline to be consistent with the modifications made on Fig.1, Fig.5, Fig.7, Fig. 9, and Fig. 13.

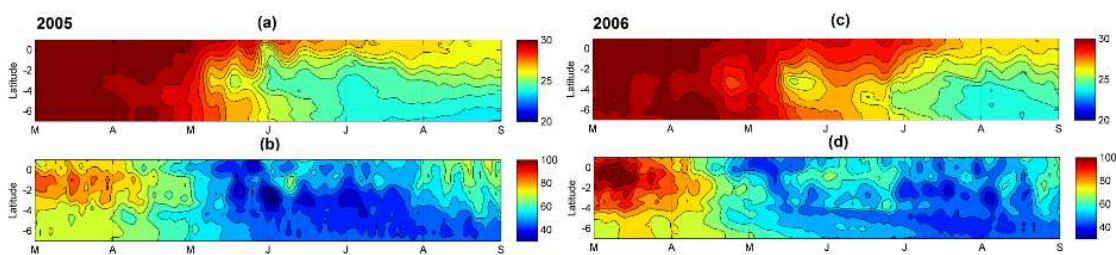


Figure 3: (a & c) Latitude-time diagram of the sea surface temperature (°C) averaged between 5°E and 12°E; (b & d) Latitude-time diagram of the 20° C-isotherm depth (m) averaged between 5° E and 12° E; from 1st March to 31 August 2005 (left panels) and 2006 (right panels).

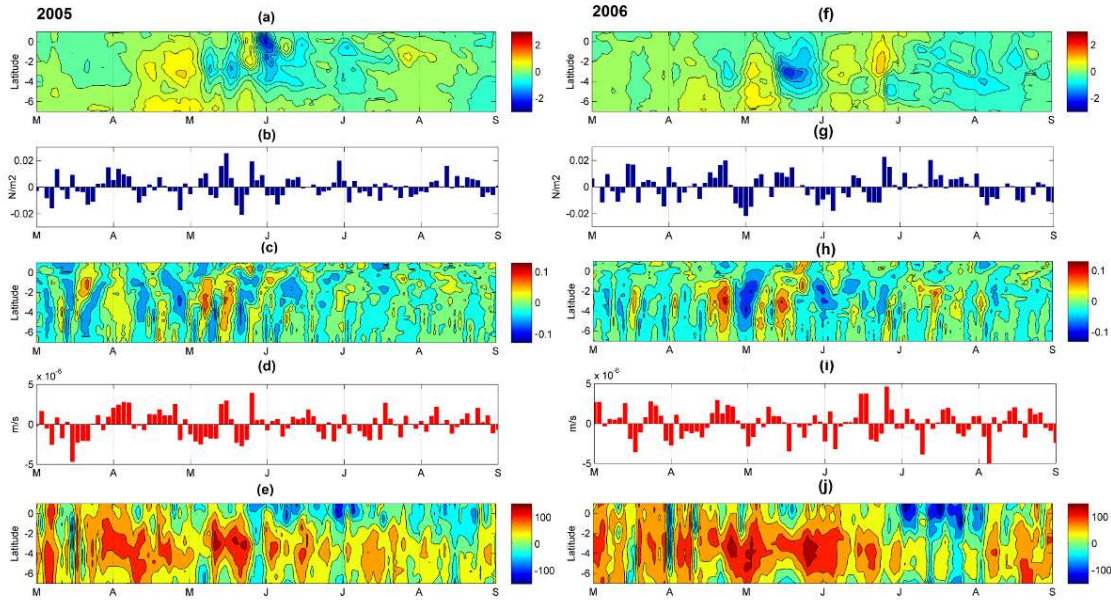


Figure 4: (a & f) Time-latitude diagram, from 7° S to 1° N, of the intraseasonal variations of sea surface temperature (in ° C) averaged between 5° E and 12° E; (b & g) Time evolution of the intraseasonal variations of wind stress amplitude (N.m⁻²) averaged between 5° E and 12° E and between 3° S and 0° S; (c & h) Latitude-time diagram of the intraseasonal variations of the maximum of the current vertical shear magnitude (m.s⁻¹) averaged between 5° E and 12°E; (d & i) Longitude-time diagram of the intraseasonal variations of Ekman Pumping (m.s⁻¹) averaged over the CLR. Ekman pumping values >0 indicate upwelling; (e & j) Latitude-time diagram of the net heat flux (W.m⁻²) averaged between 5° E and 12° E; from 1st March to 31 August 2005 (left panels) and 2006 (right panels). For details about calculations of intraseasonal variations, see Sect. 2.

13. RC: Lines 275-276: Is the reader supposed to be comparing Fig. 3b with 3d to see the correlation between wind stress and Ekman pumping? If so, it is not clear that this relationship is seen. Also, I don't know how we can see 8degE in this figure. If this correlation is not shown, please say so and let us know what the correlation coefficient is.

AC & MC: The Figures 3 and 4 have been modified. We removed the low-pass filtering (cutoff frequency of 30 days) to the total field. The filtered Ekman pumping velocities have been averaged over the area. Thus, the correlation with wind stress is more clearly visible (see the new Figure 3 and 4 in response to the previous question). The text has been modified (section 4.2.1) :

“The Ekman pumping velocity w_e averaged over the CLR for 2005 and 2006 is shown on Fig. 4d & 4i respectively. The dates of intraseasonal upward velocities are quite well correlated with the dates of intraseasonal wind events (with correlation coefficient equal to 0.55 for 2005 and 0.41 for 2006),

maximum being during the early-April, mid-May and end-May 2005 events and during late April, mid-June and end-June 2006. However, for comparable wind intensification, the boreal spring and summer wind events were not associated with comparable intensity of Ekman pumping velocity.”

14. RC: It might be more telling to try to show the SST/heat content changes in the eastern Atlantic due to each of the processes (upwelling, or even split that into wind stress and vertical mixing, and surface heat fluxes). I'm not sure the best way to suggest this, but perhaps regressions would be suitable. This way, it might be more clear that the May 2005 event was an outlier in terms of short wave cloud radiation.

AC: Thanks for the suggestion. Showing the heat content changes in the eastern Atlantic due to each of the processes would be indeed interesting. However, we consider that showing the Ekman pumping, vertical current shear, and surface heat flux bring the relevant information needed to explain the main processes at play.

MC: However, in order to better highlight the particularity of each wind event, we have modified the figure, zoomed from 1st March to 31 August 2005 and 2006 and shown the intraseasonal variations for SST, wind, Ekman pumping, and vertical current shear. The net surface heat flux have been not filtered in order to highlight the events characterized by negative heat flux, such as the end-May 2005 event and the beginning of April 2006 event.

15. RC: Lines 330-332: I do not see the difference between 2005 and 2006 from Fig. 8. It appears that both Kelvin waves reach the east around the same time and originate in the west around the same time. Figure 6 is also unclear. For 2006, I see many episodes of negative SSH (Feb., Mar., May, June), so why are you only picking the one that occurred in Mar-Apr? I do see a negative value in the east starting a tad earlier in 2006, but not by much. I also see a larger anomaly in 2006 in the east in July-Aug. Why is this not discussed...why only the Mar-Apr event? Is it because you are only focused on the boreal spring event?

AC: Do you mean « Fig. 5 » instead of “Fig. 8” ?

On Fig.5 and 6, discussed on lines 330-332, the Kelvin waves in 2005 and 2006 are delayed by about 15 days. Even weak, such a 15 days difference contributes to make the thermocline shallower when the mid-May wind burst occurs in 2005. However, it is true that the difference is not so easy to observe from Figure 5 & 6.

MC: Therefore, for more clarity, the sentence on line 330-332 (section 4.2.2.a) has been modified as follows:

“In 2005, negative SSH and z_{20} anomalies occurred in the West in early March-early April and in mid-May, whereas they occurred around late-February – mid-March and early May and June in 2006. The first Kelvin wave thus reached the CLR slightly earlier in 2006 than 2005, at the beginning of May. In addition, the two upwelling Kelvin waves followed each other more closely in 2005 than in 2006.”

Moreover, the figures have been modified and we have plotted the anomalies only for the period March-August for better clarity. We focus on negative SSH occurred in Mar-Apr in the west because that is this event which induces a shallower thermocline in the east few weeks later, in April-May. Indeed, we focused on the boreal spring events in the east.

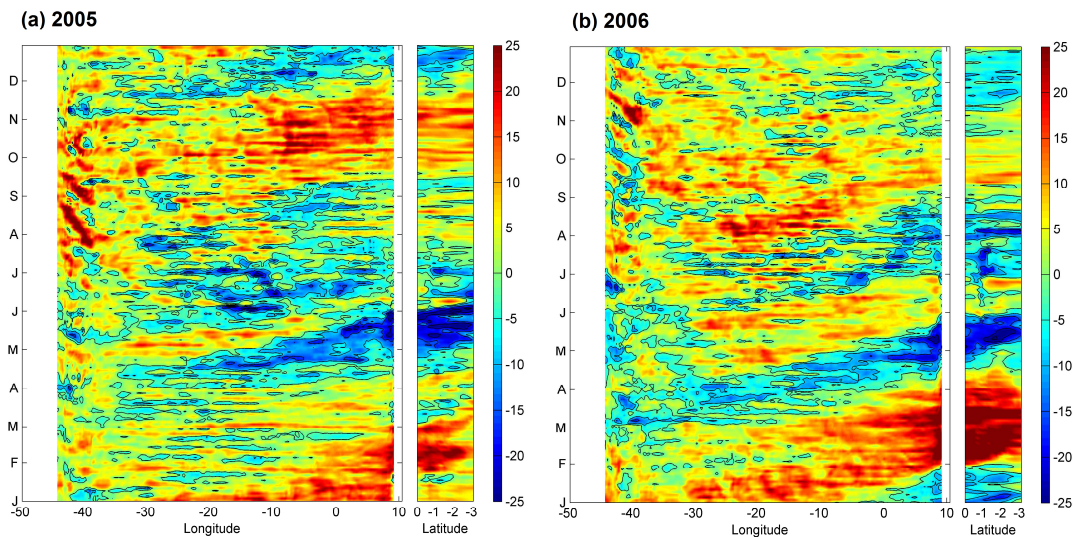


Figure 5: Time evolution of the intraseasonal anomaly of 20° C-isotherm depth (m) along the equator (between 54° W and 12° E) and along 9° E (between the equator and 3° S) for 2005 (left) and 2006 (right). Negative values indicate a 20° C isotherm depth closer to the surface. For details about calculations of the anomalies, see Sect. 2.

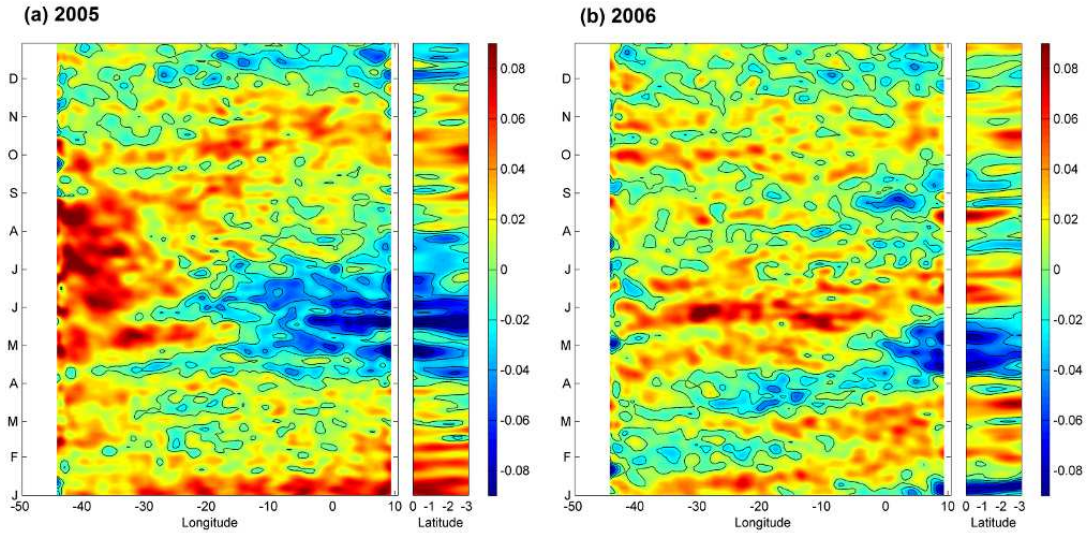


Figure 6: Time evolution of the sea level anomaly (m) along the equator (between 54° W and 12° E) and along 9° E (between the equator and 3° S) for 2005 (left), and 2006 (right) from AVISO data.

16. RC: The text on Fig. 7 is nearly impossible to read.

AC & MC: Sorry for that. Modifications have been made on the figure 7 for more clarity.

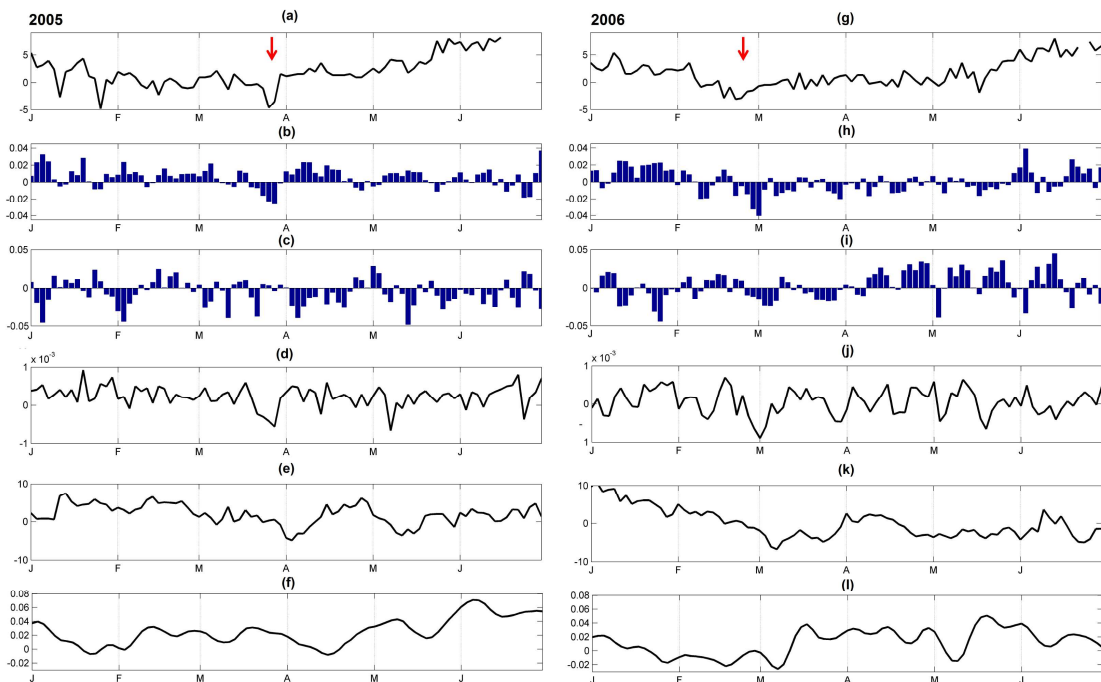


Figure 7: Time evolution, from 2-days averaged model outputs over Jan-June 2005 (left) and Jan-June 2006 (right); of (a & g) the position (in latitude, between 5° S and 10° N) where the meridional wind stress value equal zero (indicator of the position of the ITCZ); (b & h) the intraseasonal anomaly of the meridional wind stress (N.m^{-2}) averaged between 50° W and 35° W and between 1° S and 1° N; (c & i) same as (b & h) but for intraseasonal anomaly of zonal wind stress (N.m^{-2}); (d & j) the intraseasonal anomaly of the wind stress curl

($\text{N}\cdot\text{m}^{-2}$); (e & k) the intraseasonal anomaly of the 20°C isotherm depth (m); (f & l) the intraseasonal anomaly of the sea level (m). The red arrow in (a & g) indicates the southward shift of the ITCZ before the excitation of the Kelvin wave (see text). For details about the calculations of anomalies, see Sect. 2.

17. RC: Lines 409-416: This discussion is about southerly wind bursts in the eastern basin, I assume along the coast, but in Fig. 8, I do not see many arrows in that region, so it is difficult to make this connection from the figure.

This paragraph also suggests a linkage between SST variability in the Cape Lopez region and the equatorial region. You might explain this a bit further by discussing the climatological behavior of this connection (like when it occurs and how it develops). I assume that this is not a feature specific to 2005. I believe that the Bates and Okumura et al. papers might refer to this connection too.

AC & MC: The figure 8 has been modified for better visibility.

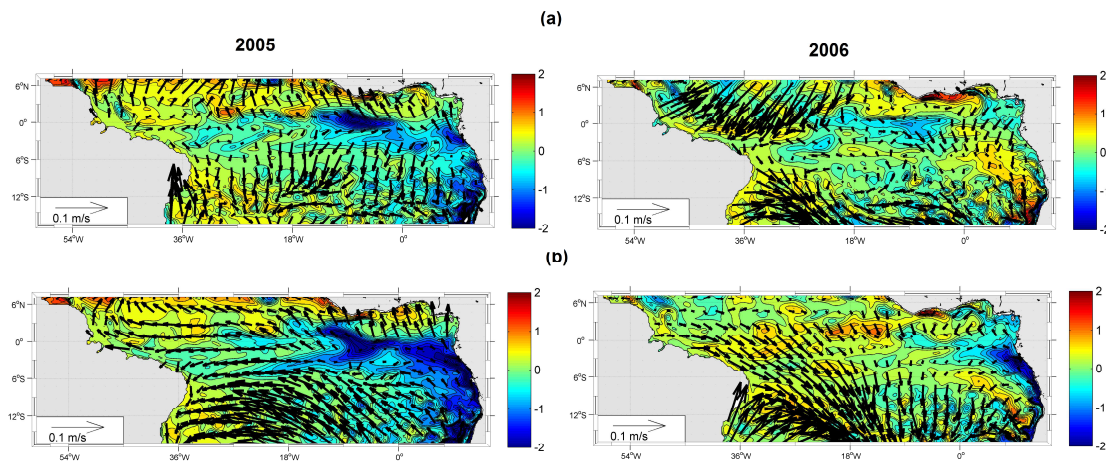


Figure 8: (a) intraseasonal anomaly of sea surface temperature ($^\circ\text{C}$; color) superimposed with intraseasonal anomaly of wind stress intensity (arrows) averaged over 1-12 May 2005 (up panel) and over 14-30 May 2005 (down panel); (b) same but for 2006. For details about the calculations of the anomalies, see Sect.2.

Indeed, the connection between the Cape-Lopez region around 3°S and the southern edge of the equatorial cold tongue is not specific to 2005 and 2006. The westward extension of the cold SST takes place every year over 1998-2008 period (our period of study) but starts at different time. It occurs generally from June-July, when the cooling events usually occur in the east at this location, and is thus closely linked with the shoaling of the thermocline due to the arrival of the Kelvin upwelling wave at the coast. In 2005, the strongest cooling events induced by strong southerly winds occur earlier, in May, combined with anomalous shallower thermocline due to early arrival of Kelvin upwelling wave. The cooling in the CLR also reaches more coastal area due to anomalous strong wind events in the east part of the basin

while it does not reach the coast at this location (3°S) in boreal spring for the most years over 1998-2008 period. In addition, the westward surface currents are usually maximum in boreal spring (as visible on the seasonal cycle shown on Fig.1) and extend over the most coastal area in the east during southerly wind events. They can thus even more contribute to the westward extension of cold coastal waters in May 2005.

In 2006, the westward extension of cold waters established from the beginning of July. Yet, coastal cooling occurred at the end of May but no westward extension of the cold waters is observed at this period. In 2005, the two upwelling Kelvin wave followed each other closely while in 2006, the first Kelvin upwelling wave reaches the coast in May and the second in July. In addition, the wind event responsible of the cooling at the end of May 2006 is rather isolated and less strong than the one in mid-May 2005 (which is preceded and followed by another wind bursts few days before and after). In order to clarify these points in the paper, we added a figure for the year 2006 and modified the comments in the text as follows:

“To better understand the oceanic processes implied in this cooling extension, we compared the z_{20} , SLA and zonal velocities along 3°S from March to September 2005 (Fig. 9 b-d) and 2006 (Fig.9 e-h). In 2005, the cooling westward extension was associated with a westward propagation of a shallower thermocline and negative SLA from the African coast up to $5^{\circ}\text{-}10^{\circ}\text{W}$ combined with enhanced surface westward current fluctuations at the dates of the successive events from April-June. The fluctuations of the westward surface current occurring off Gabon with periods of $\sim 8\text{-}10$ days were related to the strengthening of southerly winds during the wind bursts at the same periods (Fig. 4b & f). The surface current in this area is part of the westward SEC which is known to intensify during the cold season (Okumura and Xie, 2006). Our study implies shorter time scales than seasonal scale but the intensification of the SEC during wind bursts through Ekman transport processes might contribute to the westward extension of the cooling by advection of cold eastern upwelled water. This is in agreement with DeCoëtlogon et al. (2010) who found from model results that at short time scale (a few days), more than half of the cold SST anomaly around the equatorial cooling could be explained by horizontal oceanic advection controlled by the wind with a lag of a few days. In addition, minimum z_{20} and SLA values propagating westward at 3°S (Fig. 9b & c), initiated from the coast with a propagating speed of around $10\text{ cm}\cdot\text{s}^{-1}$, which is very close to the phase speed of Rossby waves. Indeed, the generation of the westward waves at the coast coincided with the arrival of Kelvin waves (see Fig. 5a) suggesting the possibility of Kelvin wave’s reflection processes into symmetrical westward propagating Rossby waves. A westward propagation of z_{20} and SLA minimums, although less obvious, was presently also identified at 3°N (not shown).

In 2005, the locally wind-forced component of the wave might reinforce the remote part of the reflected wave signal at the coast by the sea level slope which balanced the strengthening of alongshore winds blowing during the mid-May and late-May events. The quantitative and respective contributions of local and remote wind forcing to this wave is out of the scope of this study and would require further analysis. This phenomenon is supported in 2005 by anomalous eastward expanded southerly wind bursts observed in May 2005. The month of May is besides a period when westward surface currents are usually maximum (as visible on the mean seasonal cycle shown on Fig.1c). Thus, the combined effects of westward surface currents (via advection and vertical mixing through horizontal current vertical shear), local wind influences (via vertical mixing) and wave westward propagation, resulted in the extension of cold upwelled water from the eastern coast to near 20° W.

In 2006, the westward extension of cold waters established later, from the beginning of July. A coastal cooling occurred on 18-26 May but no westward extension of the cold waters is observed at this period (Fig. 9e). In 2005, the two upwelling Kelvin waves followed each other closely while in 2006, the first Kelvin upwelling wave reached the coast in May and the second in July (Fig.5b & Fig. 6b and Fig. 9f). In addition, the intraseasonal wind strengthening responsible of the coastal cooling on 18-26 May 2006 is less intense (wind stress mean in the CLR $\sim 0.04\text{N.m}^2$) than the one in mid-May 2005 ($\sim 0.06\text{N.m}^2$; which is preceded and followed by another wind bursts few days before and after; Fig. 3b & Fig. 4b).

The analysis over 1998-2008 period shows that the westward extension of the cold SST takes place every year but begins at different times of the year (not shown). It occurs generally from June-July, when the cooling events usually occur in the east at this location, and is thus closely linked with the shoaling of the thermocline due to the arrival of a Kelvin upwelling wave at the eastern coast”

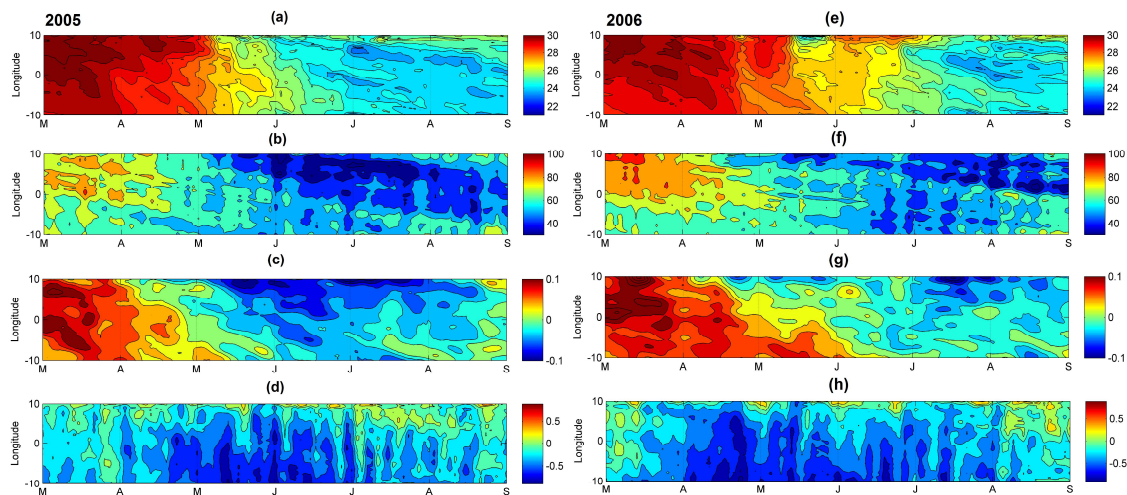


Figure 9: Time-longitude diagrams at 3° S between 10° W and 10° E, and from 2-days averaged model outputs from 1st March to 31 August 2005 and 2006, of (a & e) the sea surface temperature (° C); (b & f) the 20° C isotherm-depth (m); (c & g) the sea level anomalies from AVISO data (m); and (d & h) the zonal component of surface velocity (m.s⁻¹).

18. RC: Figure 10 is impossible to read, and the features difficult to pick out, especially for the top row and bottom two rows. It would be helpful to mask out the land in all panels and make each panel larger. The text describes a precipitation pattern consistent with a wave train, but I cannot see it because the plot is too small and the arrows seem to be covering the precip pattern.

AC & MC: The figure 10 has been modified. The precipitation and wind patterns have been separated and the plots enlarged.

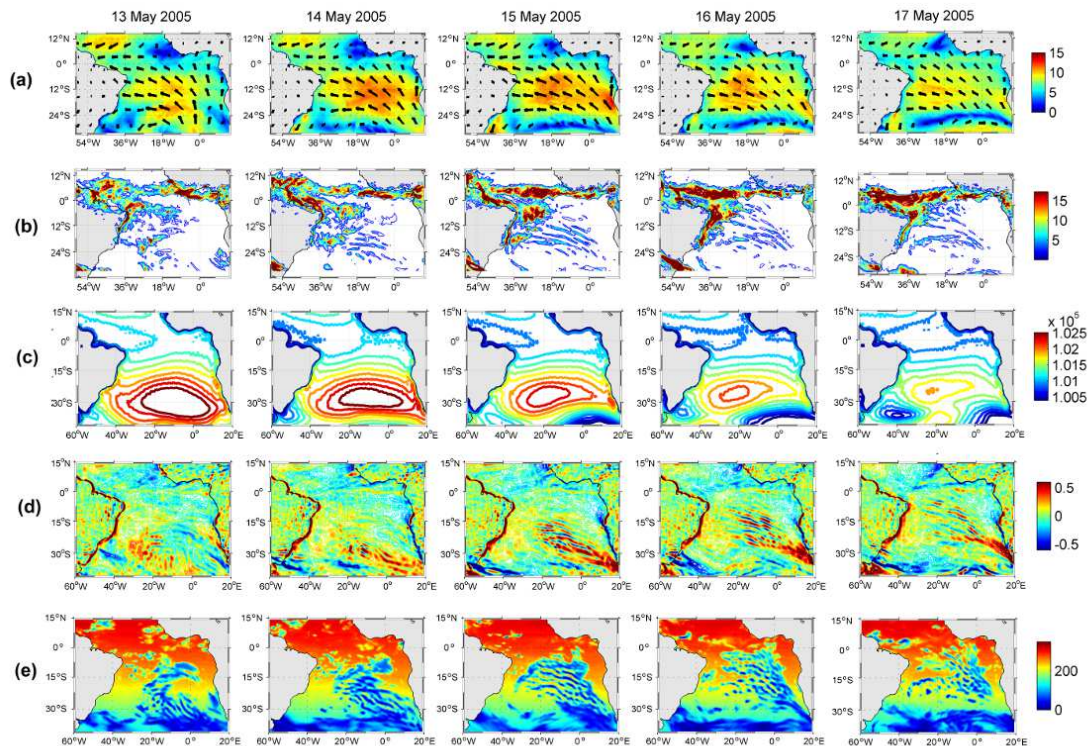


Figure 10: Daily-averaged, from 13 May to 17 May 2005 (left to right panels), of (a) wind magnitude (color field) (m.s⁻¹) superimposed with wind vectors from CFSR fields; (b) precipitation rate (kg.m⁻²/day)⁻¹) from CFSR fields; (b) surface pressure (hPa) from ERA-20C reanalysis; (c) wind speed curl (m.s⁻¹) computed from CFSR wind speed fields; and (d) downward short-wave radiation (W.m²) from CFSR fields.

19. RC: Figure 11: It doesn't seem that you have referred to this figure in the text, though I believe the discussion is on page 21. I do not see what the authors describe in the figure. Perhaps you could be more specific as to the pattern the reader should notice in the plots.

AC & MC: We decided to remove the figure 11. The text has thus been modified as follows:
“The precipitation fields during the mid-May event (Fig. 10a) also evidence rainfall pattern typical of atmospheric gravity wave train characterized by a horizontal wave length ~500 km and initiated by a front system (forming the northern boundary of a low pressure system) which developed around 17° S on 14 May and traveled northeastward until 17 May. The rainfall train was associated with oscillatory wind stress curl train alternating between positive and negative anomalies (Fig. 10c) as well as alternating downward shortwave radiation minimum (Fig. 10d) associated with the wave clouds. Gravity waves are known to play an important role in transporting the momentum and energy through long distances (Fritts, 1984). Here, they would be a way to carry momentum and energy from South Atlantic to the equator during the strong event.”

20. RC: Figure 13: It is very difficult to decipher anything from these plots because they are so small and the contour lines are so close together. It is impossible to tell if an event is stronger or not than others. The text says that the 2005 event “appears to be” one of the strongest over the period, but I cannot tell that from this plot. The authors could confirm this by giving the reader a value of wind stress from this period and state that it is confirmed that this is the strongest.

AC & MC: The figure 13 has been modified for more clarity: vertical black lines have been added to separate the years and the value of wind stress anomaly during the 2005 event has been added in the text (up to 0.13N.m² around 15°S and 0.05N.m² in equatorial region). In addition, we decided to show the fields after removing the 30 days-low pass filtered field averaged over 1998-2008 period, except for the first panel which shows the SST total field.

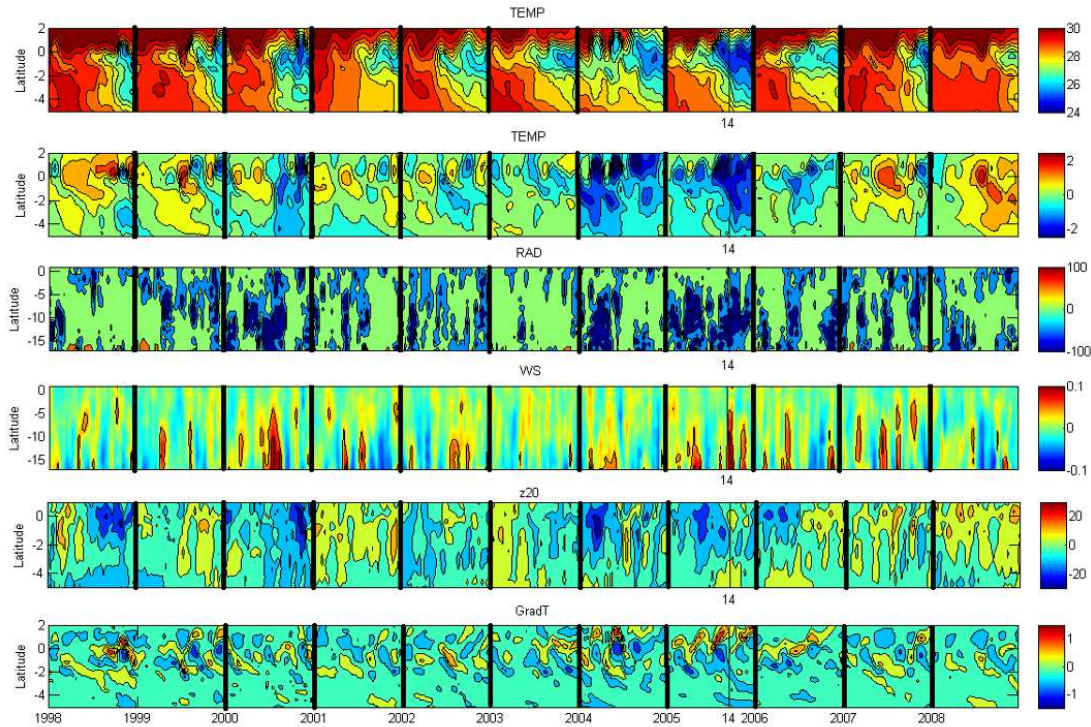


Figure 13 (“Figure 12” in the revised manuscript): Time-latitude diagrams for April-May along the 1998-2008 period, of 2-days average, from top to bottom i) SST (°C); ii) intraseasonal anomaly of SST (°C); , iii) intraseasonal anomaly of wind stress magnitude (N.m^{-2}) from CFSR fields; iv) intraseasonal anomaly of short-wave radiation surface flux (W.m^2) from CFSR fields; v) intraseasonal anomaly of 20°C-isotherm depth (m) computed from the forced model SST; vi) intraseasonal anomaly of meridional SST gradient (every 0.5° of latitude), from the forced model; averaged over 10°W - 6°W . The vertical black thin line indicates the date of 14 May, 2005. For details about the calculations of the anomalies, see Sect. 2.

Modifications have also been made on the plot of 20°C-isotherm depths : weaker values of 20°C-isotherm depths indicate shallower thermocline to be consistent with the modifications made on the Fig. 1, Fig.3, Fig.5, Fig. 9, and Fig. 7.

21. RC: Lines 575-577: Is the statement about winds north of the equator relevant to this study? If so, how is this piece of information important?

AC: The wind-strengthening events north of the Equator during boreal spring in the Gulf of Guinea is implied in the rainfall coastal onset and is linked to the intraseasonal southerly wind burst. Indeed, from Leduc Leballeur et al. (2013), the enhancement and maintenance of southerly winds north of the equator in the Gulf of Guinea is linked to a coincident installation of a deep circulation and a northward shift of the low atmospheric local circulation. This wind strengthening on the northern side of the Equator contributes to the

northward migration of humidity and convection, and pushes precipitation to the continent. It is an indication of the “rainfall coastal onset” of the monsoon.

In section 4.2, we show that as of date of the mid-May 2005 event, the wind north of the equator becomes and remains strong indicating that the mid-May 2005 event is the trigger event of the rainfall coastal onset. The strengthening of winds north of the equator is due to the meridional SST gradient created at the equator during the event. The figure 13 (Figure 12 in revised manuscript) shows that the meridional SST gradient during May 2005 is indeed anomalous strong compared to April-May usual conditions. That what we noted by the sentence in Sect. 5.3: *“This meridional SST gradient was responsible for the wind surface intensification north of the equator (Fig. 11a and Fig. 12, fourth panel) through air-sea interaction mechanisms as described by Leduc-Leballeur et al. (2011).”*

22. RC: Lines 585-593: Is this relevant to the monsoon discussion? Does the deep convection in the Gulf of Guinea lead to rain and a surface cooling? Is that the impact we should take from this paragraph?

AC: The wind strengthening results in equatorial surface cooling, which in turns intensifies the southerlies north of the Equator through air-sea interaction. This increases convection in the northern Gulf of Guinea, accompanied with a northward shift of the precipitation. Generally, in May the low atmospheric local circulation (LALC) appears briefly due to southeastern wind burst and collapses within a few days. The establishment of the LALC at a self-sustaining level appears usually at the end of May-beginning of June, triggered by a significantly stronger southeasterly wind burst. We show that in 2005, the mid-May event is this significantly stronger southeasterly wind burst. It is especially particular because it appears 15 days before the averaged reference date computed by Leduc-Leballeur et al. (2011) over the 2000-2009 period.

MC: The paragraph on lines 585-593 and the figure 14 have been deleted, and the high pressure in St Helena anticyclone region and the low pressures in Gulf of Guinea are now shown on figure 10, section 5.1.1. Moreover, we have deleted the comments about the pressure gradient in section 5.3 and added the lines below in section 5.1.1: *“The strong winds during the event were associated with high pressure core of the Saint Helena Anticyclone, especially on 13-14 May, also associated with particularly low pressure under the ITCZ 4 days later (Fig. 10c). The pressure fall during the mid-May 2005 event appeared as the lowest in May over the whole decade (not shown). The meridional surface pressure gradient during the event is thus found to be the strongest over 1998-2008 period. That suggests strong Hadley circulation intensity during the mid-*

May event and therefore strong equatorward moisture flux, allowing the deep atmospheric convection in the Gulf of Guinea to be triggered at a self-sustaining level, as previously described in Sect. 5.2.”

.23. RC: Lines 599-602: This paragraph was particularly confusing as to where the wind stress and wind bursts mentioned were located.

AC: The wind burst mentioned lines 599-602 is the one evidenced on figure 13 (Figure 12 in revised version) during the year 2000, over 10°W-6°W region.

MC: The sentence on line 599-600 has been modified as follows (Section 5.3): *“Another southerly wind burst of comparable intensity occurred at the beginning of May 2000 (Fig. 12, fourth panel) while the thermocline was shallow, causing SST cooling at the equator (Fig. 12, first and second panels).”*

24. RC: Lines 716-171: Why exactly does this region need more attention? Because of the effect on the African Monsoon? Please elaborate here to make your conclusion points better known.

AC: The South Atlantic region, and in particular the St. Helena Anticyclone variability, need more attention because of the impact of its fluctuations on the SST variability in the tropical Atlantic and in particular on the equatorial cold tongue development, as showed in the paper. The energy from South Atlantic is indeed carried toward lower latitudes by different ways : i) direct effect of the southerly winds in the east, ii) energy transport via atmospheric gravity waves, iii) excitation of Kelvin wave in the West by southeasterly winds.

In our paper, we show that intraseasonal wind bursts, related to St Helena Anticyclone fluctuations have an impact on SST variability in the CLR generating cold events in boreal spring/summer. Other studies, as the one realized by Marin et al. (2009) showed that they also impact the SST variability in the cold tongue region. In addition, the influence of the cold tongue on West African monsoon onset has been suggested by many authors (e.g. Okumura and Xie, 2004; Caniaux et al., 2011; Nguyen et al., 2011; Thorncroft et al., 2011). In 2005, we show that a particularly strong wind burst is responsible for a particularly early coastal monsoon onset. Thus, a better understanding of the variability of St. Helena Anticyclone at intraseasonal time scales would allow to bring further information about these processes.

In addition to modifications listed above, many English/grammar corrections have been made in the text.

Authors' response to Referee 3

Journal: Ocean Sciences

Title of paper: Impact of intraseasonal wind bursts on SST variability in the far eastern Tropical Atlantic Ocean during boreal spring 2005 and 2006. Focus on the mid-may 2005 event.

Authors: Herbert Gaëlle, Bourlès Bernard.

We thank Reviewer 3 for his comments and suggestions that allowed improvements of our paper. We have made all needed modifications to make the figures easily understandable and conforming with general publications criteria (figures size, labels, etc). We have also made effort to make the main narrative of the manuscript easier to follow. A more in-depth analysis would have been obviously interesting but we first aimed to understand the different processes acting in the region. In addition, a more in-depth analysis of one or two particular processes would have prevented the description of the succession of the processes as a whole.

RC: Referee's comment; **AC:** Authors' comment; **MC:** Manuscript changes

Response to specific comments:

RC: Why focus on this particular region? Is SST in it important for rainfall in a given region?

AC: The initial reason that motivates the study of the SST variability in the Cape-Lopez region is the observation in satellite SST data of cold coastal waters independent from those observed off shore in the cold tongue region around 10°W (see the map of satellite SST data for the 8 June 2005 shown on the Figure X1) which raises the question of the link of such cooling with the cold tongue development.

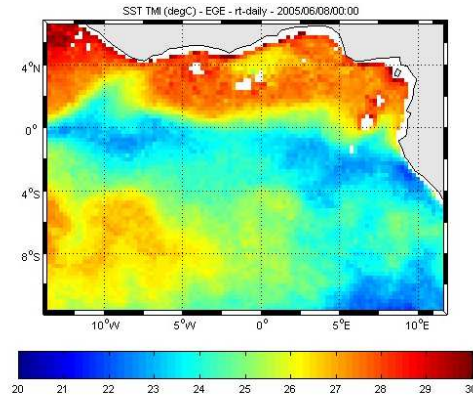


Figure X1: SST (°C) from TMI satellite data on 8 June 2005.

The equatorial region and the processes implied in the cold tongue development are largely studied contrary to the Cape-Lopez region. Other several studies focus on SST variability in more southern region such as Angola-Benguela front, but very few in the Cape-Lopez region. However, we thought that better describe the SST variability in the Cape-Lopez region is needed and interesting especially because of the numerous processes in play notably due to the presence of the coast and the proximity of the equator. In addition, some studies (such as DeCoëtlogon et al., 2010) suggest that at short time scale (a few days), more than half of the cold SST anomaly around the equatorial cooling could be explained by horizontal oceanic advection controlled by the winds. Therefore, a better understanding of the SST variability in CLR may also help to better understand the SST variability in equatorial region.

MC: Some lines have been added in the Introduction:

“The question of the processes implied in the SST variability in the Cape-Lopez region was raised based on an observation in satellite SST data of cold coastal waters during spring independent from those observed off shore in the cold tongue region around 10°W which also raised the question of the link of such cooling with the cold tongue development.” [...] “In addition, some studies (such as DeCoëtlogon et al., 2010) suggest that at short time scale (a few days), more than half of the cold SST anomaly around the equatorial cooling could be explained by horizontal oceanic advection of upwelled cold coastal waters controlled by the winds. Therefore, a better understanding of the SST variability in the CLR may also help to better understand the SST variability in the equatorial region.”

RC: How are conditions in the CLR related to the cold tongue farther west? What is the correlation between SST in the eastern box and in cold tongue box, for example?

AC: Given that the CLR and cold tongue region are submitted to the similar atmospheric forcing, the SST variability in both regions is quite close (cooling event at the same date). However, the processes responsible of the cooling differ from CLR region to cold tongue region due in particular to the presence of the coast. From many authors (Yu et al., 2006; Peter et al., 2006; Wade et al., 2011; Jouanno et al., 2011), the cooling in the cold tongue region would be regulated by a coupling between thermocline shoaling and subsurface dynamics such as turbulent mixing, vertical advection and entrainment, as well as horizontal advection.

In the CLR, we showed that upwelling processes are involved in particular around 3-4°S, as well as vertical current shear implying the SEC, which is enhanced during southerly wind bursts. Our analysis for the year 2005 and 2006 has also shown that during particular events (at the end of May and beginning of April 2006), a decrease of short wave radiation in CLR due to increased cloud cover contributes to the cooling. This phenomenon does not concern the equatorial region east of 0°W. In addition, for a given wind burst, the intensity of SST response in CLR and cold tongue region will modulate by subsurface conditions which are under the influence of equatorial Kelvin wave. For example in May 2005, the Kelvin wave reached the eastern coast while three wind bursts occurred, thus the thermocline was shallower in the east than west of 0°W. We also highlighted westward extension of cold eastern upwelled water around 3°S through combined effects of westward surface currents, local wind influences and wave westward propagation which may contribute to the cooling in the southern edge of the cold tongue region.

MC: Some lines about this have been added at the end of the section 4:

“In conclusion to this section 4, the SST variability in the CLR at intraseasonal time scales is the result of combination between basin preconditioning by remotely forced shoaling of the thermocline via Kelvin wave, local mixing induced by current vertical shear, and upwelling processes in response to strong southerly winds. As highlighted for the 26-28 May 2005 and 2 April 2006 events, the net heat flux may also contribute to cool the surface waters, through enhanced cloud cover which decrease the incoming solar radiation. The cold upwelled waters around 3°S extend then westward from the eastern coast to near 20°W by combined effect of the westward propagating Rossby waves as well as vertical mixing and advection processes. The cool water may thus contribute to the cooling in the southern edge of the cold tongue region. Although the processes implied differ slightly due to the presence of the coast, the SST variability in the CLR is quite close to the one in the equatorial cold tongue region (not shown), due to similar atmospheric forcing. However, for a given wind burst, the intensity of SST response in the CLR and in the cold tongue region is modulated by subsurface conditions which are under the influence of equatorial Kelvin wave. In May 2005, the Kelvin wave

reached the eastern coast while three wind bursts occurred. The thermocline was thus shallower in the east than west of 0°W , providing favorable subsurface conditions making the coupling between making the SST more reactive to wind intensification occurred during this month. In addition, the decrease short wave radiations due to enhanced cloud cover during the 26-28 May 2005 event or 2 April 2006 event, which contribute to the cooling in the CLR, did not concern the equatorial region east of 0°W .”

RC: It is difficult to see the differences between Figs. 3 and 4. I suggest replacing with a figure showing differences, or adding a new figure.

AC & MC: The figures 3 and 4 have been modified. The filtered SST (where the 30days-low pass filtered field has been removed to the total field) has been added in order to better highlight the cold episodes. In addition, a zoom over March-August period has been made for better clarity.

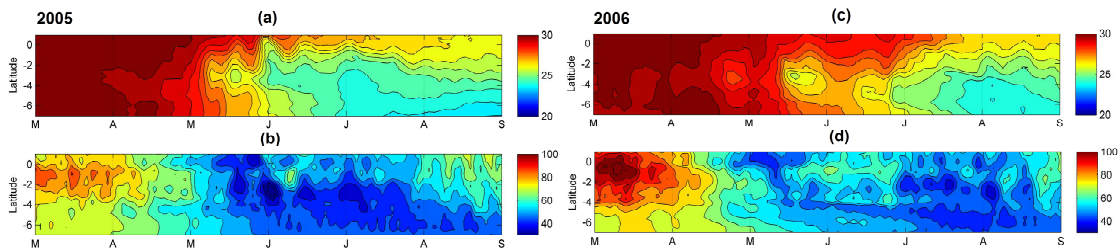


Figure 3: (a & c) Latitude-time diagram of the sea surface temperature ($^{\circ}\text{C}$) averaged between 5°E and 12°E ; (b & d) Latitude-time diagram of the 20°C -isotherm depth (m) averaged between 5°E and 12°E ; from 1st March to 31 August 2005 (left panels) and 2006 (right panels).

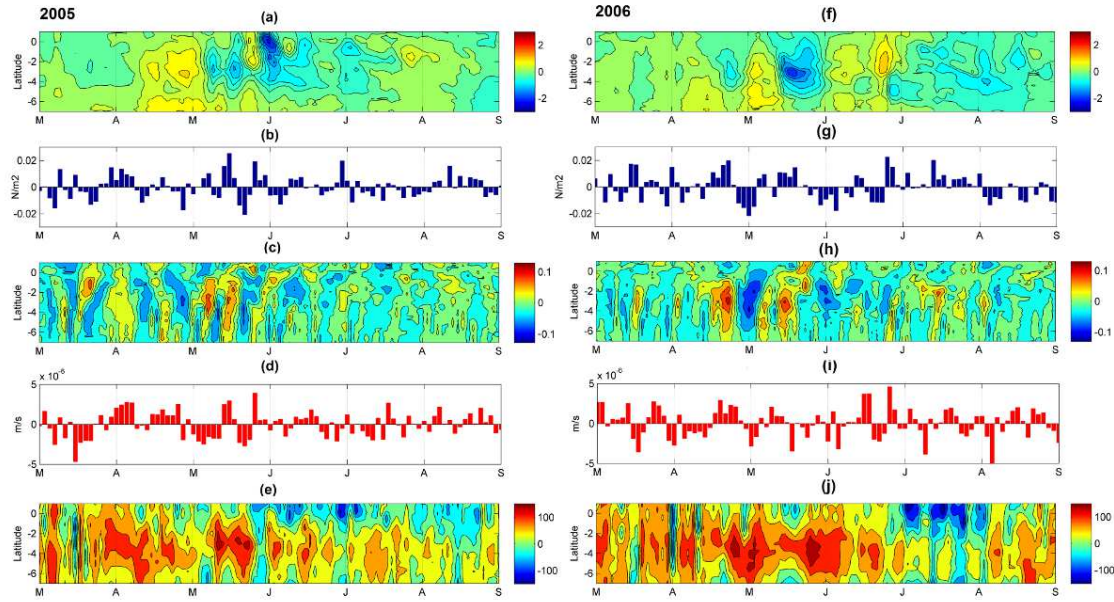


Figure 4: (a & f) Time-latitude diagram, from 7° S to 1° N, of the intraseasonal variations of sea surface temperature (in °C) averaged between 5° E and 12° E; (b & g) Time evolution of the intraseasonal variations of wind stress amplitude (N.m⁻²) averaged between 5° E and 12° E and between 3° S and 0° S; (c & h) Latitude-time diagram of the intraseasonal variations of the maximum of the current vertical shear magnitude (m.s⁻¹) averaged between 5° E and 12°E; (d & i) Longitude-time diagram of the intraseasonal variations of Ekman Pumping (m.s⁻¹) averaged over the CLR. Ekman pumping values >0 indicate upwelling; (e & j) Latitude-time diagram of the net heat flux (W.m⁻²) averaged between 5° E and 12° E; from 1st March to 31 August 2005 (left panels) and 2006 (right panels). For details about calculations of intraseasonal variations, see Sect. 2.

Modifications have also been made on the plot of 20°C-isotherm depths : weaker values of 20°C-isotherm depths indicate shallower thermocline to be consistent with the modifications made on the Fig.1, Fig.5, Fig.7, Fig. 9 and Fig. 13 (Fig. 12 in revised version) in response to the other reviewers' comments.

RC: How are the results different (or confirm) previous studies of cold tongue variability? It's not clear.

AC: Our study does not focus on the cold tongue variability but, first, on SST variability more eastern, in the Cape-Lopez region. Marin et al. (2009) show that the cooling in 10°W-4°W region is the result of successive cooling events related to intraseasonal wind bursts. The two regions are under the influence of similar atmospheric forcing but the processes implied are rather different. We show that the SST in the CLR also reacts to the intraseasonal wind

bursts. However, the processes responsible of the cooling differ from the CLR region to the cold tongue region due in particular to the presence of the coast (see our response to the previous question “How are conditions in the CLR related to the cold tongue farther west? What is the correlation between SST in the eastern box and in cold tongue box, for example?”).

The cold tongue region is mentioned in the second part of our paper when we focus on the mid-May 2005 wind burst and its impact on coastal monsoon onset. Indeed, we aim to describe the wind burst impacting the Cape-Lopez region at more global scale, so we analyzed its impact in the Cape-Lopez region and also in the cold tongue region through its role in West African Monsoon onset.

RC: Negative values in Figs. 3c, 4c to me mean shallower than normal thermocline, but it seems you are using the opposite sign so that positive values mean shallower. This is a little confusing. I recommend switching signs or making it clear in the Fig. 3 caption that negative means deeper. Also indicate in the caption that Ekman pumping values >0 indicate upwelling (I assume this is the case?).

AC & MC: Thanks for this suggestion. We have modified the figures 3c and 4c in this sense and we have added that Ekman pumping values >0 indicate upwelling in the captions of the figures.

RC: Lines 279-292: Do zonal or meridional current variations dominate for the vertical shear, and are they driven by the anomalous meridional winds?

AC & MC: The vertical shear is dominated by zonal current variations, related to the fluctuations of dominant southerly winds. We have modified the figure 3 and 4 where we plotted the vertical shear magnitude (see the response to the previous comment: “It is difficult to see the differences between Figs. 3 and 4. I suggest replacing with a figure showing differences, **or** adding a new figure.”). On the new figures, we also removed the 30-days low-pass filtered field to the total field.

RC: Lines 317-318: What do you mean by "steeper thermocline slope?" Do you mean stronger dT/dz within the thermocline, or shallower thermocline, or stronger horizontal gradients of thermocline depth...

AC: By ‘steeper thermocline slope’ we mean ‘shallower thermocline’.

MC: We have clarified this in the text.

RC: Data/methods section: How are anomalies calculated? It is not stated anywhere, yet shown frequently in the figures. Was the mean seasonal cycle (monthly mean climatology) removed before making Fig. 5, Fig. 6?

AC: For the Figure 5, we applied a 30-days low-pass filter to the total field, averaged the result over 1998-2008 period and removed it to the total field of each year.

MC: Indications about how the calculations have been made for each figure have been added in the text, in Section 2 : “*Note that throughout the whole text and figure captions, the term “intraseasonal variations” is used to designate the field obtained after the removing of the 30 days low-pass filtered field to the total field of the given year, while “intraseasonal anomaly” refers to the field obtained after the removing of the 30 days low-pass filtered field averaged over 1998-2008 to the total field of the given year.*”

RC: I don’t see a good correspondence between Figs. 5 and 6. Maybe plotting anomalies from the seasonal cycle would help (if not done already). Otherwise, another method to validate the model’s Z20 anomalies is needed.

AC: The figures 5 and 6 have been modified. Negative values of 20°C-isotherm depth now show shallower thermocline, to better highlight the correspondence between Fig. 5 and Fig. 6. The values plotted on Fig.5 are obtained by removing the 30-days low pass filtered field, averaged over 1998-2008 period to the total field.

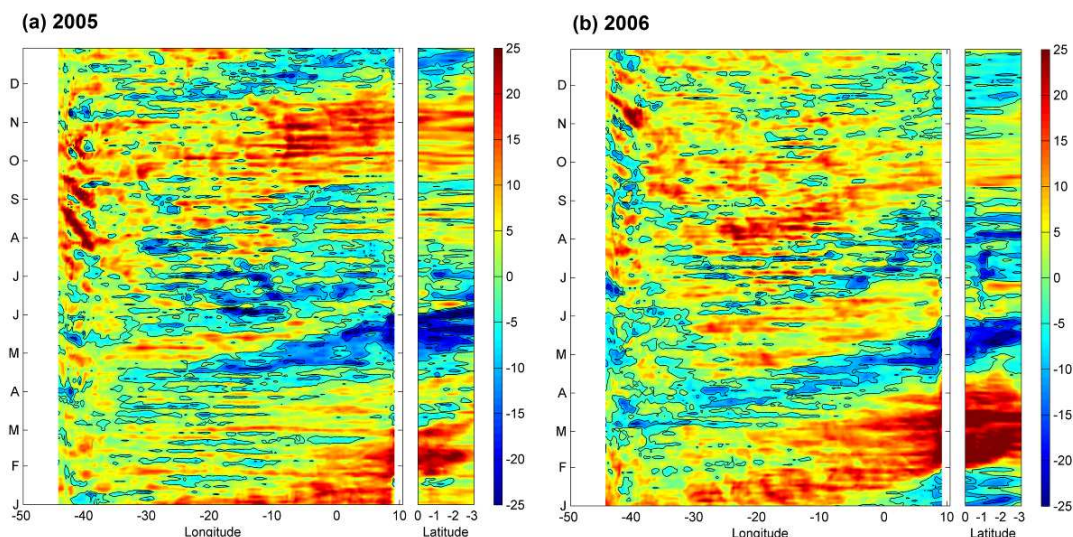


Figure 5: Time evolution of the intraseasonal anomaly of the 20° C-isotherm depth (m) along the equator (between 54° W and 12° E) and along 9° E (between the equator and 3° S) for 2005 (left) and 2006 (right).

Negative values indicate a 20°C isotherm closer to the surface.

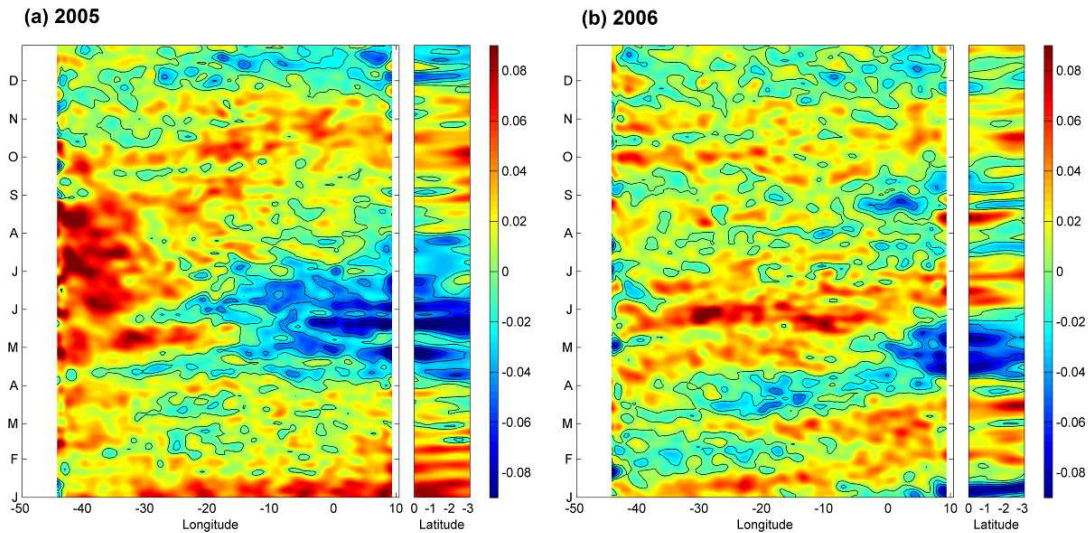


Figure 6: Time evolution of the sea level anomaly (m) along the equator (between 54° W and 12° E) and along 9° E (between the equator and 3° S) for 2005 (left), and 2006 (right) from AVISO data. For details about calculations of the anomalies, see Sect. 2.

RC: Line 386: Do you mean Fig. 7c instead of Fig. 6c?

It's difficult to follow the discussion and reasoning on line 380-390. A figure showing spatial patterns of wind anomalies might help to visualize the changes in Ekman pumping and ITCZ shifts.

AC: Yes, sorry for that, we indeed mean Fig. 7c instead of Fig. 6c. We are not sure that it is necessary to add additional figure. We think that what we want to show is clearly visible on the plot of Fig. 7.

RC: What is the main result of the analysis discussed on p. 14-15? Why is it important that the southward movement of the ITCZ was more abrupt in 2005 and the winds following the event were different compared to 2006? Please state at the end of the section or mention that it will be discussed in later sections. If it didn't clearly affect later conditions, it should not be shown.

AC: In the previous section (4.2), we show that the intraseasonal cold SST variability in the CLR is the result of combination of local and remote forcing. The remote forcing is made through Kelvin wave eastward propagation associated with minimum z20 and SSH. For the years 2005, the May wind events were responsible for strong SST response, supported by favorable subsurface conditions. Since the subsurface conditions in the east are largely influenced by the arrival of Kelvin wave excited in the west, it seems to us interesting to

better understand what are the atmospheric conditions associated with the Kelvin wave excitation in the west and how they are different in 2005 and 2006. It is the aim of the section 4.2.2b. The main result of the analysis is that the anomalous strengthening of easterly winds occurs some days after the ITCZ to be at its southernmost location. In 2005, the ITCZ reaches its southernmost location through a sudden southward shift and returns to its initial position just after, whereas in 2006, the southernmost position of the ITCZ is reached less sharply and in the continuity of the evolution of the ITCZ's position, as it is moving southward. In order to better highlight the phenomenon discussed, we have plotted the intraseasonal variations anomalies (the 30 days low-pass filtered field averaged over 1998-2008 period have been removed to the total field) of wind stress magnitude, z20, and SLA on figure 7. It also shows another way in which intraseasonal wind event impact the SST in the eastern Atlantic (even few weeks later), via the generation of Kelvin wave in the West.

MC: Few lines have been added at the end of the section 4.2.2b:

“These results highlight another way in which wind intraseasonal events may impact the SST variability in the East part of the basin, through the generation of Kelvin wave in the West which shoals the thermocline in the East few weeks later”

RC: Lines 414-415: How does Fig. 8 show an enhancement of SST cooling after May 10? It only shows SST averaged for May and for May 1-10.

AC: The enhancement of SST cooling after May 10 was deduced for the difference between the average over May and the average over May 1-10.

MC: For better clarity, we have modified the figure 8 and shown the mean for 1-12 May 2005 and for 14-31 May 2005. For comparison, the same calculation has been made for 2006.

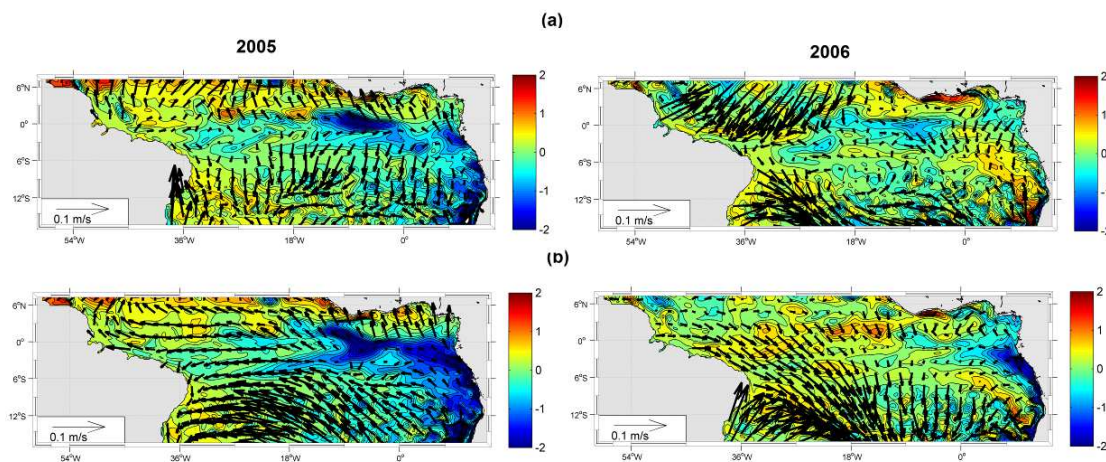


Figure 8: (a) intraseasonal anomaly of sea surface temperature ($^{\circ}$ C; color) superimposed with intraseasonal anomaly of wind stress intensity (arrows) averaged over 1-12 May 2005 (up panel) and over 14-30May (down panel); (b) same but for 2006. For details about the calculations of the anomalies, see Sect.2.

The comments of the figure 8 have therefore been modified as follows:

“To evidence the effect of these events on SST, maps of intraseasonal SST anomaly and intraseasonal wind stress anomaly averaged from 1 to 12 May (before the strong 2005 events; Fig. 8a) and from 14 to 31 May (during and after the strong 2005 events; Fig. 8b) are presented on Fig. 8. The same calculations have been for 2006 for comparison. The results illustrate an enhancement after 10 May of the cooling in the east associated with southerly wind intensification and an extension of the cooling especially south of the equator up to 20 $^{\circ}$ W.”

RC: Figure 10: Why not show anomalies for all fields instead of only for winds?

It seems like sections 5.1.2 and 5.1.3 are not essential and could be eliminated.

AC & MC: We modified the Figure 10 and decided to show the total field for all fields and to separate the wind pattern and the precipitation pattern for more visibility. The aim is to describe the atmospheric conditions associated to the mid-May event 2005.

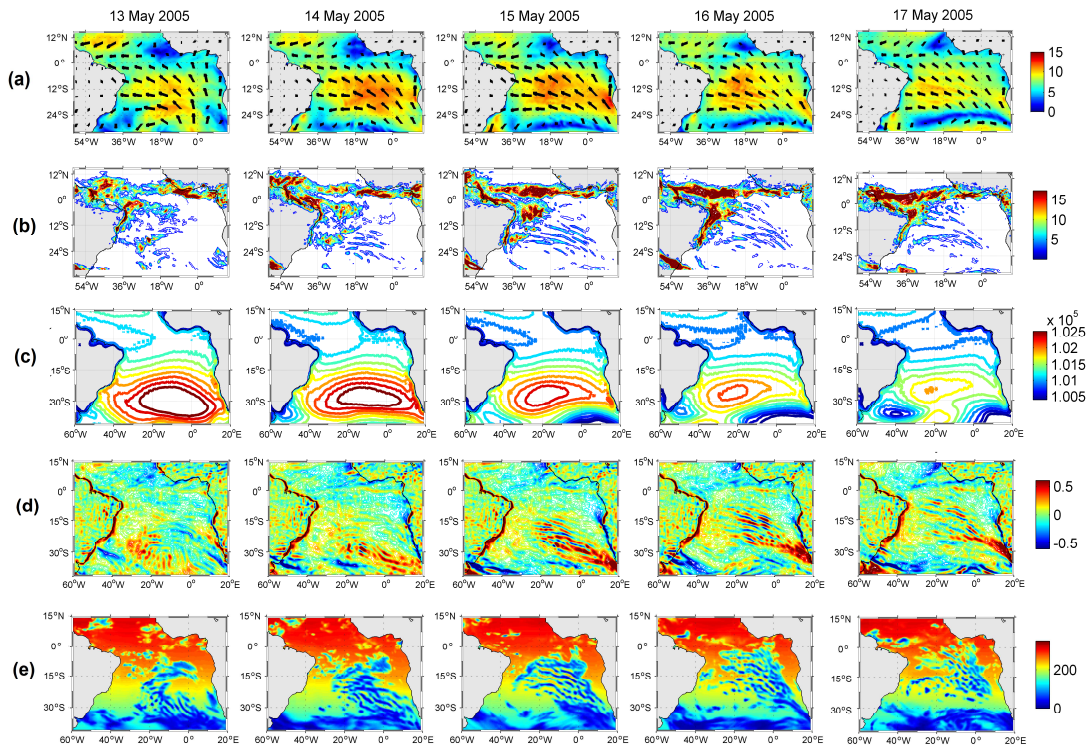


Figure 10: Daily-averaged, from 13 May to 17 May 2005 (left to right panels), of (a) wind magnitude (color field) (m.s^{-1}) superimposed with wind vectors from CFSR fields; (b) precipitation rate ($\text{kg.m}^{-2}/\text{day}^{-1}$) from CFSR fields; (b) surface pressure (hPa) from ERA-20C reanalysis; (c) wind speed curl (m.s^{-1}) computed from CFSR wind speed fields; and (d) downward short-wave radiation (W.m^{-2}) from CFSR fields.

However, we do not agree with the reviewer and do think that sections 5.1.2 and 5.1.3 are useful. Presently, the purpose of the second part of the paper is to better understand how the mid-May 2005 event is singular in addition to the anomalous strong southerly winds. These two sections show the particular conditions which accompanies the mid-May event. The section 5.1.2 shows that, through its time of occurrence and its impact on SST, the mid-May 2005 wind event has also an impact on precipitation pattern off northeast Brazil. In the section 5.1.3, we notice that the event is associated with atmospheric gravity wave which quickly propagates from south Atlantic to equatorial region, that highlights a way to carry momentum and energy of from South Atlantic region to tropical/equatorial region and raises the question of the representation of the impact of such phenomenon on the SST variability in equatorial and eastern tropical region. So, we prefer to keep these sections.

Additional authors 'comments :

In addition to modifications listed above, modifications have been made to make the figures clearer and more easily understandable.

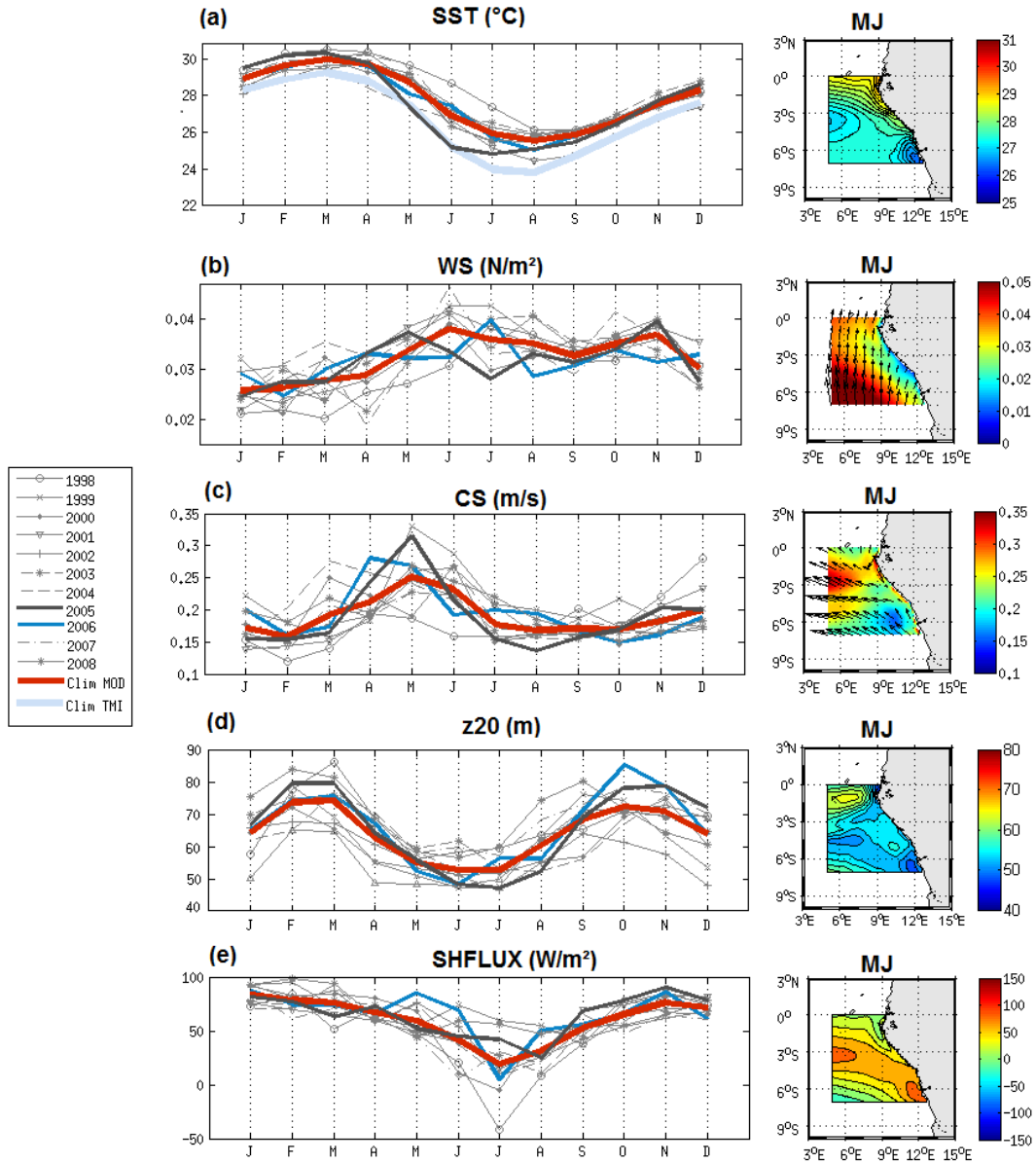


Figure 1: Monthly average of the (a) sea surface temperature ($^{\circ}\text{C}$); (b) wind stress direction (vectors) and magnitude (color field) ($\text{N}\cdot\text{m}^{-2}$); (c) horizontal surface current direction (vectors) and speed (color field) ($\text{m}\cdot\text{s}^{-1}$); (d) 20°C -isotherm depth (m); and (e) surface heat flux ($\text{W}\cdot\text{m}^{-2}$; positive values indicate downward flux) from January to December from 1998 to 2008 and for the climatology (averaged over 1998-2008) simulated by the model (red curve) and from the observations : monthly average TMI 3-daily SST data (light blue curve in (a)); averaged over 5°E - 14°E and 7°S - 0°S . Right panel: maps of each variable over May-June.

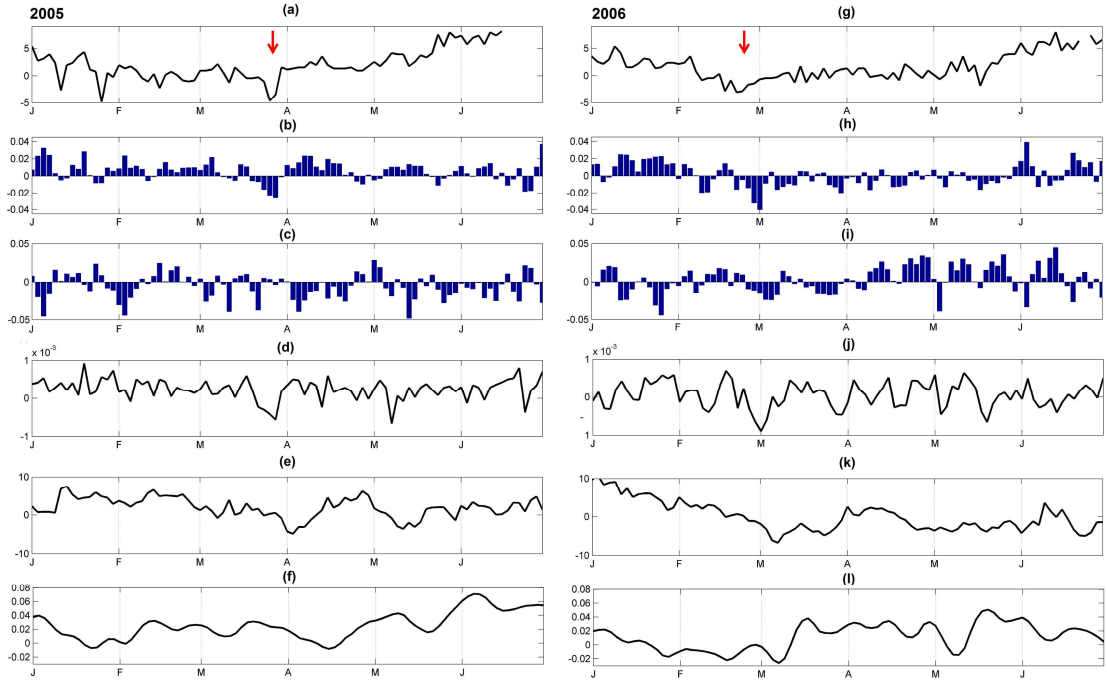


Figure 7: Time evolution, from 2-days averaged model outputs over Jan-June 2005 (left) and Jan-June 2006 (right); of (a & g) the position (in latitude, between 5° S and 10° N) where the meridional wind stress value equal zero (indicator of the position of the ITCZ); (b & h) the intraseasonal anomaly of the meridional wind stress (N.m^{-2}) averaged between 50° W and 35° W and between 1° S and 1° N; (c & i) same as (b & h) but for intraseasonal anomaly of zonal wind stress (N.m^{-2}); (d & j) the intraseasonal anomaly of the wind stress curl (N.m^{-2}); (e & k) the intraseasonal anomaly of the 20° C isotherm depth (m); (f & l) the intraseasonal anomaly of the sea level (m). The red arrow in (a & g) indicates the southward shift of the ITCZ before the excitation of the Kevin wave (see text). For details about the calculations of anomalies, see Sect. 2

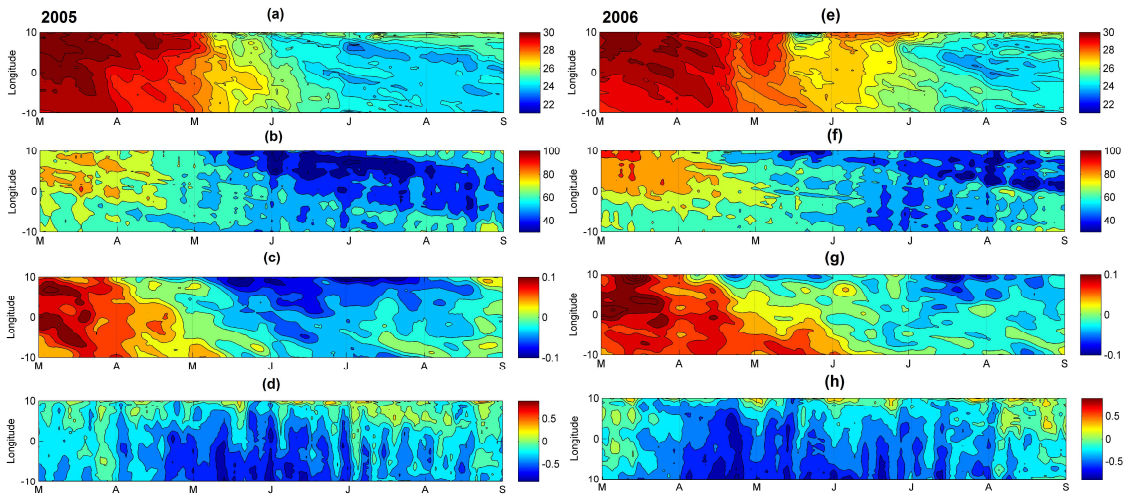


Figure 9: Time-longitude diagrams at 3° S between 10° W and 10° E, and from 2-days averaged model outputs from 1st March to 31 August 2005 and 2006, of (a & e) the sea surface temperature (° C); (b & f) the 20° C isotherm-depth (m); (c & g) the sea level anomalies from AVISO data (m); and (d & h) the zonal component of surface velocity (m.s⁻¹).

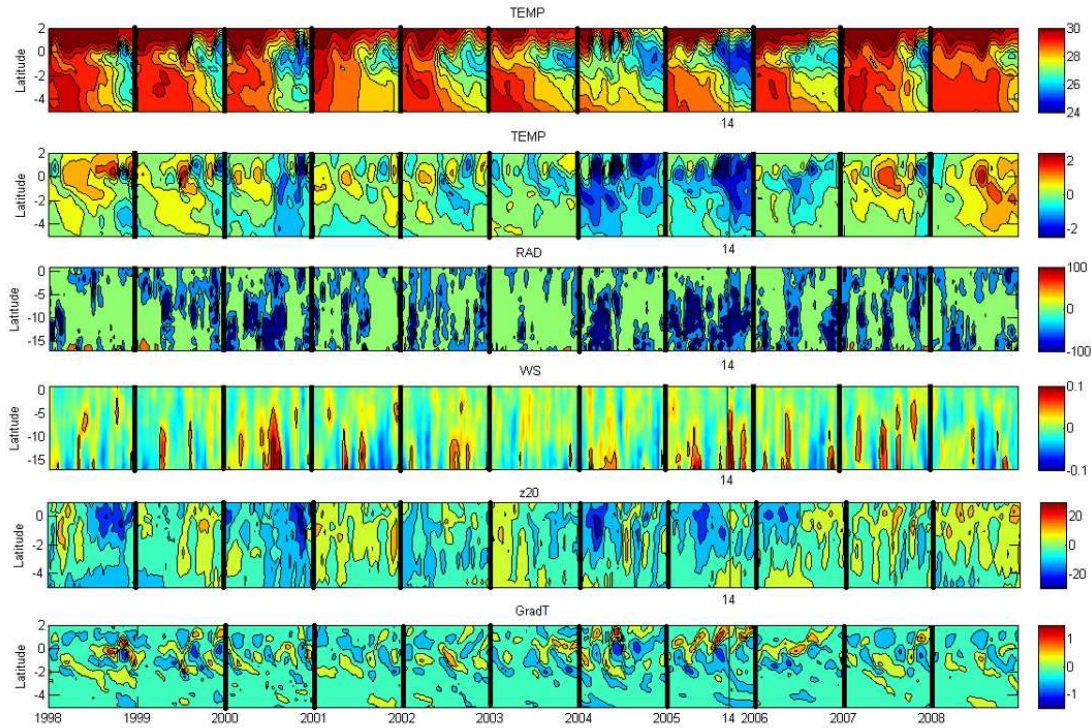


Figure 13 (“Figure 12” in the revised manuscript): Time-latitude diagrams for April-May along the 1998-2008 period, of 2-days average, from top to bottom i) SST (°C); ii) intraseasonal anomaly of SST (°C); , iii) intraseasonal anomaly of wind stress magnitude (N.m⁻²) from CFSR fields; iv) intraseasonal anomaly of short-wave radiation surface flux (W.m²) from CFSR fields; v) intraseasonal anomaly of 20°C-isotherm depth (m) computed from the forced model SST; vi) intraseasonal anomaly of meridional SST gradient (every 0.5° of latitude), from the forced model; averaged over 10° W-6° W. The vertical black thin line indicates the date of 14 May, 2005. For details about the calculations of the anomalies, see Sect. 2.

Many English/grammar corrections have also been made in the text.

Impact of intraseasonal wind bursts on SST variability in the far eastern Tropical Atlantic Ocean during boreal spring 2005 and 2006. Focus on the mid-May 2005 event.

Gaëlle Herbert¹, Bernard Boulès¹

¹:Institut de Recherche pour le Développement (IRD), Laboratoire d'Etudes Géophysiques et Océanographie Spatiale (LEGOS), Brest, France.

Correspondence to: Gaëlle Herbert (gaelle.herbert@ird.fr)

Abstract. The impact of **boreal** spring intraseasonal wind bursts on sea surface temperature variability in the eastern Tropical Atlantic Ocean in 2005 and 2006 is investigated using numerical simulation and observations. We specially focus on the coastal region east of 5° E and between the equator and 7° S that **has not been studied in detail so far**. For both years, the southerly winds strengthening induced **cooling episodes** through i) upwelling processes; ii) vertical mixing due to vertical shear of zonal current; and for **some particular events** iii) a decrease of incoming surface shortwave radiation. The strength of the **cooling episodes** was modulated by subsurface conditions affected by the arrival of Kelvin waves from the west influencing the depth of the thermocline. Once impinging the eastern boundary, the Kelvin waves excited westward-propagating Rossby waves which, combined with the effect of enhanced westward surface currents, contributed to the westward extension of the cold water. A particularly strong wind event occurred in mid-May 2005 and caused an anomalous strong cooling off Cape-Lopez and in the whole eastern Tropical Atlantic Ocean. From the analysis of oceanic and atmospheric conditions during this particular event, it appears that anomalous strong **boreal** spring wind strengthening associated to anomalous strong Hadley cell activity made the event as a decisive event which prematurely triggered the rainfall coastal onset in the northern Gulf of Guinea, **making it the earliest over 1998-2008 period**. Results show that no similar atmospheric conditions were observed **in May** over the 1998-2008 period. It is also found that the anomalous oceanic and atmospheric conditions associated to the event exerted strong influence on rainfall off Northeast Brazil. This study highlights the different processes through which the wind power from South Atlantic is brought to the ocean in the Gulf of Guinea and emphasizes the need to further document and monitor the South Atlantic region.

1.Introduction

The eastern equatorial Atlantic Ocean shows a pronounced seasonal cycle in sea surface temperature (SST) (Wauthy, 1983; Mitchell and Wallace, 1992). One strong signature **of** the SST seasonal cycle in the eastern equatorial Atlantic is the Atlantic cold tongue (ACT) (Zebiak, 1993) characterized by a fast drop of SST (up to

7° C) in **boreal** spring and summer slightly south of the equator and east of 20°W (Merle, 1980; Picaut, 1983). During boreal summer, the southern boundary of this cooler temperature connects progressively with the austral winter cooling of the Southern hemisphere SSTs. A number of observational (Merle, 1980; Foltz et al., 2003) and modeling (Philander and Pacanowski, 1986; Yu et al., 2006; Peter et al., 2006) studies show that the development of the ACT is driven by the seasonal increase of the Southern Hemisphere trade winds during late boreal winter to early summer (Brandt et al., 2011) associated to the meridional displacement of the Inter-Tropical Convergence Zone (ITCZ) (Picaut, 1983; Colin, 1989; Waliser and Gautier, 1993; Nobre and Shukla, 1996). The equatorial cooling would be regulated by a coupling between thermocline shoaling, subsurface dynamics (Yu et al., 2006; Peter et al., 2006; Wade et al., 2011; Jouanno et al., 2011) including turbulent mixing, vertical advection and entrainment, as well as horizontal advection. The equatorial thermocline shoaling is the consequence of local and remote wind forcing: the strengthening of easterly winds in the western equatorial Atlantic remotely forces the seasonal upwelling in the eastern part of the basin via equatorial Kelvin waves (Moore et al., 1978; Adamec and O'Brien, 1978; Busalacchi and Picaut, 1983; McCreary et al., 1984).

Besides the dominant seasonal cycle, the eastern tropical Atlantic is under the influence of meridional southerly winds (Picaut, 1984) which fluctuate with a period close to 15 days (Krishnamurti, 1980; de Coëtlogon et al., 2010; Jouanno et al., 2013). These intraseasonal wind fluctuations are therefore expected to be a major contributor to the seasonal SST cooling and their fluctuations occur as a vector of energy and momentum from the South Atlantic to the eastern equatorial Atlantic. A connection between the strength of the St. Helena Anticyclone and SST anomalies in the southeastern tropical Atlantic has been described by Lübbecke et al. (2014). These authors suggest that the St. Helena Anticyclone variability might be an importance source of anomalous tropical Atlantic wind power which affects SST in the eastern equatorial Atlantic via several mechanisms: zonal wind stress changes in the western equatorial basin, wave adjustment, meridional advection of subsurface temperature anomalies, intraseasonal wind stress variations, and possibly even other mechanisms. Through the in situ data analysis of AMMA/EGEE cruises (Redelsperger et al., 2006; Bourlès et al., 2007) carried out in 2005 and 2006, Marin et al. (2009) show that the SST seasonal cooling at the equator east of 10° W is not smooth but results from the succession of short-duration **cooling episodes** generated by southeasterly wind bursts due to the fluctuating St. Helena Anticyclone. In addition, according to Leduc-Leballeur et al. (2013), the sharp and durable change in the atmospheric circulation in the northern Gulf of Guinea (durably strong southerlies north of equator) takes place through an abrupt seasonal transition prepared by a succession of southerly wind bursts and possibly triggered by a significantly stronger wind burst. The southerly wind bursts occurring in **boreal** spring in the Gulf of Guinea thus would play an important role in driving precipitation pattern in the area through air-sea interactions (de Coëtlogon et al., 2010; Nicholson and Dezfuli, 2013) and coupling between the ACT and the West Africa Monsoon (WAM).

Improving our understanding of the impact of such wind bursts on SST variability at intraseasonal scale in the eastern Tropical Atlantic is important through its link with the regional climate. However, while the ACT and Angola-Benguela regions have been the object of many studies, the dynamics and SST variability of the coastal eastern region is much less documented.

In this study, we therefore first focus our analysis off Cape-Lopez (defined from 0° N-7° S; 5° E-14° E and hereafter called CLR for 'Cape-Lopez region', see map shown in Fig. 2) and aim to improve understanding of its seasonal SST variability and the impact of intraseasonal winds on SST variability during boreal spring and summer. To this end, we use regional high resolution model results as well as satellite SST data and sea surface height observations. We first use model outputs from 1998 to 2008 to analyze the seasonal cycle in the CLR and to highlight its interannual variability, and then we specially focus on the years 2005 and 2006 to investigate the SST response of intraseasonal wind forcing. These two particular years were largely investigated during the African Monsoon Multidisciplinary Analyses (AMMA) experiment (Redelsperger et al., 2006). The year 2005 is characterized by the lowest SST values in the ACT during the past 3 decades (along with 1982), while 2006 is considered as a normal year (Caniaux et al., 2011). Also, 2005 exhibits the earliest development of the ACT. The study of SST variability at intraseasonal scale during these two years is thus interesting for better understanding their observed differences in SST seasonal conditions. These two particular years have been also chosen by Marin et al. (2009) to study the variability of the properties of the ACT. Their study concerned the equatorial area west of 4° E, whereas we propose to focus in the CLR, east of 5° E where coastal processes are expected to be involved.

The question of the processes implied in the SST variability in the Cape-Lopez region was raised based on an observation in satellite SST data of cold coastal waters during boreal spring independent from those observed off shore in the cold tongue region around 10°W which also raised the question of the link of such cooling with the cold tongue development. Most studies on the CLR focused on the analysis of observational dataset to examine the hydrology and its seasonal variation along the frontal (coastal) region of Congo (e.g. Merle, 1972; Piton, 1988) or on the impact of Congo River on SST and mixed layer (e.g. Matera et al., 2012; Denamiel et al., 2013; White and Toumi, 2014) but, to our knowledge, no detailed analysis of SST variability at seasonal and intraseasonal time scales have been realized. A better understanding of ocean-atmosphere interactions in this region is thus needed. Some previous studies related to the whole eastern Tropical Atlantic (Gulf of Guinea) suggest that multiple processes could be in play in CLR, coupling remote and local forcing, and combined with the very low thermal inertia of the mixed layer depth. For example, Giordani et al. (2013) show from regional model results that horizontal advection, entrainment, and turbulent mixing significantly contribute to the heat budget east of 3°W because of the very thin mixed layer. The upper layers of the north CLR might also be impacted by vertical mixing induced by the intense current vertical shear between the South Equatorial Current, flowing westward at the surface, and the subsurface eastward Equatorial Under-Current. In addition to local forcing, the area is also under the influence of the arrival of equatorial Kelvin waves from West and their reflection, once reaching the African coast, poleward as coastally trapped waves and westward as Rossby waves (Moore, 1968; McCreary, 1976; Moore and Philander, 1977). The principal source of the equatorial Kelvin waves has been usually related to the western equatorial zonal wind changes during late boreal winter to early summer (e.g.; Philander, 1990). In order to better understand the trigger mechanism of Kelvin waves generation which conditions the mixed layer properties in the CLR, another purpose of this study is thus to identify the atmospheric conditions coinciding with the Kelvin waves generation in the West of the basin during winter 2005 and 2006. In addition, some studies (such as DeCoëtlogon et al., 2010) suggest that at short time scale (a few days), more than half of the cold SST anomaly around the equatorial cooling could be explained by horizontal

oceanic advection of upwelled cold coastal waters controlled by the winds. Therefore, a better understanding of the SST variability in the CLR may also help to better understand the SST variability in the equatorial region.

Several studies (*e.g.* Okumura and Xie, 2004; Caniaux et al., 2011; Nguyen et al., 2011; Thorncroft et al., 2011) show evidence of a high correlation between the ACT and the WAM onset in the Sahelian region. Based on an analysis of 27 years of data, Caniaux et al. (2011) identified the year 2005 as the year with the earliest WAM onset date (around 19 May 2005 whereas they define the mean onset date on 23 June \pm 8 days). According to Marin et al. (2009), the time shift in the development of the ACT between 2005 and 2006 is related to a particular wind burst event in mid-May 2005. This mid-May 2005 event therefore appears as exerting a strong influence on the WAM. In a second part of the study, we thus focus on this particular wind event that preceded a strong cold event in the far eastern Tropical Atlantic along with an early ACT development. We aim to describe i) the atmospheric and oceanic conditions during this particular event; ii) to what extent it is involved in the WAM system; and iii) which processes make it an exceptional event.

The remainder of the paper is organized as follows. In Sect. 2, the model and observational data used in this study are described. The seasonal and interannual variability of SST, winds, currents, 20° C-isotherm depth and sea surface heat flux in the CLR are analyzed in Sect. 3. The cooling episodes generated in response to southerly wind bursts and the other forcing mechanisms implied in the CLR are investigated in details for the years 2005 and 2006 in Sect. 4. In Sect. 5, we focus our analysis on the unusual wind burst occurring in mid-May 2005. Finally, the main results are summarized and discussed in Sect. 6.

2. Model and data

The numerical model used in this paper is the Regional Oceanic Modeling System (ROMS) (Shchepetkin and McWilliams, 2005). The model configuration is the same as employed in Herbert et al. (2016), and the following text is derived from there with minor modifications.

ROMS is a three-dimensional free surface, split-explicit ocean model which solves the Navier-Stokes primitive equations following the Boussinesq and hydrostatic approximations. We used the ROMS version developed at the Institut de Recherche pour le Développement (IRD) featuring a two-way nesting capability based on AGRIF (Adaptative Grid Refinement In Fortran) (Debreu et al., 2012). The two-way capability allows interactions between a large-scale (parent) configuration at lower resolution and a regional (child) configuration at high resolution. The ROMSTOOLS package (Penven et al., 2008) is used for the design of the configuration. The model configuration is built following the one performed by Djakouré et al. (2014) over the Tropical Atlantic. The large scale domain extends from 60° W to 15.3° E and from 17° S to 8° N and the nested high resolution zoom focuses between 17° S and 6.6° N and between 10° W and 14.1° E domain. This configuration allows for equatorial Kelvin waves induced by trade wind variations in the western part of the basin to propagate into the Gulf of Guinea and influence the coastal upwelling (Servain et al., 1982; Picaut, 1983). The horizontal grid resolution is 1/5° (*i.e.* 22 km) for the parent grid and 1/15° (*i.e.* 7 km) for the child grid (see Herbert et al. (2016), their Fig. 1). This allows an accurate resolution of the mesoscale dynamics since the first baroclinic

Rossby radius of deformation ranges from 150 to 230 km in the region (Chelton et al., 1998). The vertical coordinate is discretized into 45 sigma levels with vertical S-coordinate surface and bottom stretching parameters set respectively to $\theta_s = 6$ and $\theta_b = 0$, to keep a sufficient resolution near the surface (Haidvogel and Beckmann, 1999). The vertical S-coordinate Hc parameter, which gives approximately the transition depth between the horizontal surface levels and the bottom terrain following levels, is set to $H_c = 10$ m. The GEBCO1 (Global Earth Bathymetric Chart of the Oceans) is used for the topography (www.gebco.net). The runoff forcing is provided from Dai and Trenberth's global monthly climatological run-off data set (Dai and Trenberth, 2002). The rivers properties of salinity and temperature are prescribed as annual mean values. One river (Amazon) is prescribed in the parent model while five rivers, that correspond to the major rivers present around the Gulf of Guinea, are prescribed in the child model (Congo, Niger, Ogoou, Sanaga, Volta). At the surface, the model is forced with the surface heat and freshwater fluxes as well as 6 hourly wind stress derived from the Climate Forecast System Reanalysis (CFSR) (horizontal resolution of $1/4^\circ \times 1/4^\circ$) (Saha et al., 2010). Our model has three open boundaries (North, South, and West) forced by temperature and salinity fields from the Simple Ocean Data Analyses (SODA) (horizontal resolution of $1/2^\circ \times 1/2^\circ$) (Carton et al., 2000a, 2000b; Carton and Giese, 2008). The simulation has been performed on IFREMER Caparmor super-computer and integrated for 30 years from 1979 to 2008 with the outputs averaged every 2 days. A statistical equilibrium is reached after ~10 years of spin-up. Model analyses are based on the 2-days averaged model outputs from year 1998 to year 2008. The model has already been validated successfully with a large set of measurements and climatological data, and more detailed information about the model validations can be found in Herbert et al. (2016).

Note that throughout the whole text and figure captions, the term “intraseasonal variations” is used to designate the field obtained after the removing of the 30 days low-pass filtered field to the total field of the given year, while “intraseasonal anomaly” refers to the field obtained after the removing of the 30 days low-pass filtered field averaged over 1998-2008 to the total field of the given year.

For SST observations, we use data obtained from measurements made by the Tropical Rainfall Measuring Mission microwave imager (TMI). The dataset is a merged product available at www.remss.com. The SST data have a spatial resolution of $1/4^\circ$ and for the present study the 10 years' time series, from 1 January 1998 to 31 December 2008, obtained as 3-daily field. The important feature of the microwave retrievals is that it can give accurate SST measurements under clouds (Wentz et al., 2000). However, the major limitation to the microwave TMI observations is land contamination which results in biases of the order of 0.6°K within about 100 km from the coast (Gentemann et al., 2010). Thus, in the Optimal Interpolation TMI product the offshore zone with no data extends at approximately 100 km from the coast. This limits to some degree the analysis of near-coastal regions, in particular those dominated by coastal upwelling dynamics.

We also use for this study daily sea surface height (SSH) data, which are available for the period 1993–2012 and maintained by the organization for Archiving, Validation, and Interpretation of Satellite Oceanographic data (AVISO; www.aviso.altimetry.fr). The sea surface height dataset is a merged product of observations from several satellite missions Ssalto/Duacs (Segment Sol multimissions d'ALTimétrie, d'Orbitographie et de localisation précise/Developing Use of Altimetry for Climate Studies) mapped onto a 0.25° Mercator projection grid. All standard corrections have been made to account for atmospheric (wet troposphere, dry troposphere and ionosphere delays) and oceanographic (electromagnetic bias, ocean, load, solid Earth and pole tides) effects.

The mean sea surface topography for the period 1993–2012 was removed from the SSH to produce sea surface height anomalies.

In addition, surface pressure data were studied using ECMWF Atmospheric Reanalysis (ERA) for the 20th Century product. The four-hourly data are daily averaged and is available on <https://rda.ucar.edu> website. The product assimilates surface pressure and marine wind observations.

3. Seasonal variability of surface conditions in CLR

The purpose of this section is to describe the seasonal atmospheric and ocean surface conditions in the CLR.

The seasonal variability of SST, surface winds stress, horizontal current intensity, depth of 20° C-isotherm (hereafter referred to as z20), and the surface net heat flux from monthly averaged model outputs in the CLR for each year from 1998 to 2008 and averaged over the period are shown on Fig. 1. The reliability of the model is also provided by comparing the simulated and the corresponding TMI SST climatological seasonal cycle in the CLR (Fig. 1a). The SST variations display an annual cycle with highest temperature in boreal winter (warm season), when the ITCZ reaches its southernmost position and the trade winds are weakest, and minimum values in boreal summer (cold season), when the trades intensify. The most salient features of the atmospheric and hydrographic fields during May-June are also illustrated on Fig. 1 by May-June averaged maps. **Despite a warm bias (~1°C) compared to satellite observations, the model well reproduces the satellite pattern. While this warm bias in the eastern tropical Atlantic is well known in coupled climate models (e.g. Zeng et al., 1996; Davey et al., 2002; Deser et al., 2006; Chang et al., 2007; Richter and Xie, 2008), results from Large and Danabasoglu (2006) suggest indeed that a warm SST bias may also be present along the Atlantic coast of southern Africa in forced ocean-only simulation.** The SST May-June average map indicates that the boreal summer SST minimum is **related to** intensified cool SST around 6°S, in the Congo mouth region. In this region, the coast is oriented parallel to the trade flow which reinforces in boreal summer, thus favorable to coastal upwelling processes. The mean alongshore wind stress during May-June reveals in fact that upwelling conditions are observed over most of the CLR. Wind stress magnitude exhibits a semi-annual variability with a second maximum in October–December and a weakening during July-September season (Fig. 1b). The strengthening of winds in **boreal** spring is associated with a strengthening of mean current speed, particularly off Cape-Lopez between 2° S to 4° S and west of 8° E in May-June (Fig. 1c). The orientation of surface current is mostly westward for the May-June season, while it is northward from October to January (not shown). This general picture of surface circulation is consistent with observations (Merle, 1972; Piton, 1988; Rouault et al., 2009).

The region is also characterized by a shallow thermocline which depicts a strong semi-annual cycle (Fig. 1d). The evolution of z20 reveals a shoaling of the thermocline during May-July and a deepening up to October-November when it exhibits a maximum depth, in agreement with previous studies such as the one realized by Schouten et al. (2005) who find a similar seasonal cycle from SSH altimetric data.

The surface net heat flux exhibits a maximum in boreal winter and a minimum in July (Fig. 1e), following the seasonal cycle of solar shortwave radiations. As visible on the May-June average map, greater heating is found over cool waters, due to weaker heat loss via latent heat flux in these areas.

The seasonal cycle is modulated by strong year-to-year variations. The mean SST in the CLR in 2005 cools as early as March from TMI data and April from the model data. SST reaches weaker values than the climatologic ones, as observed by Marin et al. (2009) and Caniaux et al. (2011) west of 4° E. This 2005 cold anomaly is associated with positive wind speed and surface current speed anomaly in April-May (Fig. 1b&c) as well as shallower-than-average thermocline depth. In 2006, SST variations are very close to the climatologic ones.

Thus, the April-June season in the CLR appears as a transitional period characterized by strong seasonal evolution, primarily governed by the local winds which generate coastal upwelling in Congo mouth region and modulated by the variation of thermocline depth.

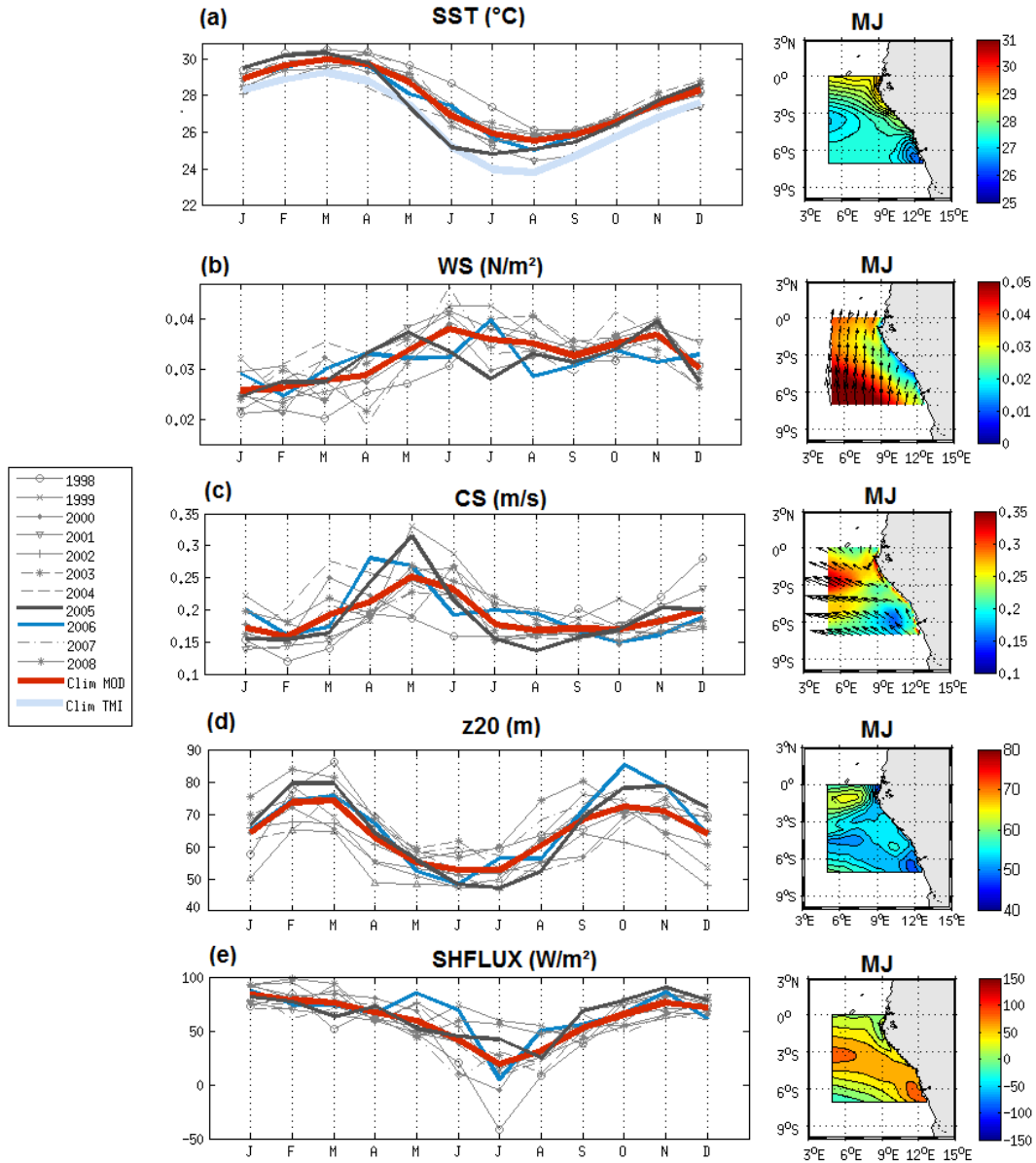


Figure 1: Monthly average of the (a) sea surface temperature ($^{\circ}\text{C}$); (b) wind stress direction (vectors) and magnitude (color field) ($\text{N}\cdot\text{m}^{-2}$); (c) horizontal surface current direction (vectors) and speed (color field) ($\text{m}\cdot\text{s}^{-1}$); (d) 20°C -isotherm depth (m); and (e) surface heat flux ($\text{W}\cdot\text{m}^{-2}$; positive values indicate downward flux) from January to December from 1998 to 2008 and for the climatology (averaged over 1998-2008) simulated by the model (red curve) and from the observations : monthly average TMI 3-daily SST data (light blue curve in (a)); averaged over 5°E - 14°E and 7°S - 0°S . Right panel: maps of each variable over May-June..

4. Analysis of **cooling episodes** in the CLR in 2005 and 2006

In this section, we examine the impact of intraseasonal wind bursts on SST in **the** CLR during the particular years 2005 and 2006 (Marin et al., 2009; Caniaux et al., 2011). We propose here to analyze in details the SST conditions in CLR, east of 5° E, for both years.

4.1 SST variations

In order to delineate the sequence of **cooling episodes**, we analyze the SST variations from 2-days averaged model outputs in 2005 and 2006 over the CLR, i.e. between 5° E and 12° E. **Both the SST (Fig. 3a & c) and intraseasonal variations of SST (Fig. 4a & f) have been shown.** In 2005, the intraseasonal **cooling episodes** took place on 22-24 April, 8-12 May, 16-20 May, 26-30 May, 12-16 June and 30 June-2 July, with a temperature drop ranging between -0.2°C to -1.7°C (Fig 4a). The cooling episodes occurred east of 5° E from May to September. They concerned especially the southern equatorial region (around ~3-4° S), except for the strongest events where they reached more northern equatorial regions, especially for the mid-May and late-May 2005 events. These latter were associated with an intense meridional SST front between the cold water south of the equator and the warmer water north of the equator, as visible on SST map for 12 May 2005 presented on Fig. 2. We can see cold waters extending along the eastern coast and in ACT region west of 5° W. In the model, cold waters are deflected offshore off Cape-Lopez, due to recursive bias in warm water intrusion toward the south.

Besides, model SST fields (Fig. 3a) indicate that the SST minimum (~24° C) in 2005 was reached in July, i.e. one month earlier than in 2006, as also noticed in seasonal variations of SST averaged in the region (Fig. 1a). These results illustrate the important role of the succession of quick and intense **cooling episodes** in the establishment of persistent cold anomalies **in the CLR**, as highlighted by Marin et al. (2009) in the equatorial region.

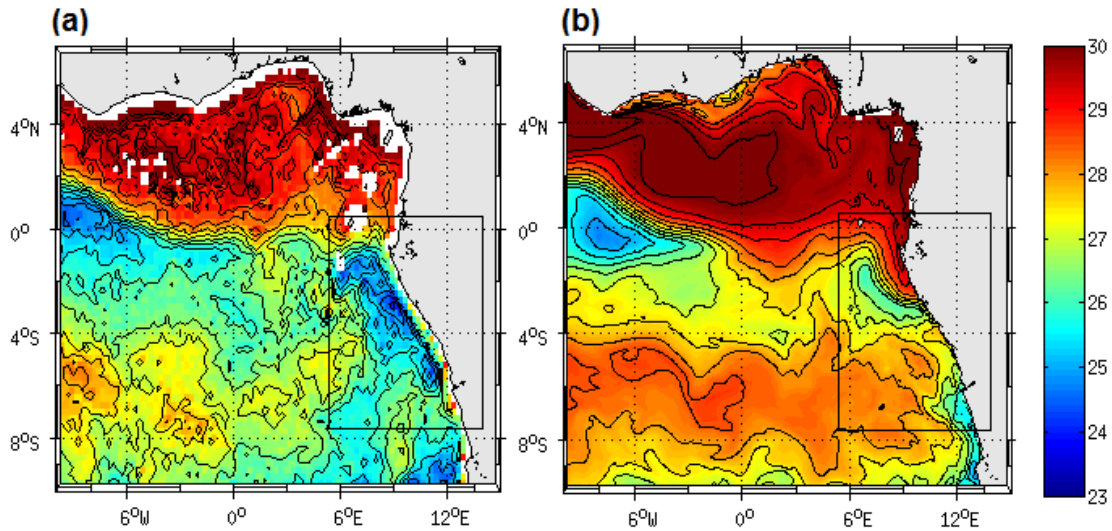


Figure 2: Map of the sea surface temperature ($^{\circ}$ C) on 12 May 2005 from 3-days average TMI data (a) and from the 2-days average model output (b). Note that for the model it corresponds to 11-12 May average whereas for TMI data it is 10-11-12 May average. The black square indicates the Cape-Lopez region (called ‘CLR’).

4.2 Forcing mechanisms

4.2.1. Local forcing

To examine the local forcing mechanisms responsible for the observed **cooling episodes** in CLR, the **intraseasonal variations of wind stress magnitude** are examined and compared in 2005 and 2006 (Fig. 4b & 4g). In 2005, successive periods of 6-16 days wind intensification occurred from late-March to late-May. The main **cooling episodes** described above are associated with positive intraseasonal wind stress speed occurring on 4-6, 12-16 & 24-28 May, and 10-12 & 28 June with a maximum for the 12-16 May event peaking on 14 May (at $\sim 0.025 \text{ N.m}^{-2}$). Another period of wind intensification is evidenced in late March – early April but it did not generate significant cooling despite comparable or even higher wind intensity than following wind events. In 2006, **periods of wind intensification extended from mid-March to July**. The main wind events occurred in 14-16 March, 2-4 & 16-24 April, 4-6 & 12-18 May, 12-14 & 24-26 June and 10-12 July with maximum intraseasonal wind stress magnitude in 16-24 April (0.019 N.m^{-2}) and 24-26 June (0.022 N.m^{-2}). Also, the wind event in late April 2006 did not generate a surface cooling as strong as the mid-May 2006 one, despite higher wind stress magnitude. To depict the subsurface conditions during **cooling episodes** in the CLR for both years, the 20° C-isotherm depths averaged from 5° E to 12° E are presented on Fig. 3b & 3d. They indicate strong correlation with SST variations on intraseasonal time scale with **minimum depths ($< 35 \text{ m}$) observed during the mid-May 2005 and end-May event**. In early April 2005 and before the late-April 2006, the thermocline was deeper, that can explain why wind intensification did not generate a surface cooling at these times. Indeed, at the time of the strong 16-24 April 2006 wind event, the z_{20} values was higher south of the equator than during the 14-16 May 2005 event, making the SST less reactive to comparable wind intensification. The same feature is observed in early May 2006, when the **higher z_{20} values indicate** deeper thermocline south of the equator

around 3-4° S than a few days later. Besides, the thermocline appeared globally shallower south of the equator in 2005 than in 2006, in agreement with the difference of the cooling intensity observed between the two years.

The Ekman pumping velocity w_e averaged over the CLR for 2005 and 2006 is shown on Fig. 4d & 4i respectively. The dates of intraseasonal upward velocities are quite well correlated with the dates of intraseasonal wind events (with correlation coefficient equal to 0.55 for 2005 and 0.41 for 2006), maximum being during the early-April, mid-May and end-May 2005 events and during late April, mid-June and end-June 2006. However, for comparable wind intensification, the boreal spring and summer wind events were not associated with comparable intensity of Ekman pumping velocity.

Another process that may contribute to the cooling in the upper layer is the vertical mixing due to intense vertical shear of the current. The maximum of the vertical shear magnitude fields in the CLR, averaged between 5° and 12° E for 2005 and 2006 (Fig. 4c & 4h), exhibited intensification south of the equator, centered around 3-4° S. Weaker intensification also occurred occasionally at the equator (located around 80 m depth between the westward surface South Equatorial Current – SEC – and the eastward subsurface Equatorial Under- Current). Around 3-4°S, the vertical shear was driven by the SEC, reinforced by prevailing southerly winds events through Ekman transport. It thus occurred at the date of wind events previously identified for 2005 and 2006, with stronger vertical shear occurring in early May 2005 and late April 2006. The intensity of the maximum of vertical shear magnitude during the events was quite similar between 2005 and 2006. The main difference lied in their meridional extent, related to the meridional extent of the strengthened southerly winds which reached equatorial region during the May 2005 events (not shown). We can also notice that for comparable wind intensification, the boreal spring and summer wind events were not associated with comparable intensity of vertical shear. The meridional wind component favorable to westward Ekman transport was actually stronger during April and May events than during summer ones (not shown).

The heat content within the mixed layer is also impacted by the sea surface heat fluxes. The net heat fluxes averaged between 5° E and 12° E are shown on Fig. 4e & 4j for 2005 and 2006 respectively. They indicate a net heating ($\sim 50-100 \text{ W.m}^{-2}$) over the 2° S - 5° S latitude band, where the SST cooling was strongest, suggesting other mechanisms involved. However, we notice some particular events during which the net heat flux was negative over most of the region. A strong net cooling (-30 W.m^{-2}) occurred during the 26-28 May 2005 event. It was mainly due to a sudden decrease of incoming surface short wave radiation (drop of about 80 W.m^{-2} in the CLR between 22 and 28 May; not shown) suggesting increased cloud cover. Another strong net cooling occurred on 2 April 2006 with a mean value in the CLR reaching -95 W.m^{-2} . It is more sudden than the end-May 2005's one, and was almost exclusively restricted to the CLR region with values reaching locally -185 W.m^{-2} (not shown). For both events, the net cooling did not concern the equatorial region west of 0°W.

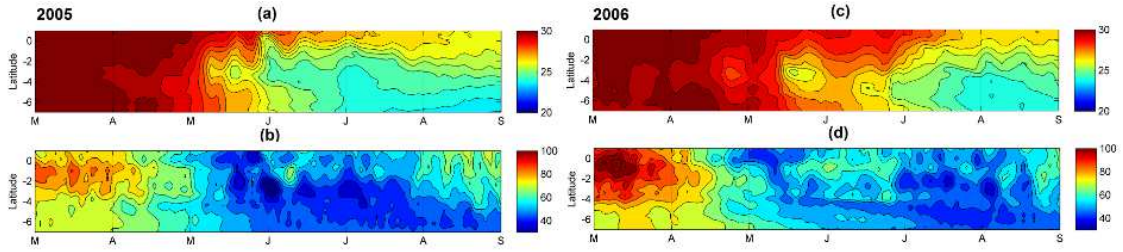


Figure 3: (a & c) Latitude-time diagram of the sea surface temperature (°C) averaged between 5°E and 12°E; (b & d) Latitude-time diagram of the 20° C-isotherm depth (m) averaged between 5° E and 12° E; from 1st March to 31 August 2005 (left panels) and 2006 (right panels).

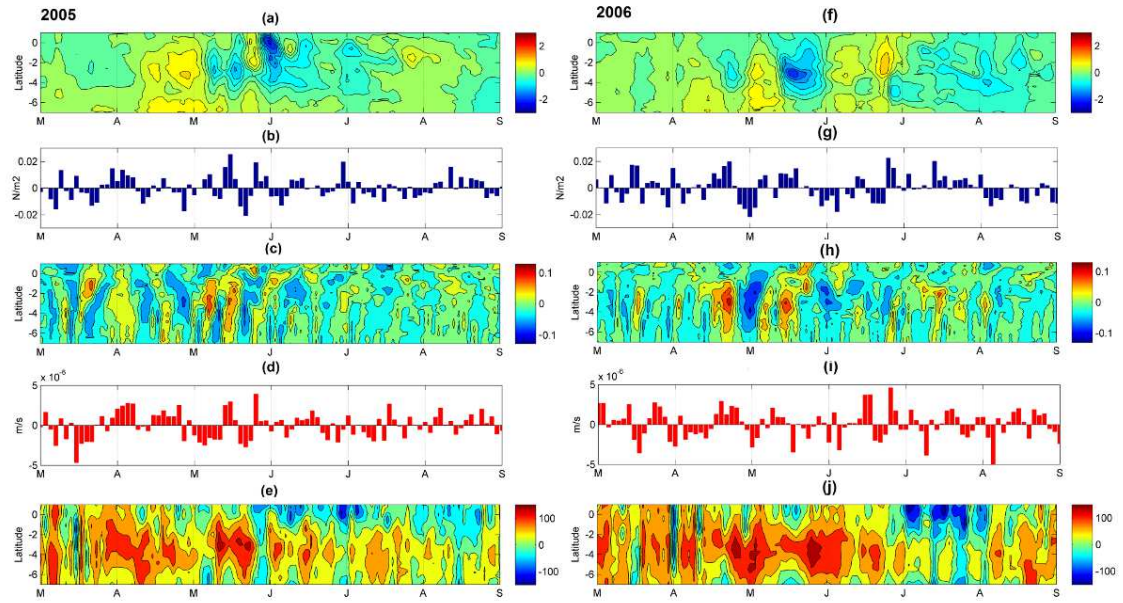


Figure 4: (a & f) Time-latitude diagram, from 7° S to 1° N, of the intraseasonal variations of sea surface temperature (in ° C) averaged between 5° E and 12° E; (b & g) Time evolution of the intraseasonal variations of wind stress amplitude (N.m⁻²) averaged between 5° E and 12° E and between 3° S and 0° S; (c & h) Latitude-time diagram of the intraseasonal variations of the maximum of the current vertical shear magnitude (m.s⁻¹) averaged between 5° E and 12°E; (d & i) Longitude-time diagram of the intraseasonal variations of Ekman Pumping (m.s⁻¹) averaged over the CLR. Ekman pumping values >0 indicate upwelling; (e & j) Latitude-time diagram of the net heat flux (W.m⁻²) averaged between 5° E and 12° E; from 1st March to 31 August 2005 (left panels) and 2006 (right panels). For details about calculations of intraseasonal variations, see Sect. 2.

4.2.2. Remote forcing

a. Highlighting of Kelvin wave propagation

As previously shown, the time of occurrence of the cold events in the CLR coincides with **shallow thermocline** which allows a mixed layer temperature to be more reactive to surface forcing. Indeed, because of its proximity to the equator, the thermocline in the CLR is affected by the arrival of equatorial waves, initiated in the **western** part of the basin. Pairs of alternate downwelling and upwelling Kelvin waves occur usually in February-March, July-September and October-November. Upon impingement with the eastern boundary, the incoming equatorial Kelvin wave excites westward-propagating Rossby waves and poleward-propagating coastal Kelvin waves (Moore, 1968; Moore and Philander, 1977; Illig et al., 2004; Schouten et al., 2005; Polo et al., 2008). The 20° C-isotherm depth anomalies along the equator and along 9°E are presented on Fig. 5 and clearly evidence large **negative** anomalies indicating shallower-than-average thermocline, propagating eastward along the equator and then southeastward for both years. The eastward propagation of Kelvin wave along the equator and southeastward along the coast is also well visible in the basin-wide SSH anomalies (Fig. 6) with a phase velocity of about 1.1-1.3m.s⁻¹, which fits well in the range between the second and third baroclinic equatorial Kelvin wave modes. **In 2005, negative SSH and z20 anomalies occurred in the West in early March- early April and in mid-May, whereas they occurred around late-February – mid-March and early May and June in 2006. The first Kelvin wave thus reached the CLR slightly earlier in 2006 than 2005, at the beginning of May. In addition, the two upwelling Kelvin waves followed each other more closely in 2005 than in 2006.**

Thus, the intensity of the cold events observed in **boreal** spring and summer 2005 and 2006 resulted from both the basin preconditioning by remotely forced shoaling of the thermocline, local mixing and upwelling processes in response to strong southerly local winds, as well as heat flux variations. In 2005, stronger wind intensification and favorably preconditioned oceanic subsurface conditions, made the coupling between surface and subsurface ocean processes more efficient than in 2006, resulting in stronger cooling.

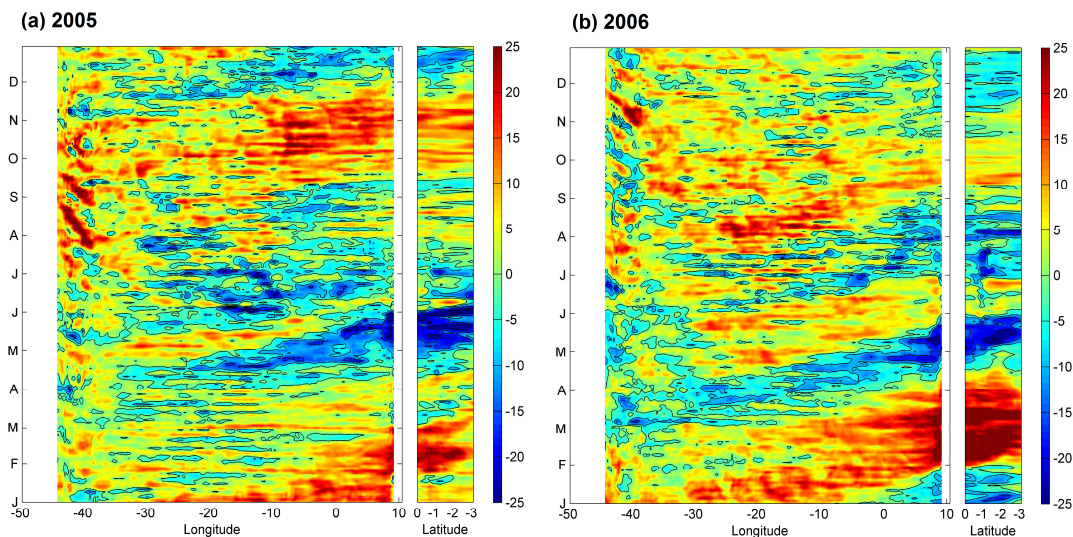


Figure 5: Time evolution of the intraseasonal anomaly of 20° C-isotherm depth (m) along the equator (between 54° W and 12° E) and along 9° E (between the equator and 3° S) for 2005 (left) and 2006 (right). Negative values indicate a 20°C isotherm depth closer to the surface. For details about calculations of the anomalies, see Sect. 2.

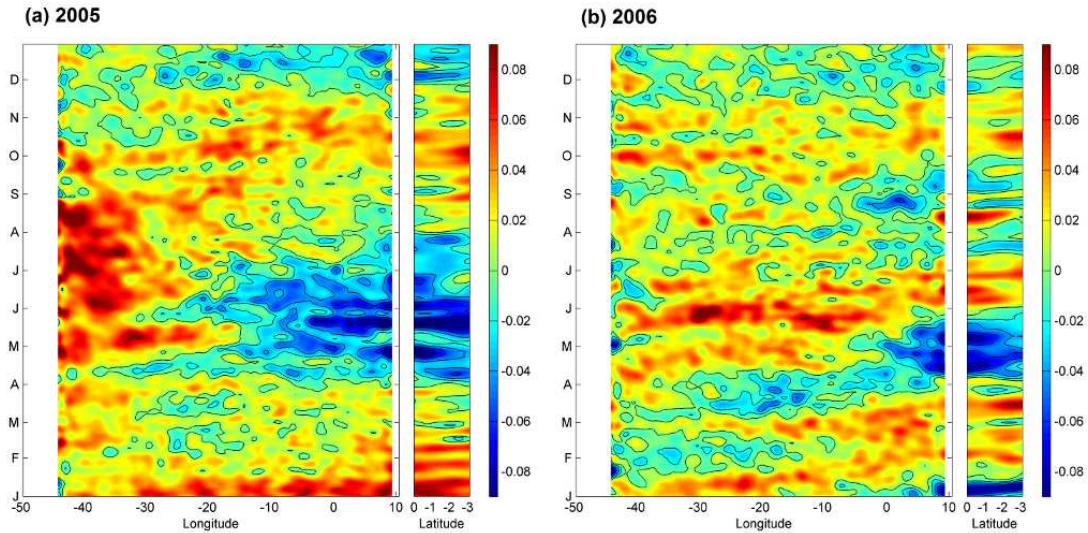


Figure 6: Time evolution of the sea level anomaly (m) along the equator (between 54° W and 12° E) and along 9° E (between the equator and 3° S) for 2005 (left), and 2006 (right) from AVISO data.

b. Kelvin wave generation and coinciding atmospheric conditions in the West

In order to identify the wind activity which accompanies the **generation** of Kelvin upwelling waves in winter 2005 and 2006 in the western part of the basin, we analyze the position of the ITCZ (averaged over 50° W-35° W) identified as the latitude where the meridional wind stress goes to zero (Fig. 7a & g). The intraseasonal anomaly of the zonal and meridional components of the wind stress (Fig. 7b-c & 7h-i), the intraseasonal anomaly of wind stress curl (Fig. 7d & j), as well as the intraseasonal anomaly of the z20 and SSH (Fig. 7e-f & k-l), averaged in the equatorial band (over 1° S and 1° N), are also presented. Many authors suggest that the source of the equatorial Kelvin wave is mainly related to a sudden change of the western equatorial zonal wind (e.g. Picaut, 1983; Philander, 1990): a symmetric westerly (easterly) wind burst along the equator will generate Ekman convergence (divergence) and thus force downwelling (upwelling) anomalies which then propagate eastward as a Kelvin wave (Battisti, 1988; Giese and Harrison, 1990). In 2005, shallower-than-average thermocline, evidenced by **negative z20 and SSH** anomalies, occurred in the end of March-beginning of April in the west part of the basin (Fig. 7e & f). The intraseasonal anomalies of meridional and zonal wind stress indicate that the maximum of thermocline slope anomaly was associated with a strengthening of northeast trades followed by a strengthening of southeast trades from either side on the equator. At the equator, we notice indeed a sudden reversing of meridional winds which turned southward on 27-28 March 2005 related to an abrupt southward displacement of the ITCZ which was then found south of the equator in the west part of the basin (Fig. 7a & b). The ITCZ returned its initial position four days later followed by a strengthening of easterlies which persisted for ~20 days (Fig. 7c). Climatologically, the latitudinal position of the ITCZ varies from a minimum close to the equator in **boreal** spring (March-May) in the west to a maximum extension of 10° N –

15°N in late boreal summer (August) in the east. Positive (negative) wind stress curl is found north (south) of the ITCZ. When the ITCZ is north of the equator, it induces upward (downward) Ekman pumping to the north (south) of the ITCZ. Thus, the southward shift of the ITCZ on 27-28 March 2005 accompanied with strong northerlies led to negative anomaly of wind stress curl south of the equator resulting in upward Ekman pumping. Results show indeed a strong negative anomaly on 22-26 March 2005 associated with the southward shift of the ITCZ just before the upwelling signal, initiated on 28 March. These changes contributed to a rise in the oceanic thermocline with a time lag of some days (Fig. 7e & f). The upwelling signal might then be reinforced by the symmetric easterly wind which concerned a large part of the western basin. Besides, we identify on Fig. 7d another peak of negative wind stress curl anomaly on 6-8 May 2005, more sudden than the previous winter one. It was associated with negative **z20 SSH anomalies** indicator of a thermocline rise initiated on 6 May 2005 in the west of the basin and which propagated eastward along the equator. The zonal wind stress anomalies (Fig. 7c) also indicate an easterly wind strengthening initiated in the beginning of May, which a maximum on 8-10 May, just after the minimum of wind stress curl.

In 2006, the upwelling Kelvin wave is identified in the first half of March in the west part of the basin (Fig. 7k & l). The coinciding atmospheric conditions were slightly different than the ones identified in 2005. In winter, the position of the ITCZ had a more southern position in 2006 than in 2005. It crossed the equator during a longer period (about 10 days from ~ Feb. 10 2006), reaching minimum latitude on 22-24 February. This location south of the equator induced a negative wind stress curl anomaly (Fig. 7j). As in 2005, the reversion of the meridional wind at the equator was followed by a strengthening of westward component of the wind stress few days after, which lasted for about ten days (Fig. 7i); however, it was of a lesser magnitude compared to 2005 and only concerned the westernmost part of the basin. In addition, the negative zonal wind anomaly concerned mainly the northeasterlies rather than the southeasterlies, leading to an anti-symmetric meridional wind pattern as well as symmetric zonal wind pattern on either side on the equator (not shown). These wind patterns were expected to generate Ekman convergence at the Equator and thus to reinforce the observed upwelling anomalies.

Thus, for both years, Kelvin upwelling wave occurred in the west while easterly winds were strengthened from either side of the equator after the ITCZ reached its southernmost location. This latter was observed one month earlier in 2006 than in 2005, and was associated with a negative wind stress curl anomaly. In winter 2005, the ITCZ was found south of the equator after a very sudden southward shift and was followed by strong easterlies during ~20 days, while in winter 2006, the ITCZ was found closer to the equator less sharply and during a longer period, followed by weaker easterlies compared to 2005. **These results highlight another way in which wind intraseasonal events may impact the SST variability in the East part of the basin, through the generation of Kelvin wave in the West which shoals the thermocline in the East few weeks later.**

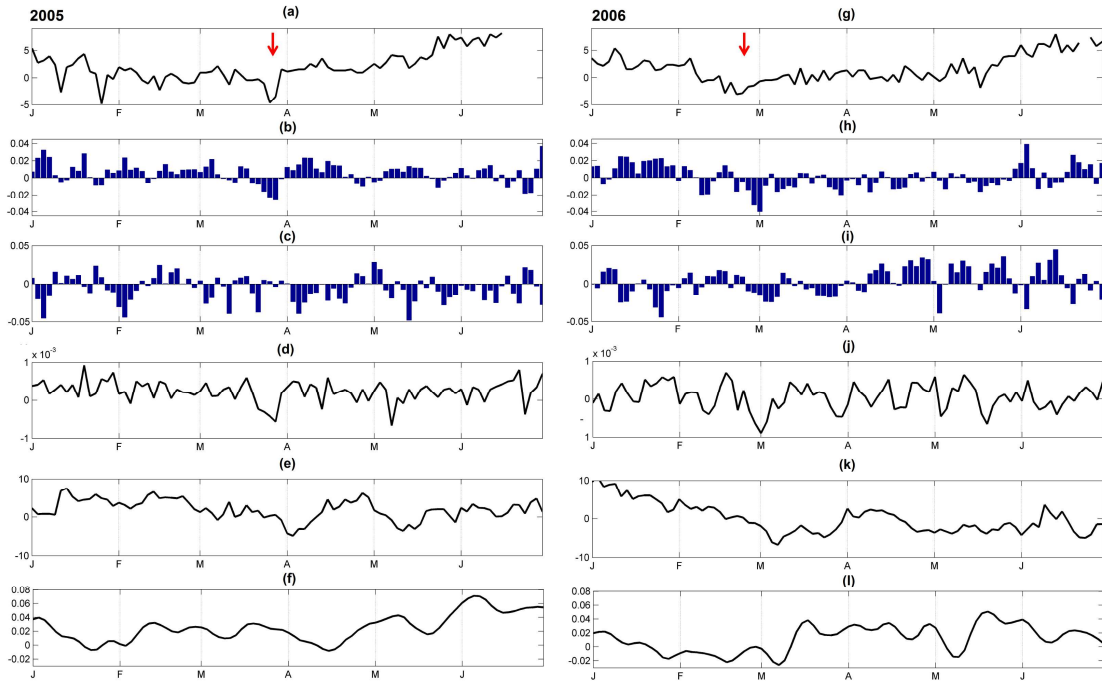


Figure 7: Time evolution, from 2-days averaged model outputs over Jan-June2005 (left) and Jan-June 2006 (right); of (a & g) the position (in latitude, between 5° S and 10° N) where the meridional wind stress value equal zero (indicator of the position of the ITCZ); (b & h) the intraseasonal anomaly of the meridional wind stress ($N.m^{-2}$) averaged between 50° W and 35° W and between 1° S and 1° N; (c & i) same as (b & h) but for intraseasonal anomaly of zonal wind stress ($N.m^{-2}$); (d & j) the intraseasonal anomaly of the wind stress curl ($N.m^{-2}$); (e & k) the intraseasonal anomaly of the 20° C isotherm depth (m); (f & l) the intraseasonal anomaly of the sea level (m). The red arrow in (a & g) indicates the southward shift of the ITCZ before the generation of the Kevin wave (see text). For details about the calculations of anomalies, see Sect. 2.

4.3. Westward extension of the CLR cooling

In the east, the cooling generated by southerly wind bursts in the CLR then progressively extended westward to connect with the southern boundary of the equatorial ACT. This phenomenon was more obvious in 2005 when the cooling which first concerned coastal area extended further offshore a few days after the two strong events occurring in the second half of May. To evidence the effect of these events on SST, maps of intraseasonal SST anomaly and intraseasonal wind stress anomaly averaged from 1 to 12 May (before the strong 2005 events; Fig. 8a) and from 14 to 31 May (during and after the strong 2005 events; Fig. 8b) are presented on Fig. 8. The same calculations have been for 2006 for comparison. The results illustrate an enhancement after 10 May of the cooling in the east associated with southerly wind intensification and an extension of the cooling especially south of the equator up to 20°W.

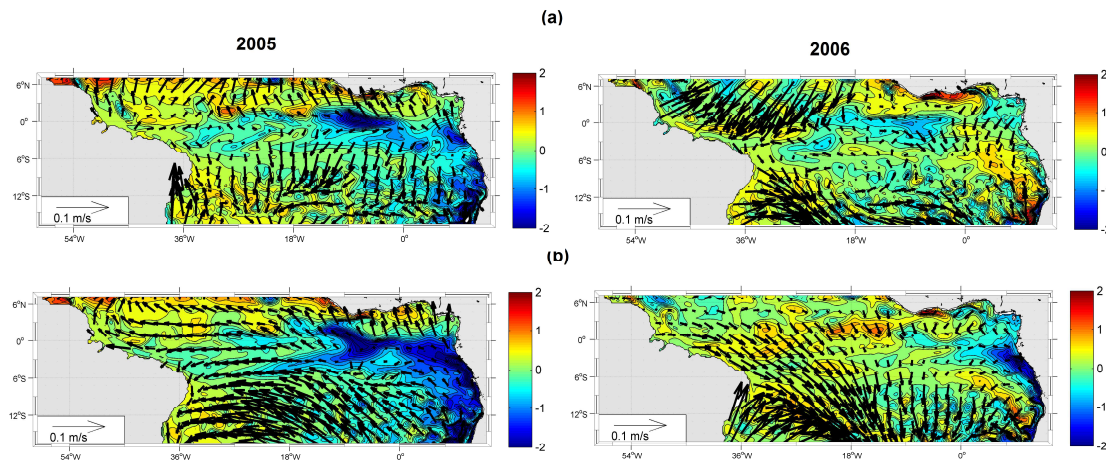


Figure 8: (a) intraseasonal anomaly of sea surface temperature ($^{\circ}$ C; color) superimposed with intraseasonal anomaly of wind stress intensity (arrows) averaged over 1-12 May 2005 (up panel) and over 14-30 May 2005 (down panel); (b) same but for 2006. For details about the calculations of the anomalies, see Sect.2.

To better understand the oceanic processes implied in this cooling extension, we compared the SST, z20, SLA and zonal velocities along 3° S from March to September 2005 (Fig. 9 a-d) and 2006 (Fig.9 e-h). In 2005, the cooling westward extension was associated with a westward propagation of a shallower thermocline and negative SLA from the African coast up to 5° - 10° W combined with enhanced surface westward current fluctuations at the dates of the successive events from April-June. The fluctuations of the westward surface current occurring off Gabon with periods of \sim 8-10 days were related to the strengthening of southerly winds during the wind bursts at the same periods (Fig. 4b & g). The surface current in this area is part of the westward SEC which is known to intensify during the cold season (Okumura and Xie, 2006). Our study implies shorter time scales than seasonal scale but the intensification of the SEC during wind bursts through Ekman transport processes might contribute to the westward extension of the cooling by advection of cold eastern upwelled water. This is in agreement with DeCoëtlogon et al. (2010) who found from model results that at short time scale (a few days), more than half of the cold SST anomaly around the equatorial cooling could be explained by horizontal oceanic advection controlled by the wind with a lag of a few days. In addition, minimum z20 and SLA values propagating westward at 3° S (Fig. 9b & c), initiated from the coast with a propagating speed of around 10 cm.s^{-1} , which is very close to the phase speed of Rossby waves. Indeed, the generation of the westward waves at the coast coincided with the arrival of Kelvin waves (see Fig. 5a) suggesting the possibility of Kelvin wave's reflection processes into symmetrical westward propagating Rossby waves. A westward propagation of z20 and SLA minimums, although less obvious, was presently also identified at 3° N (not shown).

In 2005, the locally wind-forced component of the wave might reinforce the remote part of the reflected wave signal at the coast by the sea level slope which balanced the strengthening of alongshore winds blowing during the mid-May and late-May events. The quantitative and respective contributions of local and remote wind forcing to this wave is out of the scope of this study and would require further analysis. This phenomenon is supported in 2005 by anomalous eastward expanded southerly wind bursts observed in May 2005. The month of

May is besides a period when westward surface currents are usually maximum (as visible on the mean seasonal cycle shown on Fig.1c). Thus, the combined effects of westward surface currents (via advection and vertical mixing through horizontal current vertical shear), local wind influences (via vertical mixing) and wave westward propagation, resulted in the extension of cold upwelled water from the eastern coast to near 20° W.

In 2006, the westward extension of cold waters established later, from the beginning of July. A coastal cooling occurred on 18-26 May but no westward extension of the cold waters is observed at this period (Fig. 9e). In 2005, the two upwelling Kelvin waves followed each other closely while in 2006, the first Kelvin upwelling wave reached the coast in May and the second in July (Fig.5b & Fig. 6b and Fig. 9f). In addition, the intraseasonal wind strengthening responsible of the coastal cooling on 18-26 May 2006 is less intense (wind stress mean in the CLR $\sim 0.04\text{N.m}^2$) than the one in mid-May 2005 ($\sim 0.06\text{N.m}^2$; which is preceded and followed by another wind bursts few days before and after; Fig. 3b & Fig. 4b).

The analysis over 1998-2008 period shows that the westward extension of the cold SST takes place every year but begins at different times of the year (not shown). It occurs generally from June-July, when the cooling episodes usually occur in the east at this location, and is thus closely linked with the shoaling of the thermocline due to the arrival of a Kelvin upwelling wave at the eastern coast

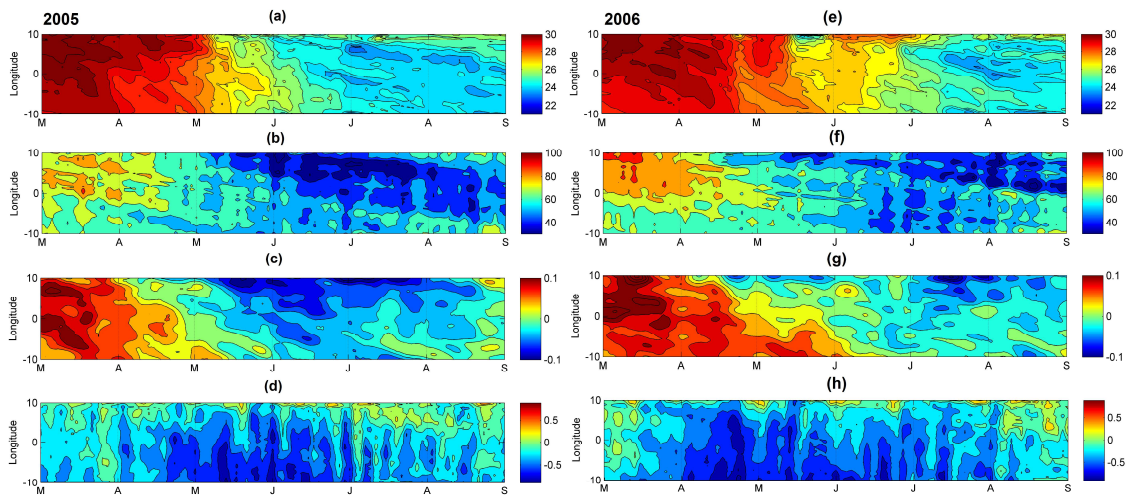


Figure 9: Time-longitude diagrams at 3° S between 10° W and 10° E, and from 2-days averaged model outputs from 1st March to 31 August 2005 and 2006, of (a & e) the sea surface temperature (° C); (b & f) the 20° C isotherm-depth (m); (c & g) the sea level anomalies from AVISO data (m); and (d & h) the zonal component of surface velocity (m.s⁻¹).

In conclusion to this section 4, the SST variability in the CLR at intraseasonal time scales is the result of combination between basin preconditioning by remotely forced shoaling of the thermocline via Kelvin wave, local mixing induced by current vertical shear, and upwelling processes in response to strong southerly winds. As highlighted for the 26-28 May 2005 and 2 April 2006 events, the net heat flux may also contribute to cool the surface waters, through enhanced cloud cover which decrease the incoming solar radiation. The cold upwelled waters around 3°S extend then westward from the eastern coast to near 20°W by combined effect of

the westward propagating Rossby waves as well as vertical mixing and advection processes. The cool water may thus contribute to the cooling in the southern edge of the cold tongue region. Although the processes implied differ slightly due to the presence of the coast, the SST variability in the CLR is quite close to the one in the equatorial cold tongue region (not shown), due to similar atmospheric forcing. However, for a given wind burst, the intensity of SST response in the CLR and in the cold tongue region is modulated by subsurface conditions which are under the influence of equatorial Kelvin wave. In May 2005, the Kelvin wave reached the eastern coast while three wind bursts occurred. The thermocline was thus shallower in the east than west of 0°W , providing favorable subsurface conditions making the coupling between making the SST more reactive to wind intensification occurred during this month. In addition, the decrease short wave radiations due to enhanced cloud cover during the 26-28 May 2005 event or 2 April 2006 event, which contribute to the cooling in the CLR, did not concern the equatorial region east of 0°W .

5. Focus on the mid-May 2005 event

We have previously identified five main cold events in 2005 (22-24 April, 8-12 May, 16-20 May, 26-30 May and 14-18 June), characterized by a temperature drop ranging from -0.2°C to -1.7°C in the model. Analysis of intraseasonal wind stress magnitude (Fig. 4b) has revealed that each event is associated with strengthening of equatorward winds, especially during the 14-16 May event when the intraseasonal wind stress magnitude averaged over the CLR is the strongest one. This particular event has been found to be responsible for the sudden and intense SST cooling in the eastern equatorial Atlantic and identified as part of manifestation of temporal variability of the St. Helena Anticyclone (Marin et al., 2009). In this section, we focus on this mid-May event, to better understand the processes **at play** during this unusual event.

5.1 Atmospheric conditions

5.1.1 Wind and surface atmospheric pressure

The spatial distribution of the mid-May 2005 wind event can be inferred from Fig. 10 where CFSR wind speed fields superimposed with daily precipitation fields, surface pressure, wind speed curl, and downward shortwave radiation, are presented from 13 May to 17 May. The event was characterized by intense southeasterly wind east of 15°W and from 30°S to the equator from 13-14 May, concomitant with a strengthening of the easterlies west of 30°W between 30° and 15°S (Fig. 10a). The strong southeasterly winds drifted then westward up to 15-16 May when the maximum was located in the western part of the basin off northeastern Brazilian coast. Simultaneously, a strengthening of southerly winds occurred north of the equator in the Gulf of Guinea. **The strong winds during the event were associated with high pressure core of the Saint Helena Anticyclone, especially on 13-14 May, also associated with particularly low pressure under the ITCZ 4 days later (Fig. 10c). The pressure fall during the mid-May 2005 event appeared as the lowest in May over the whole decade (not shown). The meridional surface pressure gradient during the event is thus found to be the strongest over 1998-2008 period. That suggests strong Hadley circulation intensity during the mid-May event and therefore strong**

equatorward moisture flux, allowing the deep atmospheric convection in the Gulf of Guinea to be triggered at a self-sustaining level (see Sect. 5.2 following).

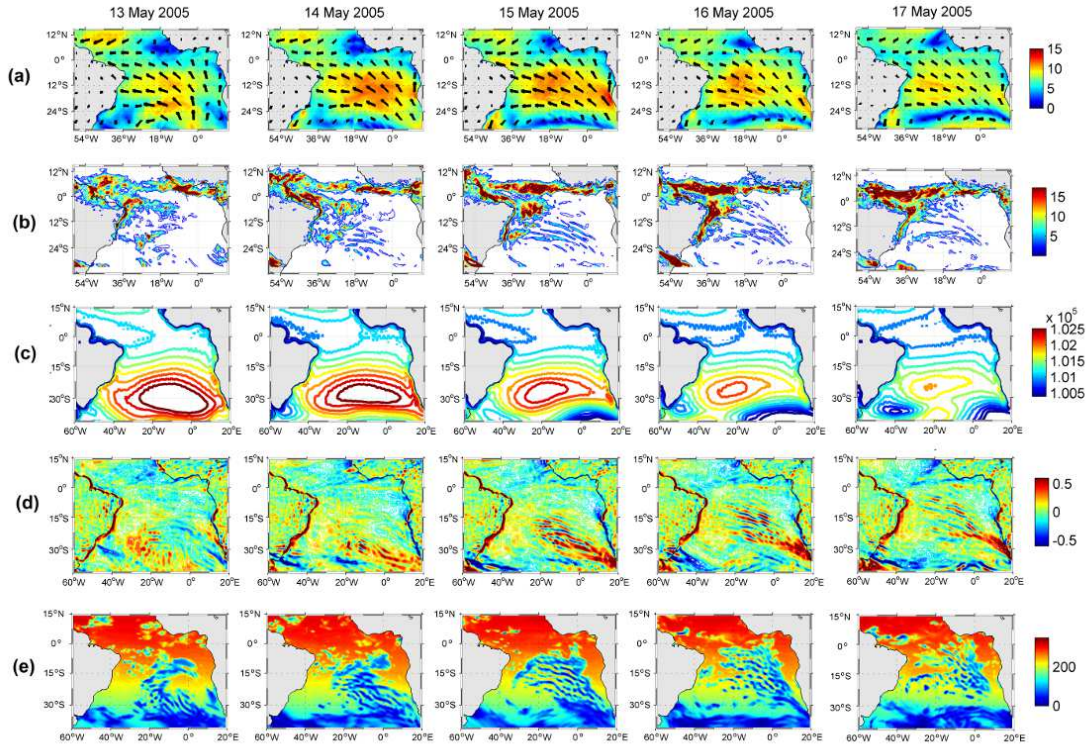


Figure 10: Daily-averaged, from 13 May to 17 May 2005 (left to right panels), of (a) wind magnitude (color field) ($\text{m}\cdot\text{s}^{-1}$) superimposed with wind vectors from CFSR fields; (b) precipitation rate ($\text{kg}\cdot\text{m}^{-2}/\text{day}^{-1}$) from CFSR fields; (b) surface pressure (hPa) from ERA-20C reanalysis; (c) wind speed curl ($\text{m}\cdot\text{s}^{-1}$) computed from CFSR wind speed fields; and (d) downward short-wave radiation ($\text{W}\cdot\text{m}^{-2}$) from CFSR fields.

5.1.2 Precipitation

The maps of precipitation rate during the event (Fig. 10b) display a band of heavy precipitation ($9\text{-}17 \text{ kg}\cdot\text{m}^{-2}/\text{day}$) between $5^{\circ} - 9^{\circ} \text{ N}$ and off northeast Brazil from the coast to 15° W and from 10° S to 3° S . The maximum precipitation rate in this region occurred on 15-16 May concomitant with the easterly winds strengthening. This convective zone, located between the ITCZ north of the equator and the South Atlantic Convergence Zone (SACZ) in southern tropics, is the Southern Intertropical Convergence Zone (SICZ) (Grotsky and Carton, 2003). This zone forms usually later, by June-August, when the southern branch of the convection separates from the ITCZ which moves north of the equator. Grotsky and Carton (2003) showed that this rainfall pattern appears closely linked to the seasonal change in SST difference between the ACT region (which they defined between $15^{\circ} \text{ W} - 5^{\circ} \text{ W}$, $2^{\circ} \text{ S} - 2^{\circ} \text{ N}$) and the SITCZ region ($25^{\circ} \text{ W} - 20^{\circ} \text{ W}$, $10^{\circ} \text{ S} - 3^{\circ} \text{ S}$). They argued that the

seasonal appearance of the ACT along the equator sets up pressure gradients within the boundary layer that induce wind convergence in the SITCZ region. Based on Grodsky and Carton (2003) results, the unusually rainfall conditions during mid-May event might thus be explained by strong SST gradient between the two regions caused by unusually early cooling in the ACT region at this time of the year.

5.1.3 Generation of atmospheric gravity wave

The precipitation fields during the mid-May event (Fig. 10b) also evidence rainfall pattern typical of atmospheric gravity wave train characterized by a horizontal wave length ~ 500 km and initiated by a front system (forming the northern boundary of a low pressure system) which developed around 17° S on 14 May and traveled northeastward until 17 May. The rainfall train was associated with oscillatory wind speed curl train alternating between positive and negative values (Fig. 10d) as well as alternating downward shortwave radiation minimum (Fig. 10e) associated with the wave clouds. Gravity waves are known to play an important role in transporting the momentum and energy through long distances (Fritts, 1984). Here, they would be a way to carry momentum and energy from South Atlantic to the equator during the strong event.

[Figure 11 and associated comments has been deleted]

5.2 A decisive event for coastal monsoon onset

The mid-May 2005 wind event was found to be involved in the early onset of the ACT development (Marin et al. 2009, Caniaux et al., 2011). The influence of the cold tongue on the WAM onset has been suggested by several authors (Okumura and Xie, 2004; Caniaux et al., 2011; Nguyen et al., 2011; Thorncroft et al., 2011). At the seasonal time-scale, Caniaux et al. (2011) suggest that it comes from strong interactions between the SST cooling and wind pattern in the eastern equatorial Atlantic: the ACT serves to accelerate (decelerate) winds in the northern (southern) hemisphere contributing to the northward migration of humidify and convection, and pushes precipitation to the continent. Thus, due to its impact on ACT development, the mid-May 2005 wind event is also linked to the onset of the WAM in 2005 which has been the earliest over 1982-2007 period from Caniaux et al. (2011). In this section we aim to better understand how this single wind event may have such impact. For further information on the WAM, the reader can refer to Leduc-Leballeur et al. (2013) and Caniaux et al. (2011).

In order to analyze the air-sea pattern in the northern Gulf of Guinea during May-June 2005, we show in Fig. 11 the wind stress magnitude, precipitation rate, and SST fields averaged from 10° W to 6° W. The wind strengthening appeared first south of the equator on 12-16 May and then north of the equator from 14-18 May. It was associated with strong rainfall extending southward up to 2° N. Equatorial cooling occurred 4 days after the event and slowed down the overlying winds by feedback mechanisms. The winds north of the equator then remained stronger than in the ACT region and strengthened again north of the Equator on 22-28 May together with precipitation maximum pushed northward (around 5° N) after the event.

Thus, this mid-May event appears as the “decisive event” which triggered the abrupt transition between the two wind patterns in the northern Gulf of Guinea, when the wind north of the equator became and remained stronger than south of the equator. It occurred 15 days earlier than the average date (31 May) identified by Leduc-

Leballeur et al. (2013) over 2000-2009 period. According to these authors, the time of occurrence of this phenomenon would be related with the strength of anomalous moisture flux. They explain that in April-May the low atmospheric local circulation is present only during an equatorial SST cooling and surface wind strengthening north of the equator, both generated by a southerly wind burst, before disappearing until the next wind burst. In June-July the low atmospheric local circulation is then always present and intensified by the wind bursts. Thus, the establishment of an abrupt seasonal transition event as observed in 2005, occurring much earlier than the reference date, supposed anomalously strong equatorial cooling caused by unusual strong southerly winds which allowed, through air-sea interactions mechanisms, to trigger the deep atmospheric convection in the Gulf of Guinea at a self sustaining level.

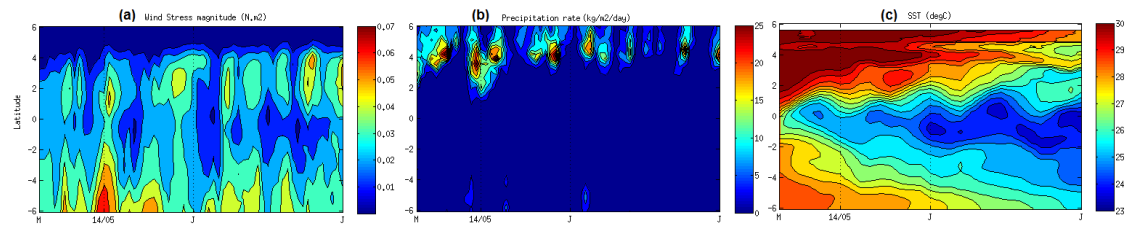


Figure 11: Time evolution, in May and June 2005 between 6° S and 6° N and averaged between 10° W and 6° W, of the (a) daily averaged wind stress magnitude (N.m^{-2}) computed from CFSR wind speed fields ; (b) daily averaged precipitation rate ($\text{kg.m}^{-2}/\text{day}$) from CFSR fields and (c) 2-daily averaged SST ($^{\circ}\text{C}$) fields, from the forced model.

5.3. Why made the mid-May 2005 event so special?

To better understand which makes the particularity of the mid-May 2005 event, the atmospheric and oceanic conditions (SST, intraseasonal SST anomalies, intraseasonal short-wave radiation flux anomalies (hereafter RADSW), intraseasonal wind stress magnitude anomalies, intraseasonal z20 anomalies, and intraseasonal meridional SST gradient anomalies) averaged over the 10° W - 6° W region and between 15° S to 5° N during April-May are analyzed over the 1998-2008 period (Fig. 12). The intraseasonal wind stress magnitude anomaly during mid-May event appears to be one of the strongest over the whole 1998-2008 period (up to 0.13N.m^{-2} around 15°S and 0.05N.m^{-2} in equatorial region). These strong wind conditions are usually met later in late boreal spring or summer, when the St. Helena Anticyclone strengthens and shifts northward toward the warm hemisphere. The wind intensification in mid-May 2005 was associated with particularly weak RADSW from South Atlantic to the northern equatorial region, suggesting cloud albedo effect during the event which tended to cool the mixed layer. We can notice that the April-May 2005 period was characterized by the weakest mean RADSW.

In addition, at the time of the event, the surface waters were already cooled by previous wind bursts (e.g. 20 April and 8 May). The SST response to the mid-May event occurred 4-6 days later, inducing the weakest equatorial SST values for April-May season over the whole 1998-2008 period (SST drop of $\sim 3^{\circ}\text{C}$ inducing SST $< 24.8^{\circ}\text{C}$). The cooling also caused an enhanced SST front around 1° N, as shown on Fig. 12 (bottom panel), which was found to be the earliest and strongest one over the 1998-2008 period. This meridional SST gradient

was responsible for the wind surface intensification north of the equator (Fig. 11a and Fig. 12, fourth panel) through air-sea interaction mechanisms as described by Leduc-Leballeur et al. (2011). Another SST gradient maximum is found at the end of May 1998 but it was not extended as eastward than during the mid-May 2005 event (not shown).

When the wind burst occurred on 14 May 2005, the 20°C-isotherm depth in the area was anomalously shallow south of the equator and slightly deeper at the equator (Fig. 12, fifth panel). The thermocline shoaling associated with the Kelvin wave appeared in fact a few days earlier providing favorable subsurface conditions which made the SST response to previous wind bursts (20 April and 8 May) more effective. At the time of the mid-May event, the wave already reached more eastern areas, as shown in previous sections.

Thus, the particularity of the mid-May 2005 event mainly lies in the i) anomalous atmospheric conditions related to strong St. Helena Anticyclone perturbation; ii) cooling initiated by the succession of previous wind bursts; and iii) favorable subsurface local ocean conditions preconditioned by equatorial waves which shoaled the mixed layer. Another wind burst of comparable intensity occurred at the beginning of May 2000 (Fig. 12, fourth panel) while the thermocline was shallow, causing SST cooling at the equator (Fig. 12, first and second panels). However, the wind strengthening was less sudden than during the mid-May 2005 event and the resulting cooling took place over a less broad region (not shown). In addition, the surface pressure drop in the ITCZ region was not as pronounced as during mid-May 2005 event.

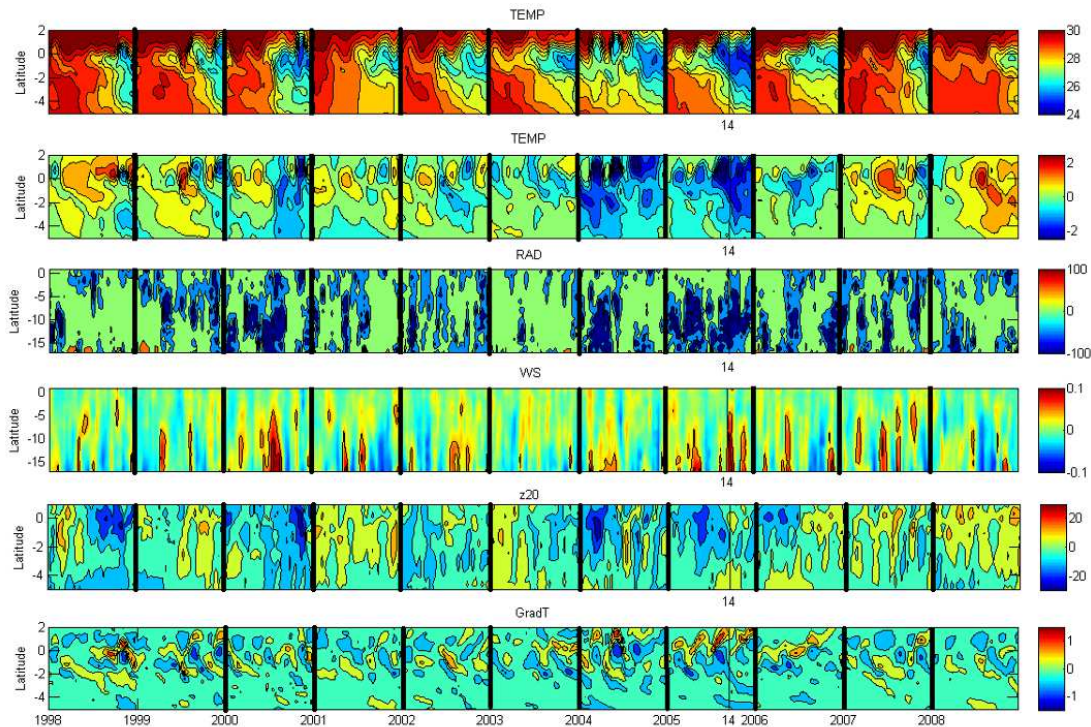


Figure 12: Time-latitude diagrams for April-May along the 1998-2008 period, of 2-days average, from top to bottom i) SST (°C); ii) intraseasonal anomaly of SST (°C); , iii) intraseasonal anomaly of wind stress magnitude ($N.m^{-2}$) from CFSR fields; iv) intraseasonal anomaly of short-wave radiation surface flux ($W.m^2$)

from CFSR fields; v) intraseasonal anomaly of 20°C-isotherm depth (m) computed from the forced model SST; vi) intraseasonal anomaly of meridional SST gradient (every 0.5° of latitude), from the forced model; averaged over 10° W-6° W. The vertical black thin line indicates the date of 14 May, 2005. For details about the calculations of the anomalies, see Sect. 2.

[Figure 14 has been deleted]

6. Summary and discussion

In this study, the impact of intraseasonal winds on SST in the far eastern Tropical Atlantic during boreal spring 2005 and 2006 has been investigated from observations and numerical simulation. We first focus our study in the Cape-Lopez region (CLR), east of 5°E and between the equator and 7° S, where the seasonal and interannual SST variability is poorly documented. There, the boreal spring (AMJ) season corresponds to a transitional period between high SST in boreal winter and weak SST in boreal summer, under the influence of local winds. Intensified cool SSTs are observed in the coastal upwelling area located around 6° S in the Congo mouth region, associated with mean alongshore wind conditions. Boreal spring season is in fact characterized by maximum winds amplitude, influence of which is made more effective by shallow thermocline depth, itself strongly influenced by remote forcing. The seasonal cycle in the CLR is modulated by strong year-to-year variations, as observed in boreal spring 2005 when cold SST anomaly are associated with shallower-than-average thermocline depth and positive wind speed anomaly.

The intraseasonal wind bursts which occurred in boreal spring 2005 and 2006 generated cooling episodes especially around 3°-4° S except for some strongest events when the cooling reached more northern equatorial region, especially during the mid-May and end-May 2005 events. The intensity of the cold events resulted from both basin preconditioning by remotely forced shoaling of the thermocline (via Kelvin wave), local mixing (induced by current vertical shear) and upwelling processes in response to strong southerly local winds. For one particular event, on 26-28 May 2005, the net heat flux also tended to cool the surface water, due to enhanced cloud cover which decreased the incoming solar radiations. In the CLR, stronger wind intensification and favorably preconditioned oceanic subsurface conditions in 2005 made the coupling between surface and subsurface ocean processes more efficient than in 2006, resulting in stronger cooling. It should be noted that the occurrence of intraseasonal wind intensification in the CLR is not specific to the boreal spring/summer 2005 and 2006 and is observed every year over the 1998-2008 period of study (not shown). However, their impact on SST variability in the region is modulated depending of the strength of wind intensification and of the subsurface preconditioning. For example, the year 1998, known as a "warm year", is characterized by anomalous warm SST in boreal spring/summer in the CLR., associated with anomalous weak winds and anomalous deep thermocline.

The preconditioning of subsurface conditions in the area via Kelvin wave at the dates of the wind bursts depended on the atmospheric conditions in the western part of the basin a few weeks earlier. Previous studies (e.g. Picaut, 1983; Philander, 1990) suggest that the source of an equatorial Kelvin wave is mainly related to a sudden change of the zonal wind in the west. Analysis of atmospheric and oceanic conditions at intraseasonal to daily scale in winter 2005 and 2006 showed that for both years, an Kelvin upwelling wave was initiated in the

west while easterly winds were strengthened from either side of the equator just after the ITCZ to be at its southernmost location. This latter was observed one month earlier in 2006 (late February – early March) than in 2005 (late March-early April), and was associated with a negative wind stress curl anomaly. In winter 2005, the ITCZ was found south of the equator after a very sudden southward shift and was followed by strong easterlies during ~20 days, while in winter 2006, the ITCZ was found closer to the equator less sharply and during a longer period, followed by weaker easterlies when compared to 2005. These results obtained for the years 2005 and 2006 years do not imply that same atmospheric conditions would be observed for winter upwelling Kelvin wave of other years. Especially, the year 2005 was very particular and also exhibited anomalously cold SSTs in the south Atlantic and anomalously warm SSTs in the north Atlantic initiated in fall 2004, signature of a meridional mode (Virmani and Weisberg, 2006; Foltz and Mc. Phaden, 2006; Hormann and Brandt, 2009).

Upon impingement at the eastern boundary, the incoming equatorial Kelvin wave excites westward-propagating Rossby waves and poleward propagating coastal Kelvin waves. In 2005, the Kelvin wave reached the coast around mid-May while southerly winds strengthened, allowing the reflected wave to be reinforced by the local wind. This resulted in westward propagation of negative z_{20} and SSH anomalies which, combined with enhanced westward surface currents, provided favorable conditions to westward extension of cold upwelled water from the eastern coast to near 20°W through advection and vertical mixing.

In the second part of the study, we specially focused on the mid-May 2005 event (13 May to 16 May) that was characterized by strong southerly wind strengthening in the eastern Tropical Atlantic Ocean. It was found to be responsible for the sudden and intense SST cooling in the Gulf of Guinea and the CLR, and involved in the early onset of the ACT development in 2005 and therefore in early onset of the WAM. The analysis of atmospheric and oceanic conditions in the Gulf of Guinea associated to this event allowed to show that the mid-May event, controlled by the St. Helena Anticyclone, can be identified as a “decisive event” which triggered the abrupt transition between two wind patterns in the northern Gulf of Guinea. Unusual strong southerly winds induced anomalously strong equatorial cooling which in turns slowed down the overlying wind feedback mechanism and generated stronger than normal southerlies north of the equator through the SST front around 1°N . This triggered the deep atmospheric convection in the Gulf of Guinea at a self-sustaining level and the beginning of coastal precipitation. The time of occurrence of this phenomenon, 15 days earlier than the averaged date (31 May from Leduc-Leballeur et al., 2013), suggests that the mid-May 2005 event was associated with anomalous strong moisture flux. The description of atmospheric conditions over the 1998-2008 period has shown that the 2005 event was characterized by the strongest surface pressure gradient between the St. Helena high pressures and the low pressures under the ITCZ, inducing strong Hadley cell activity. No similar atmospheric pattern was observed during the whole 1998-2008 period. Another wind burst of comparable wind intensity occurred at the beginning of May 2000. This event also induced a cooling at the equator but the surface pressure decrease in ITCZ region was not as pronounced than during mid-May 2005 event and the SST gradient around 1°N was weaker. In addition to coastal precipitation in the Gulf of Guinea and due to the early cooling in the ACT region, unusually rainfall conditions also occurred between the northeast coast of Brazil and 15°W within the SITCZ, which generally forms in early boreal summer.

Finally, this study highlights the impact of a strong southerly wind burst in the eastern tropical Atlantic during boreal spring season, which is a transitional period during which an anomalous strong energy input may tip the energy balance from an equilibrium state toward another one and thus impact the WAM system. The analysis of atmospheric and oceanic conditions during the mid-May 2005 wind event allows to highlight the different processes through which the wind power provided by the wind burst is brought to the ocean: i) direct effect of the wind on the SST in the eastern tropical Atlantic; ii) changes in the trade winds in the western equatorial Atlantic exciting eastward-propagating equatorial Kelvin waves; iii) energy transport via atmospheric gravity waves from South Atlantic; and iv) energy supply to Rossby wave. In addition to unusual atmospheric conditions in mid-May 2005, the ocean response intensity to this event was also enhanced by the subsurface conditions, made favorable by previous wind bursts, either local (e.g. in 6-8 May) or occurring a few weeks before in the West.

It is crucial to better describe the atmospheric and oceanic processes in play during such extreme event, notably in order to reduce the well known warm bias in the southeastern tropics in coupled models in both atmospheric and oceanic components (Zeng et al., 1996; Davey et al., 2002; Deser et al., 2006; Chang et al., 2007; Richter and Xie, 2008) as well as in forced ocean-only simulations (e.g. Large and Danabasoglu, 2006). This warm bias is well evidenced in our numerical simulation (Fig. 1&2) and our results clearly show that the cooling episodes were underestimated in the CLR, implying the need to investigate more in depth the oceanic and atmospheric processes in play in this particular region. As the intraseasonal wind bursts are related to the fluctuations of St. Helena Anticyclone, their impact on SST variability in the eastern tropical Atlantic and regional climate suggests the need of better understand the St. Helena Anticyclone variability.

It is also important to note that the mid-May 2005 event occurred during an unusually active year. The year 2005 exhibited a pronounced meridional mode pattern with strong SST gradient between the two hemispheres. Several authors (Foltz et al., 2006 ; Virmani and Weisberg, 2006 ; Marengo et al., 2008a, 2008b ; Zeng et al., 2008) studied this particular year, marked by anomalously warm SST in the tropical North Atlantic during March-July, the warmest from at least 150 years. This anomalous warming was associated with the most active and destructive hurricane season on record (Foltz et al., 2006; Virmani and Weisberg, 2006) and an extreme and rare drought in the Amazon Basin (Marengo et al., 2008a, 2008b; Zeng et al. 2008; Erfanian et al., 2017). From these authors, primary causes of the anomalous warming in 2005 were a weakening of the northeasterly trade winds and associated decrease in wind-induced latent heat loss as well as changes in shortwave radiation and horizontal oceanic heat advection. This 2005 temperature record is made even more remarkable given that, unlike the 1998's one, it occurred in the absence of any strong El Niño anomaly (Shein, 2006). Some studies (Goldenberg et al., 2001) attribute these SST increases to the Atlantic Multidecadal Oscillation (AMO), while others suggest that climate change may instead be playing the dominant role (Emanuel, 2005; Webster et al., 2005; Mann and Emanuel, 2006; Trenberth and Shea, 2006). Comparable anomalously warm tropical Atlantic SSTs have been observed in 2010 also associated with extreme drought in the Amazon. However, from time series of monthly anomalies constructed for the two basins (North and South Atlantic) by using OISST monthly mean data, Erfanian et al. (2017) show that the warmer-than-usual SSTs in the North Atlantic in 2010 was not associated with colder-than-usual SST in South Atlantic contrarily to 2005 (their Fig. S4e).

While the warming in North Tropical Atlantic during 2005 has been investigated by several authors, the cooling in South Atlantic has received less attention. This study highlights the need to further document and monitor the South Atlantic region and the St. Helena Anticyclone, through additional high resolution analysis and observations.

Acknowledgments:

The research leading to these results received funding from the EU FP7/2007-2013 under grant agreement no. 603521, PREFACE and from the EU Horizon 2020 under grand agreement no. 2014-633211, AtlantOS. These projects are gratefully acknowledged. We do thank Gildas Cambon for his help and participation on the implementation of ROMS simulations, and Frédéric Marin for his helpful comments.

References:

- Adamec, D., O'Brien, J. J.: The seasonal upwelling in the Gulf of Guinea due to remote forcing, *J. Phys. Oceanogr.*, 8, 1050-1060, 1978.
- Battisti, DS.: Dynamics and thermodynamics of a warming event in a coupled tropical atmosphere ocean model, *J. Atmos. Sci.* 45:2889 – 2919, 1988.
- Busalacchi, A., Picaut, J.: Seasonal variability from a model of the tropical Atlantic Ocean, *J. Phys Oceanogr.*, 13, 1564-1588, 1983.
- Bourlès, B., Brandt, P., Caniaux, G., Dengler, M., Gouriou, Y., Key, E., Lumpkin, R., Marin, F., Molinari, R.L., Schmid, C. : African Monsoon Multidisciplinary Analysis (AMMA): Special measurements in the Tropical Atlantic, *CLIVAR Exchange Letters*, 41 (12 2), International CLIVAR Project Office, National Oceanography Centre, Southampton, United Kingdom, 7–9, 2007.
- Brandt, P., Funk, A., Hormann, V., Dengler, M., Greatbatch, R.J., Toole, J.M.: Interannual atmospheric variability forced by the deep equatorial Atlantic Ocean, *Nature*, 473, 497–500, doi:10.1038/nature10013, 2011.
- Caniaux, G., Giordani, H., Redelsperger, J.-L., Guichard, F., Key, E., Wade, M.: Coupling between the Atlantic cold tongue and the West African monsoon in boreal spring and summer, *J. Geophys. Res.*, 116, C04003, doi:10.1029/2010JC006570, 2011.
- Carton, J. A., Chepurin, G., Cao, X., Giese, B.S.: A simple ocean data assimilation analysis of the global upper ocean 1950 –1995, part 1: Methodology, *J. Phys. Oceanogr.*, 30, 294–309, doi:10.1175/ 1520-0485(2000)030<0294:ASODAA>2.0.CO;2, 2000a.

- Carton, J. A., Chepurin, G., Cao, X.: A simple ocean data assimilation analysis of the global upper ocean 1950–1995, part 2: Results, *J. Phys. Oceanogr.*, 30,311–326, doi:10.1175/1520-0485(2000)030<0311:ASODAA>2.0.CO;2, 2000b.
- Carton, J. A., and Giese, B.S.: A reanalysis of ocean climate using simple ocean data assimilation (SODA), *Mon. Weather Rev.*, 136 ,2999–3017, doi:10.1175/2007MWR1978.1, 2008.
- Colin, C.: Sur la variabilité dans le Golfe de Guinée: Nouvelles considérations sur les mécanismes d’upwelling, Ph.D. thesis, Mus. Natl. d’Hist. Nat., Paris, 1989.
- Chang, C.-Y., Carton, J.A., Grodsky, S.A., Nigam, S.: Seasonal climate of the tropical Atlantic sector in the NCAR Community Climate System Model 3: Error structure and probable causes of errors, *J. Climate*, 20, 1053–1070, 2007.
- Chelton, D. B., deSzoeke, R.A., Schlax, M. G. , Naggar, K. E., Siwertz, N.: Geographical variability of the first-baroclinic Rossby radius of deformation, *J. Phys. Oceanogr.*, 28, 433–460, 1998.
- Dai, A., and Trenberth, K.E.: Estimates of freshwater discharge from continents: Latitudinal and seasonal variations, *J. Hydrometeorol.*, 3, 660–687, 2002.
- Danabasoglu, G., Large, W.G., Tribbia, J.J., Gent, P.R., Briegleb, B.P.: Diurnal Coupling in the Tropical Oceans of CCSM3, *Journal of Climate*, 19, 2347-2365, 2006.
- Davey, M., Huddleston, M., Sperber, K.R., et al.: STOIC: A study of coupled model climatology and variability in tropical ocean regions, *Clim. Dynam.*, 18, 403-420, 2002.
- Debreu, L., Marchesiello, P., Penven, P., Cambon, G.: Two-way nesting in split-explicit ocean models: algorithms, implementation and validation, *Ocean Modelling*, 49-50, 1-21, 2012.
- De Coëtlogon, G., Janicot, S., Lazar, A.: Intraseasonal variability of the ocean-atmosphere coupling in the Gulf of Guinea during boreal spring and summer, *Q. J. R. Meteorol. Soc.*, 136, 426–441, doi:10.1002/qj.554, 2010.
- Denamiel, C., Budgell, W.P., Toumi, R.: The Congo River plume: Impact of the forcing on the far-field and near-field dynamics, *J. Geophys. Res. Oceans*, 118, 964–989, doi:10.1002/jgrc.20062, 2013.
- Deser, C., Capotondi, A., Saravanan, R., Phillips, A.: Tropical Pacific and Atlantic climate variability in CCSM3, *J. Climate*, 19, 2451–2481, 2006.

- Djakouré, S., Penven, P., Bourlès, B., Veitch, J., Koné, V.: Coastally trapped eddies in the north of the Gulf of Guinea, *J. Geophys. Res. Oceans*, 119, 6805–6819, doi:10.1002/2014JC010243, 2014.
- Emanuel, K.: Increasing destructiveness of tropical cyclones over the past 30 years, *Nature*, 436, 686–688, 2005.
- Erfanian, A., Wang, G., Fomenko, L.: Unprecedented drought over tropical South America in 2016: significantly under-predicted by tropical SST, *Scientific reports*, 7:5811, doi: 10.1038/s41598-017_05373-2, 2017.
- Foltz, G. R., Grodsky, S. A., Carton, J. A., McPhaden, M. J.: Seasonal mixed layer heat budget of the tropical Atlantic Ocean, *J. Geophys. Res.*, 108, 3146, doi:10.1029/2002JC001584, 2003.
- Foltz, G.R. and McPhaden, M.J.: Unusually warm sea surface temperatures in the tropical North Atlantic during 2005, *Geophys. Res. Lett.*, 33: doi: 10.1029/2006GL027394. issn: 0094-8276, 2006.
- Fritts, D. C.: Wave saturation in the middle atmosphere: A review of theory and observations, *Rev. Geophys.*, 22, 275–308, 1984.
- Gentemann, C.L., Wentz, F.J., Brewer, M., et al.: Passive Microwave Remote Sensing of the Ocean: an Overview, *Oceanography from Space, Revisited*, edited by V. Barale, J. Gower, and L. Alberotanza, 13–33. Heidelberg: Springer, 2010.
- Giese, B.J, Harrison, D.E.: Aspects of the Kelvin wave response to episodic wind forcing, *J. Geophys. Res.*, 95: 7289 – 7312, 1990.
- Giordani, H., Caniaux, G., Voldoire, A.: Intraseasonal mixed-layer heat budget in the equatorial Atlantic during the cold tongue development in 2006, *J. Geophys. Res.: Oceans*, 118(2):650-671. doi: 10.1029/2012JC008280, 2013.
- Goldenberg, S.B., Landsea, C.W., Mestas-Núñez, A.M., Gray, W.M.: The Recent Increase in Atlantic Hurricane Activity: Causes and Implications, *Sciences*, Vol. 293, Issue 5529, pp. 474-479, doi: 10.1126/science.1060040, 2001.
- Grodsky, S. A., Carton, J. A.: The Intertropical Convergence Zone in the South Atlantic and the Equatorial Cold Tongue, *J. Climate*, 16, 723–733, 2003.
- Haidvogel, D.B., Beckmann, A.: *Numerical Ocean Circulation Modeling*, Imperial College Press, London; 320 pp., 1999.

- Herbert, G., Bourlès, B., Penven, P., Grelet, J.: New insights on the upper layer circulation north of the Gulf of Guinea, *J. Geophys. Res.: Oceans*, 121, doi:10.1002/2016JC011959, 2016.
- Hormann, V., Brandt, P.: Upper equatorial Atlantic variability during 2002 and 2005 associated with equatorial Kelvin waves, *J. Geophys. Res.*, 114: C03007, doi:10.1029/2008JC005101, 2009.
- Illig, S., Dewitte, B., Ayoub, N., du Penhoat, Y., Reverdin, G., Mey, P.D., Bonjean, F., Lagerloef, G.S.E.: Interannual long equatorial waves in the tropical Atlantic from a high-resolution ocean general circulation model experiment in 1981-2000, *J. Geophys. Res.: Oceans*, 109:C02022. doi: 10.1029/2003JC001771, 2004.
- Jouanno, J., Marin, F., duPenhoat, Y., Sheinbaum, J., Molines, J.M.: Seasonal heat balance in the upper 100m of the Equatorial Atlantic Ocean, *J. Geophys. Res.: Oceans*, 116:C09003. doi: 10.1029/2010JC006912, 2011.
- Jouanno, J., Marin, F., duPenhoat, Y., Molines, J.M.: Intraseasonal Modulation of the Surface Cooling in the Gulf of Guinea, *J. Phys. Oceanogr.*, 43(2):382-401. doi: 10.1175/JPO-D-12-053.1, 2013.
- Krishnamurti, T. N., Pasch, R.J., Ardanuy, P.: Prediction of African waves and specification of squall lines, *Tellus*, 32, 215-231, 1980.
- Leduc-Leballeur, M., Eymard, L., de Coëtlogon, G.: Observation of the marine atmospheric boundary layer in the Gulf of Guinea during the 2006 boreal spring, *Q. J. R. Meteorol. Soc.*, 137: 992 – 1003, 2011.
- Leduc-Leballeur, M., de Coëtlogon, G., Eymard, L.: Air – sea interaction in the Gulf of Guinea at intraseasonal time-scales: Wind bursts and coastal precipitation in boreal spring, *Q. J. R. Meteorol. Soc.*, 139, 387–400, doi:10.1002/qj.1981, 2013.
- Lübbecke, J.F., Burls, N.J., Reason, C.J.C., McPhaden, M.J.: Variability in the South Atlantic Anticyclone and the Atlantic Nino Mode, *J. Climate*, 27, doi: 10.1175/JCLI-D-14-00202.1, 2014.
- Mann, M. E., and Emanuel, K.A.: Atlantic hurricane trends linked to climate change, *Eos, Trans. Amer. Geophys. Union*, 87, 233–244, 2006.
- Marengo, J. A., Nobre, C.A., Tomasella, J., Oyama, M.D., De Oliveira, G.S., De Oliveira, R., Camargo, H., Alves, L.M., Brown, I.F. : The drought of Amazonia in 2005, *J. Climate*, 21, 495-516, 2008a.
- Marengo, J.A., Nobre, C.A., Tomasella, J., Cardoso, M.F., Oyama, M.D.: Hydro-climatic and ecological behaviour of the drought of amazonia in 2005, *Philosophical transactions of the Royal society of London, Biological sciences*, v.21, p.1-6, 2008b.

- Marin, F., Caniaux, G., Bourlès, B., Giordani, H., Gouriou, Y., Key, E.: Why were sea surface temperatures so different in the Eastern Equatorial Atlantic in June 2005 and 2006, *J. Phys. Oceanogr.*, 39, 1416–1431, doi:10.1175/2008JPO4030.1, 2009.
- Materia, S., Gualdi, S., Navarra, A., Terray, L.: The effect of Congo River freshwater discharge on Eastern Equatorial Atlantic climate variability, *Clim. Dynam.*, 39(9-10), 2109–2125, doi:10.1007/s00382-012-1514-x, 2012.
- McCreary, J.: Eastern tropical ocean response to changing wind systems with application to El Nino, *J. Phys. Oceanogr.*, 6, 632-645, 1976.
- McCreary, J., Picaut, J., Moore, D.: Effects of the remote annual forcing in the eastern tropical Atlantic Ocean, *J. Mar. Res.*, 42, 45-81, 1984.
- Merle, J. : Conditions hydrologiques saisonnières de la marge continentale du Gabon et du Congo (de 10°N a 60°S) Etude descriptive, *Dot. Sci. O.R.S.T.O.M. Pointe-Noire*, 27 : 1-20, 1972.
- Merle, J., Fieux, M., Hisard, P.: Annual signal and interannual anomalies of sea surface temperature in the eastern equatorial Atlantic Ocean, *Deep Sea Res.*, 26,77–101, 1980.
- Mitchell, T. P., Wallace, J.M.: The annual cycle in equatorial convection and sea surface temperature, *J. Climate*, 5, 1140–1156, 1992.
- Moore, D.W.: Planetary-gravity waves in an equatorial ocean, PhD Thesis, Harvard University, 201 pp., 1968.
- Moore, D.W., and Philander, S.G.H.: Modeling of the tropical ocean circulation, *The Sea*, Vol. 6, Wiley Interscience, New York, N.Y., pp. 316-361, 1977.
- Moore, D. W., Hisard, P., McCreary, J. P., Merle, J., O'Brien, J. J., Picaut, J., Verstraete, J. M., Wunsch, C.: Equatorial adjustment in the eastern Atlantic, *Geophys. Res. Lett.*, 5, 637-640, 1978.
- Nguyen, H., Thorncroft, C. D., Zhang, C.: Guinean coastal rainfall of the West African Monsoon, *Q.J.R. Meteorol. Soc.*, 137: 1828–1840. doi:10.1002/qj.867, 2011.
- Nicholson, S.E., Dezfuli, A.K.: The relationship of rainfall variability in western equatorial Africa to the tropical oceans and atmospheric circulation. Part I: The boreal spring, *J. Climate*, 26(1), 45–65, 2013.
- Nobre, P., Shukla, J.: Variations of sea surface temperature, wind stress, and rainfall over the tropical Atlantic and South America, *J. Climate*, 9 : 2464 – 2479, 1996.
- Okumura, Y., and Xie, S.P.: Interaction of the Atlantic equatorial cold tongue and the African monsoon, *J. Climate*, 17, 3589–3602, 2004.

- Okumura, Y., Xie, S.P.: Some overlooked features of tropical Atlantic climate leading to a new Niño-like phenomenon, *J. Climate*, 19(22), 5859–5874, doi:10.1175/JCLI3928.1, 2006.
- Penven, P., Marchesiello, P., Debreu, L., Lefevre, J.: Software tools for pre- and post-processing of oceanic regional simulations, *Environ. Modell. Software*, 23, 2008 660–662, 2008.
- Peter, A.-C., Le Hénaff, M., du Penhoat, Y., Menkès, C., Marin, F., Vialard, J., Caniaux, G., Lazar, A.: A model study of the seasonal mixed layer heat budget in the equatorial Atlantic, *J. Geophys. Res.*, 111, C06014, doi: 10.1029/2005JC003157, 2006.
- Philander, S., and Pacanowski, R.: A model of the seasonal cycle in the Tropical Atlantic Ocean, *J. Geophys. Res.*, 91, 14, 192–14, 206, 1986.
- Philander, S.G.: *El Nino, La Nina and the Southern Oscillation*, Academic Press, 293 pp., 1990.
- Picaut, J.: Propagation of the seasonal upwelling in the eastern equatorial Atlantic, *J. Phys. Oceanogr.*, 13, 18–37, doi: 10.1175/1520-0485, 1983.
- Picaut, J.: On the dynamics of the thermal variations in the Gulf of Guinea, *Oceanogr. Trop.*, 19 (2) : 127-53, 1984.
- Piton, B. : *Les courants sur le plateau continental devant Pointe-Noire (Congo)*, Documents scientifiques, ORSTOM, Brest, n°47, 37 p., 1988.
- Polo, I., Lazar, A., Rodriguez-Fonseca, B., Arnault, S.: Oceanic Kelvin waves and tropical Atlantic intraseasonal variability: 1. Kelvin wave characterization, *J. Geophys. Res.*, 113, C07009, doi: 10.1029/2007JC004495, 2008.
- Redelsperger, J. L., et al. : *AMMA: Une étude multidisciplinaire de la mousson Ouest-Africaine*, *Meteorologie*, 54,22–32, doi:10.4267/2042/20098, 2006.
- Richter, I. and Xie, S.-P.: On the origin of equatorial Atlantic biases in coupled general circulation models, *Clim. Dynam.*, 1:587–598, doi : 10.1007/s00382-008-0364-z, 2008.
- Rouault, M., Servain, J., Reason, C. J. R. , Bourlès, B., Rouault, M. J. , Fauchereau, N.: Extension of PIRATA in the tropical south-east Atlantic: An initial one-year experiment, *Afr. J. Mar. Sci.*,31(1),63–71, doi:10.2989/AJMS.2009.31.1.5.776, 2009.
- Saha, S., Moorthi, S., Pan, H.-L., Wu, W., Wang, J., Nadiga, S., Tripp, P., Kistler, R., Woollen, J., Behringer, D., Liu, H., Stokes, D., Grumbine, R., Gayno, G., Wang, J., Hou, Y.T., Chuang, H.-Y., Juang, H.-M.

- H., Sela, J., Iredell, M., Treadon, R., Kleist, D., Van Delst, P., Keyser, D., Derber, J., Ek, M., Meng, J., Wei, H., Yang, R., Lord, S., Van Den Dool, H., Kumar, A., Wang, W., Long, C., Chelliah, M., Xue, Y., Huang, B., Schemm, J.-K., Ebisuzaki, W., Lin, R., Xie, P., Chen, M., Zhou, S., Higgins, W., Zou, C.-Z., Liu, Q., Chen, Y., Han, Y., Cucurull, L., Reynolds, R.W., Rutledge, G., Goldberg, M. : The NCEP climate forecast system reanalysis, *Amer. Meteor. Soc.*, 91, 1015-1057, 2010.
- Schouten, M. W., Matano, R. P., Strub, T. P.: A description of the seasonal cycle of the equatorial Atlantic from altimeter data, *Deep Sea Res., Part I*, 52, 477–493, doi:10.1016/j.dsr.2004.10.007, 2005.
- Servain, J., Picaut, J., Merle, J.: Evidence of remote forcing in the equatorial Atlantic Ocean, *J. Phys. Oceanogr.*, 12, 457–463, 1982.
- Shein, K. A.: State of the climate in 2005, *Bull. Am. Meteorol. Soc.*, 87, s1–s102, doi: 10.1175/BAMS-87-6-shein, 2006.
- Shchepetkin, A., McWilliams, J.C.: The Regional Oceanic Modeling System (ROMS): A split-explicit, free-surface, topography-following-coordinate ocean model, *Ocean Modell.* 9, 347–404, 2005.
- Thorncroft, C. D., Nguyen, H., Zhang, C., Peyrillé, P.: Annual cycle of the West African monsoon: regional circulations and associated water vapour transport, *Q. J. R. Meteorol. Soc.*, 137, 129-147, doi:10.1002/qj.728, 2011.
- Trenberth, K.E., Shea, D.J.: Atlantic hurricanes and natural variability in 2005, *Geophys. Res. Lett.*, vol. 33, L12704, doi: 10.1029/2006GL026894, 2006.
- Virmani, J. I., and Weisberg, R.H.: The 2005 hurricane season: An echo of the past or a harbinger of the future?, *Geophys. Res. Lett.*, 33, L05707, doi: 10.1029/2005GL025517, 2006.
- Wade, M., Caniaux, G., du Penhoat, Y.: Variability of the mixed layer heat budget in the eastern equatorial Atlantic during 2005–2007 as inferred using Argo floats, *J. Geophys. Res.*, 116, C08006, doi: 10.1029/2010JC006683, 2011.
- Yu, L., Jin, X., Weller, R.A.: Role of net surface heat flux in seasonal variations of sea surface temperature in the tropical Atlantic ocean, *J. Climate*, 19, 6153–6169, 2006.
- Waliser, D. E., and Gautier, C.: A satellite-derived climatology of the ITCZ, *J. Climate*, 6, 2162–2174, 1993.
- Wauthy, B. : Introduction à la climatologie du Golfe de Guinée, *Oceanogr. Trop.*, 18, 103–138, 1983.

- Webster, P.J., Holland, G. J., Curry, A., Chang, H.R.: Changes in tropical cyclone number, duration, and intensity, in warming environment, *Science*, 309, 1844-1846, 2005.
- Wentz, F.J., and Meissner, T.: Algorithm Theoretical Basis Document (ATBD), version 2, AMSR-E Ocean Algorithm, Remote Sensing Systems Tech. Rep., RSS 121599A-1, 55 pp., 2000.
- White, R.H. and Toumi, R.: River Flow and Ocean Temperatures: The Congo River, *J. Geophys. Res. -Oceans*, 119, 25016–2517, doi:10.1002/2014JC009836, 2014.
- Zebiak, S.: Air-sea interaction in the equatorial Atlantic region, *J. Climate*, 6(8), 1567–1586, doi:10.1175/1520-0442(1993)006<1567:AIITEA>2.0.CO;2, 1993.
- Zeng, N., Dickinson, R.E., Zeng, X.: Climatic impact of Amazon deforestation-A mechanistic model study, *J. Climate*, 9, 859–883, 1996.
- Zeng, N., Dickinson, R.E., Zeng, X.: Causes and impacts of the 2005 Amazon drought, *Env. Res. Lett.*, 3, doi: 10.1088/1748-9326/3/1/014002, 2008.